



HAL
open science

CRUISE REPORT of the TONGA oceanographic campaign (R/V L'Atalante, oct 31-dec 6, 2019)

Cécile Guieu, Sophie Bonnet

► To cite this version:

Cécile Guieu, Sophie Bonnet. CRUISE REPORT of the TONGA oceanographic campaign (R/V L'Atalante, oct 31-dec 6, 2019): This is the cruise report of the TONGA (shallow hydroThermal sOurces of trace elemeNts: potential impacts on biological productivity and the bioloGicAl carbon pump) oceanographic campaing that explored the Western Tropical South Pacific (WTSP) Ocean on board R/V L'Atalante, oct 31-dec 6, 2019.. CNRS; IRD - Institut de recherche pour le developpement. 2023. hal-04383234

HAL Id: hal-04383234

<https://hal.science/hal-04383234>

Submitted on 9 Jan 2024

HAL is a multi-disciplinary open access archive for the deposit and dissemination of scientific research documents, whether they are published or not. The documents may come from teaching and research institutions in France or abroad, or from public or private research centers.

L'archive ouverte pluridisciplinaire **HAL**, est destinée au dépôt et à la diffusion de documents scientifiques de niveau recherche, publiés ou non, émanant des établissements d'enseignement et de recherche français ou étrangers, des laboratoires publics ou privés.

OCEANOGRAPHIC CAMPAIGN REPORT

(UPDATED VERSION November 2023)

TONGA

shallow hydroThermal sOurces of trace elemeNts: potential impacts
on biological productivity and the bioloGicAl carbon pump



FUNDED by: ANR-18-CE01-0016, INSU-LEFE-CYBER & GMMC, Fondation A-MIDEX (Aix-Marseille University), FOF Fonds de Soutien, IRD

Navire : ATALANTE	
Dates de la campagne : 31/10/2019 to 06/12/2019 Nombre de jours sur zone/en transit : 35 jours sur zone	Zone(s) : Pacific Ocean (Eaux inter.): -20° 0' 0" -24° 0' 0" -166° 0' 0" 165° 0' 0"
Chief scientist : Cécile Guieu, LOV, CNRS. Sophie Bonnet, M.I.O, IRD Nombre de chercheurs et d'enseignants-chercheurs : 12 en mer / 39 à terre Nombre d'ingénieurs et de techniciens : 10 en mer / 16 à terre Nombre d'étudiants: 7 doctorants en mer / 2 doctorants à terre (more in the future)	

Authors : Cécile Guieu/Sophie Bonnet

Date de rédaction ou d'actualisation de la fiche: Mars 2020, mise à jour novembre 2023

Adresse : LOV, Villefranche, M.I.O Marseille

Email : cecile.guieu@imev-mer.fr, sophie.bonnet@ird.fr



Table des matières

1.	Factual info (web sites, data base, publications, outreach, students and post-doc etc.): updates on november 2023	5
2.	Scientific framework of the campaign	6
3.	Main objectives	6
4.	Overview of the work performed	8
4.1	Specific strategy to study the shallow volcanoes	9
4.1.1	Volcano 1 and its maximum echo anomaly PANAMAX	9
4.1.2	Strategy for volcano at LD10.	10
3.1	Work at Station: summary	12
5.	Detailed work performed at sea and preliminary results.....	16
4.2	Physical environment	16
4.2.1	CTDs.....	16
4.2.2	Microturbulence measurements	18
4.3	Stocks/diversity measurements (work at stations)	20
4.3.1	Chemical elements	20
4.3.1.1	Nutrients and core parameters.....	20
4.3.1.2	Metals	21
4.3.1.3	Gases: Methane in the water column.....	25
4.3.1.4	Physical and Chemical tracing of hydrothermal plumes	27
4.3.2	Diversity within the planktonic communities	33
4.3.3	Essential traits of Plankton and elemental (iron, Lithium) concentrations and quotas.....	34
4.3.4	Phytoplankton communities and bio-optics at stations	36
4.4	Fluxes measurements, processes studies at stations	37
4.4.1	Heterotrophic prokaryotic production	37
4.4.2	Primary production and N ₂ Fixation rates	38
4.4.3	Phosphate availability and microbial P cycle	39
4.5	Characterization of export pathways	40
4.5.1	Export at 200 m and 1000 m on short time scale close to the shallow volcanoes	40
4.5.2	Mesopelagic remineralization of sinking particles.....	41
4.5.3	Biogeochemical and microbial characterization of export material and fluxes accross Fe/hydrothermal gradients	43
4.5.4	Study of export at 200 m and 1000 m the annual time scale	45
4.6	Stocks, diversity and processes in the sediment	48
4.7	Underway work	49
4.7.1	Atmosphere	49
4.7.2	Surface waters underway	51

4.7.2.1	Role of fine scale dynamics in structuring diazotrophic activity & diversity	51
4.7.2.2	High spatio-temporal characterization of photosynthetic activity.....	52
4.7.2.3	How biological activity impacts marine emissions.....	53
4.8	Process Studies.....	54
4.8.1	Mixing experiments in minicosms	54
4.8.2	Effect of different DOP molecules on N ₂ fixation, DOP acquisition, gene expression and methane production	57
4.8.3	Impacts of P and Fe availability on colony formation in <i>Trichodesmium</i> spp.....	58
4.9	Autonomous instruments launched during TONGA.	59
4.9.1	BGC ARGO and ARVOR floats.....	60
4.9.2	SVP buoys	63
4.10	Supporting data	64
4.10.1	Ariane simulations	64
4.10.2	SPASSO.....	66
6.	References in the text	67
7.	Annexe 1: Participants on board	68
8.	Annexe 2: Participants on land	69
9.	Annexe 3: Publications (published or accepted) and communications (update nov 2023)	71
10.	ANNEXE 4: Students involved in TONGA.....	72

1. FACTUAL INFO (WEB SITES, DATA BASE, PUBLICATIONS, OUTREACH, STUDENTS AND POST-DOC ETC.): UPDATES ON NOVEMBER 2023

- TONGA expedition is GEOTRACES process study (GPpr14) <https://www.geotraces.org/geotraces-process-studies/>
- French Fleet Web sites of the TONGA 2019 expedition : <https://campagnes.flotteoceanographique.fr/campagnes/18000884/>
- French Fleet Web sites of the TONGA-RECUP 2020 expedition : <https://campagnes.flotteoceanographique.fr/campagnes/18001357/fr/>
- Web site of the project: <http://tonga-project.org/web/>
- Database LFE-CYBER: <https://www.obs-vlfr.fr/proof/php/TONGA/tonga.php>
- Published database: <https://www.seanoe.org/data/00770/88169/>
- Videodocuments:
 - Le Réveilleur (2022) L'interview du Réveilleur avec C Guieu et S Bonnet: www.echosciences-paca.fr/articles/video-echoscientifique-n-23 Dans le cadre du projet Echosciences Provence-Alpes-Côte d'Azur <https://www.echosciences-paca.fr>
 - Le Réveilleur (2022) Pourquoi la Vie Galère dans l'océan : <https://www.youtube.com/watch?v=3105ScO53fo> Dans le cadre du projet Echosciences Provence-Alpes-Côte d'Azur <https://www.echosciences-paca.fr> avec Cécile Guieu (CNRS / Laboratoire d'Océanographie de Villefranche) & Sophie Bonnet (IRD / l'Institut Méditerranéen d'Océanologie).
 - The TONGA oceanographic expedition, (2021) Film 26' Director: Hubert Bataille Co-production: IRD-CNRS , Scientific advisors: Sophie Bonnet (IRD), Cécile Guieu (CNRS). English version: <https://www.youtube.com/watch?v=UeABf-cVR-k>
 - Mission TONGA à la recherche des volcans sous-marins du Pacifique, (2020) Film 26' Réalisateur : Hubert Bataille Co-production : IRD-CNRS Conseillères scientifiques: Sophie Bonnet (IRD), Cécile Guieu (CNRS) Copyright IRD 2020. Version française: <https://www.youtube.com/watch?v=e5kAd0i6Dck>
- Publications and communications: see at the end of the document (p 71)
- Students involved in TONGA: see at the end of the document (p 72)

2. SCIENTIFIC FRAMEWORK OF THE CAMPAIGN

The Western Tropical South Pacific (WTSP) Ocean has recently been identified as a hotspot of N₂ fixation and harbors among the highest rates reported in the global ocean, and supports nearly all new primary production during the summer season. N₂-fixing organisms have high iron (Fe) quotas relative to non-diazotrophic plankton and their success in the WTSP has been attributed to the alleviation of Fe limitation in this region. A shallow source (<500 m) of hydrothermal Fe was discovered during the OUTPACE campaign in the WTSP (Guieu et al., 2018), resulting in high dissolved iron concentrations (> 4 nM) into the euphotic layer (~ 0-150 m). To date, the potential impact of such inputs on Fe regional budgets and on the biogeochemical cycles of biogenic elements (C, N, P) has never been studied.

In this context, the objective of the TONGA campaign was to study the control of productivity and carbon sequestration by these micronutrients of shallow hydrothermal origin. The 37-day oceanographic survey over a large area of the WTSP allowed for the acquisition of numerous results on both the atmosphere and the entire water column (up to the sediment). Part of these results will feed into important modeling work. The launching of a fixed mooring line (recovered in Nov. 2020) as well as the 7 ARGO floats and 20 drifting buoys that were launched during the campaign will provide a broader temporal context. An important focus of the campaign was the trace metal characterization of the entire water column. For this, TONGA has been labeled by the international program GEOTRACES. The impact on biological communities of fluids is supported by the international IMBER program. The TONGA project is also part of the LEFE program (funding by LEFE-CYBER and LEFE-GMMC), the ANR (Appel à projets génériques) and the Fondation A-MIDeX of the Aix-Marseille Université. An important component of the outreach was linked to the adopt-a-float project (<http://www.monoceanetmoi.com/web/index.php/fr/adopt-a-float>).

3. MAIN OBJECTIVES

The objectives of the cruise were to investigate at least 2 active volcanoes where shallow (< 500 m) hydrothermal sites could release chemical elements both able to fertilize and/or bring toxicity to the planktonic food web. More specifically, the task 1 of the TONGA cruise was to characterize chemically and optically the hydrothermal fluids and to compare the source from below (shallow hydrothermal fluids) with the source from above (atmospheric deposition); the task 2 was related to the dynamical dispersion of the fluids at small and regional scale; the third task was to investigate the impact of the shallow hydrothermal sources on the biological activity and diversity, and the feedback to the atmosphere via the oceanic emissions of primary and secondary aerosols (figure 1). An important objective was to communicate about the campaign mainly by the feed of a Tweeter account (<https://twitter.com/tongaproject>, now X); several short movies were posted. The outreach component of the campaign was done in collaboration with the adopt-a-float project and during the campaign, two float have been 'adopted' by kids from two schools (one in Nouméa and one in Abu Dhabi).

The position of the sampling station has been constantly re evaluated during the campaign to fulfill the objectives: a long west to east (up to the blue waters of the gyre) transect allowed to characterize the different biogeochemical provinces crossed and a focus in the region of the Lau Basin allowed to investigate the impact of shallow hydrothermal sources. A series of short and long stations allowed to fully characterizing the stocks and the fluxes in the different provinces. Short-term (up to 10 days) processes studies have been conducted (drifting moorings and minicosms experiments). A fixed mooring was deployed in the Lau Basin to study the carbon/metals export at the annual time scale. In addition to the team embarked on board the R/V Atalante, several scientists assisted us on land to advice on the potential active sites that we could visit, the dynamic condition of the targeted area and also specifically on the interpretation of acoustic survey above volcanoes.

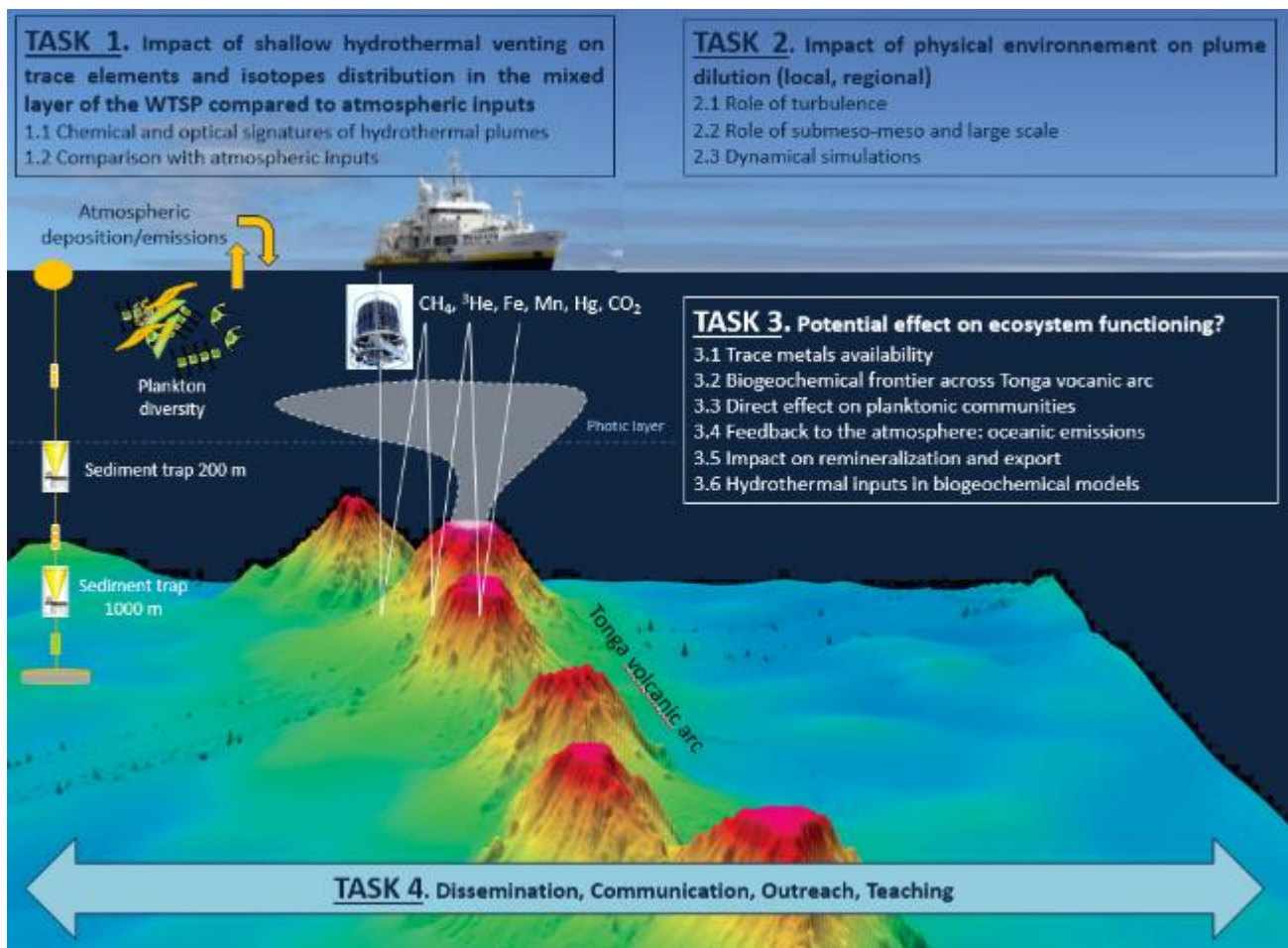


Figure 1. Scheme of the different tasks of the TONGA project and cruise.

4. OVERVIEW OF THE WORK PERFORMED

During the 6100 km covered, we occupied 12 stations: 9 'short' stations lasting 10 hours on average and 3 long stations lasting from 4 to 7 days. The depths were very variable with minimum depths above the 2 studied volcanoes (a few hundred meters) to the deepest station 8 (5400 m).

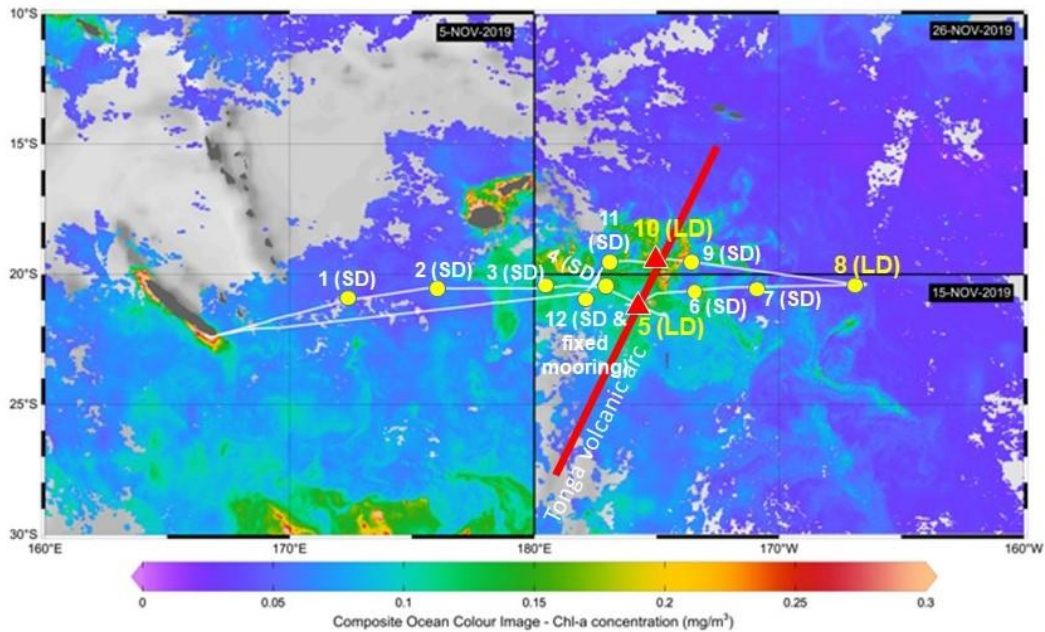


Figure 2. *Final track of the TONGA Cruise superimposed to ocean color images during the campaign. The detailed occupation of the 2 volcanoes sites « LD5» and « LD10 » can be found in the detailed sections below.*

The number of stations has been reduced compared to the original plan because the two targeted volcanoes have been better investigated than anticipated (sub-stations in the vicinity of the 2 volcanoes allowed a very good survey to both characterize the source and the impacts). A detailed description of the surveys in the vicinity of both the volcanoes is given below. Two areas have been targeted following recommendation from our geologist colleagues with the main criteria that the active source should be as shallow (<500 m) as possible. Our first target was Volcano 1 (an area also identified as a possible source of the iron anomaly measured during OUTPACE, see Guieu et al., 2018). The exploration strategy was first based on an acoustic survey using the hull-mounted EM-122 and EM-710 echosounders of RV L'Atalante, operating at a frequency of 12 kHz (for depths >1000m), and 70 to 100 kHz (for lower depths) respectively. Given the depths of the survey area, both were implemented. Surveys were carried out above the volcanoes at <7 knots for several hours.

Our strategy was to start a precise bathymetry mapping by the mean of the multibeam echo sounder; simultaneously, all the acoustic anomalies seen directly on the screen during the survey were reported in order to get all the coordinates where anomalies could be seen. This strategy allowed us to find 2 'active' sites both at LD5 above Volcano 1 (maximum activity site named 'PANAMAX') and at LD10..

After this exploration phase, the second phase consisted in deploying a CTD-rosette fitted with NISKIN bottles and various *in situ* physical and chemical sensors to detect the presence of chemical and physical/optical anomalies related to hydrothermal activity in the water column. Several physical and chemical tracers were used: conductivity, temperature, turbidity, redox potential (Eh), pH, CH₄, Mn, Fe, and ³He. Hydrothermal tracers can be detectable some hundreds of meters above and a few kilometers around any given vent source (see following sections for detailed reports on both volcanoes).

4.1 Specific strategy to study the shallow volcanoes

4.1.1 Volcano 1 and its maximum echo anomaly PANAMAX

Available bathymetry (Massoth et al. 2007) → multibeam echo sounder → bathymetry + acoustic anomalies → pseudo towyo above the small structure where the strong acoustic anomaly has been identified 'PANAMAX' site → a series of stations between PANAMAX, the mooring site (depth ~2000 m) and up to 20 mn west of the mooring site to track physical anomalies in the water column.

Bathymetry available: from Massoth et al., 2007 paper: we decided to redo the bathy with a multibeam echo sounder survey and at the same time identify the acoustic anomalies and note their position as the survey was done.

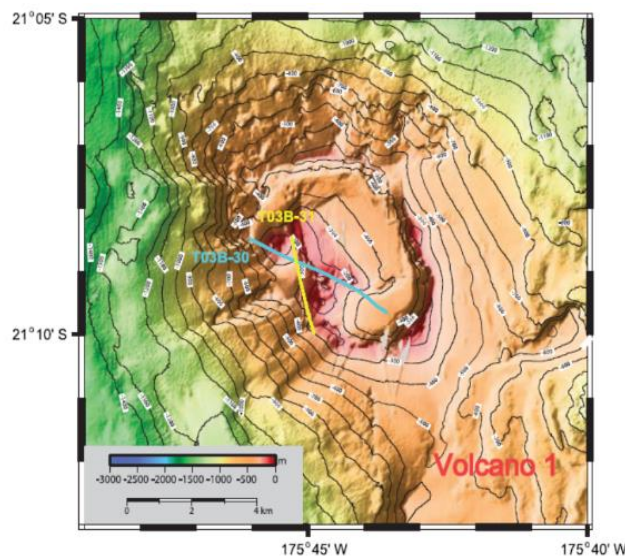


Figure 3. Initial bathymetry of Volcano 1 (Massoth et al., 2007)

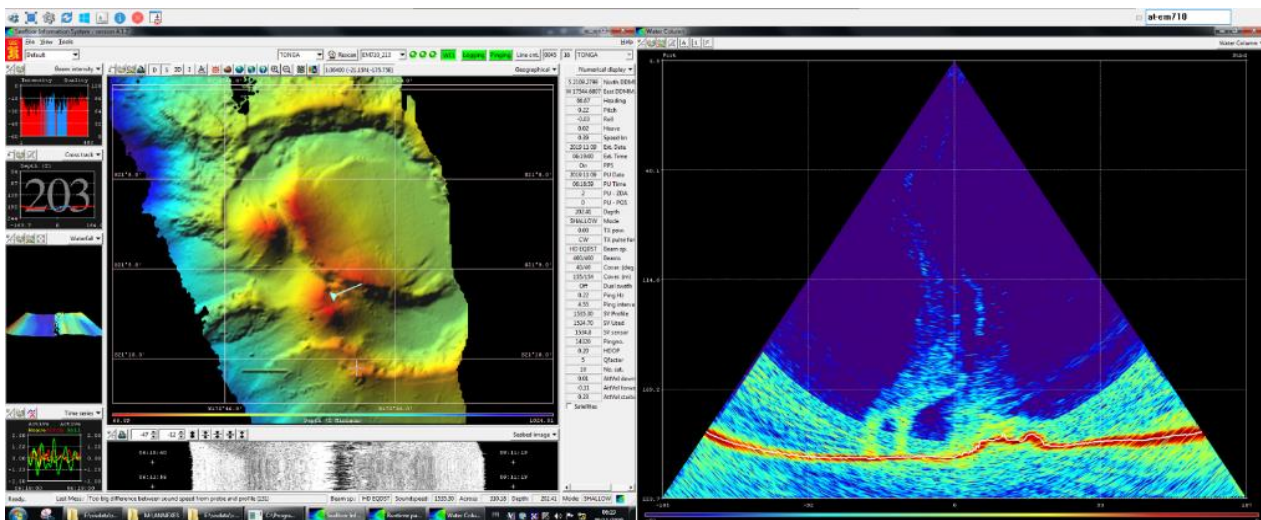


Figure 4. Bathymetry of Volcano 1 realized during TONGA and identification of PANAMAX (above the position on the R/V (small triangle on the left screen in the center of the small structure found to have a strong acoustic anomaly (right screen)).

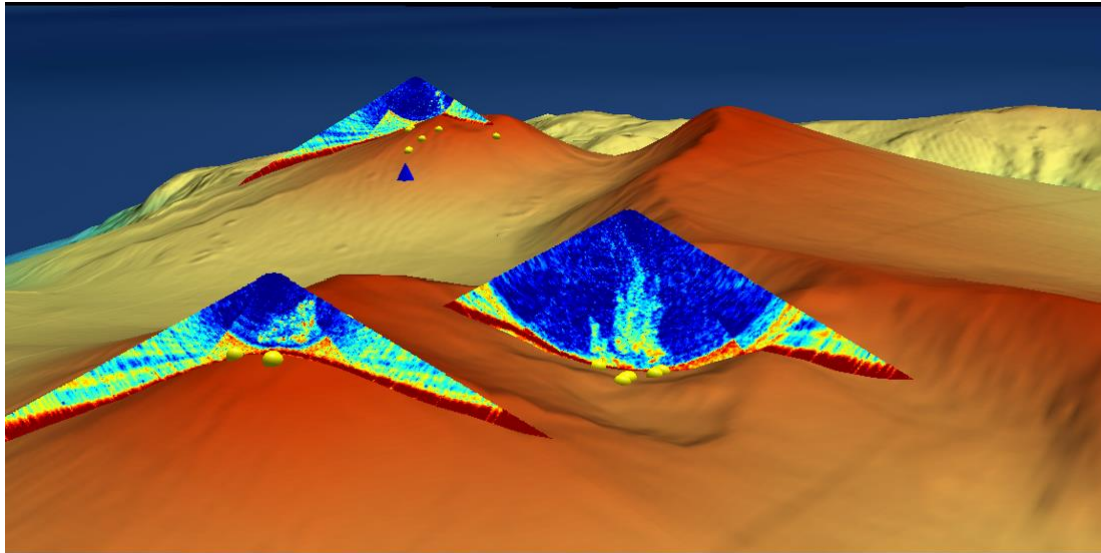


Figure 5. All the acoustic anomalies reported during the SMF survey of Volcano 1 are then introduced in a 3 D view (Figure: Carla Scalabrin).

A mooring site was then identified as close as possible of PANAMAX and on the main current direction, when the bottom reached ~2000 m (again following the multibeam echo sounder survey). This whole area was deeply investigated during 7 days thanks to a large number of CTDs between the different sub-stations reported on the map below:

(For the exact position of the different CAST : see table 1)

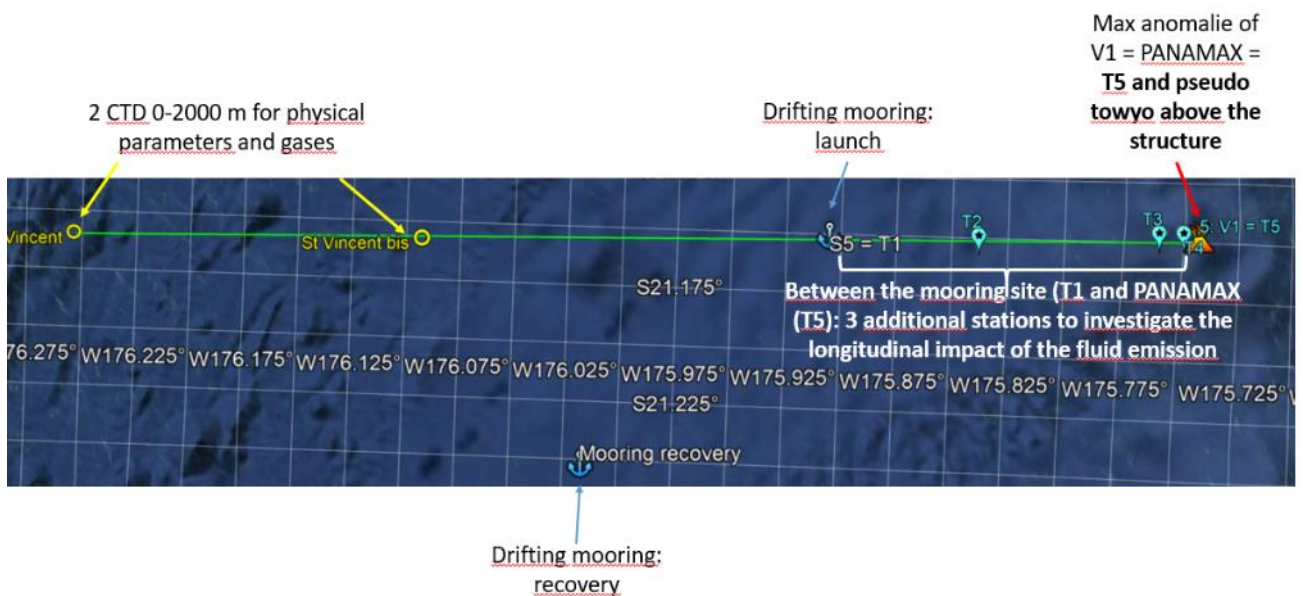


Figure 6. Long duration Station 5: Volcano 1 "V1" area was investigated between 08/11 (17h45 TU) to 15/11 (6h40 TU). The results of the physical characterisation along the whole transect can be found figure 12.

4.1.2 Strategy for volcano at LD10.

Available bathymetry before the cruise (Fernando Martinez, Univ Hawaii) → a targeted area within the large caldera indicated by our geologist colleagues → multibeam echo sounder survey restricted to that area → signal was found but not as strong as at ST5

above Panamax → more multibeam echo sounder survey to find a stronger signal followed by a towyo strategy although no evidence from optical sensors of significant anomalies.

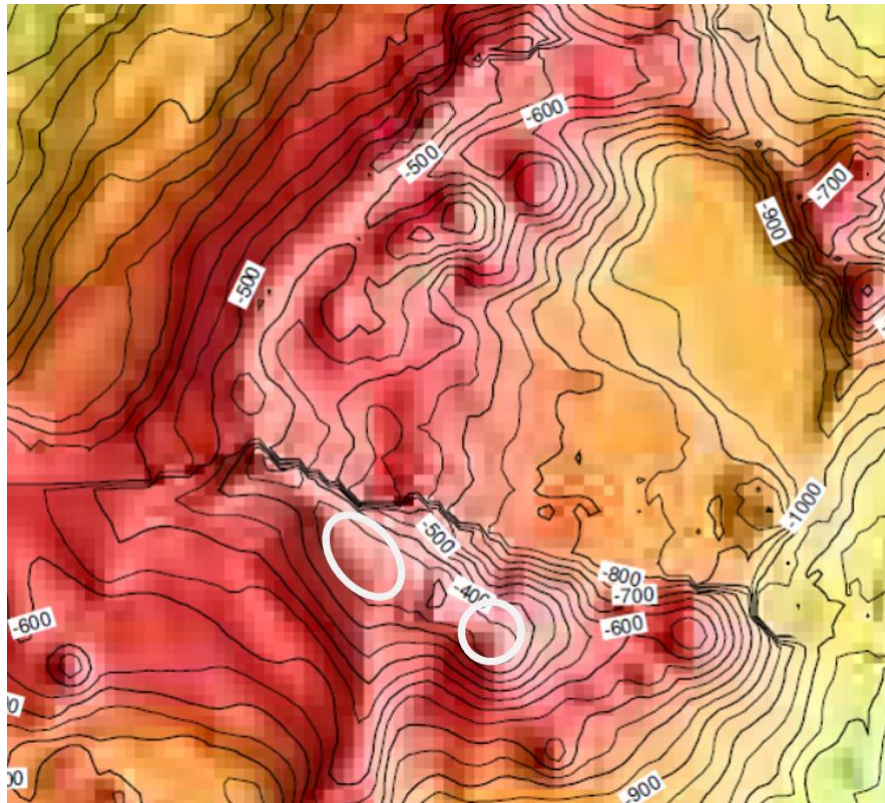


Figure 7. LD 10: Initial bathymetry of the site (Fernando Martinez, Univ Hawaii). The two area (circles) investigated were indicated as potential active zones by our geologists colleagues

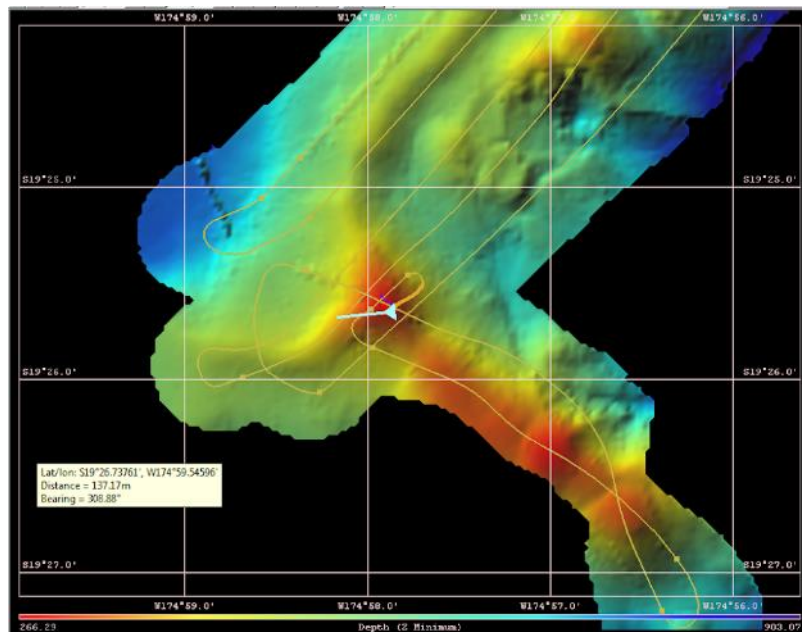


Figure 8. Due to timing issues, the whole bathymetry of the volcano was not possible. The main activity has been found above the

small western structure.

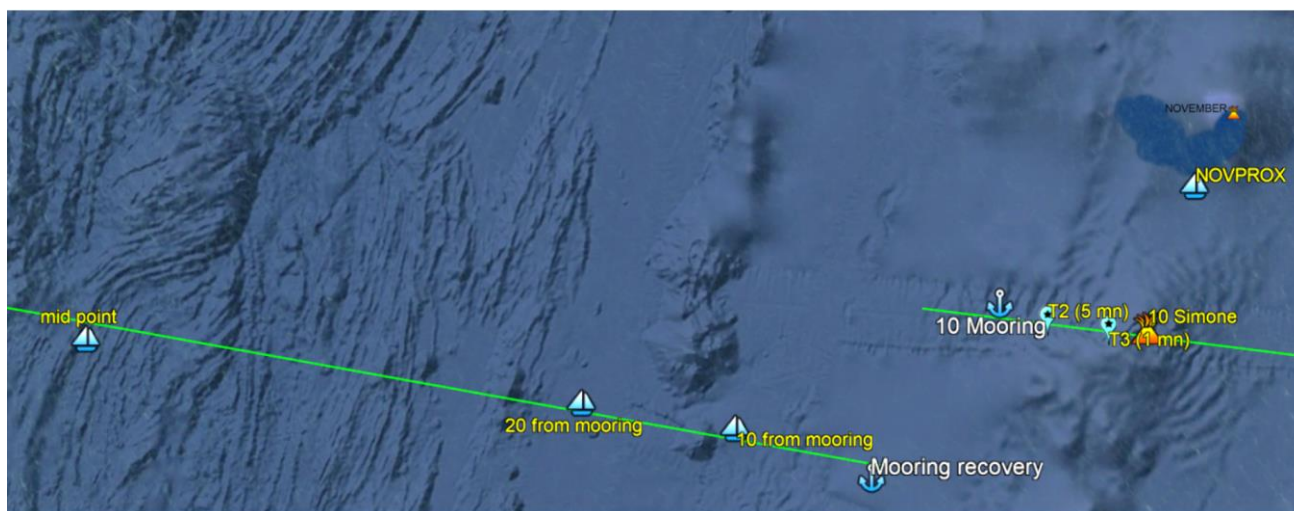


Figure 9. Station 10 was investigated between 23/11 (16h10 UT) and 28/11 (20h18 UT). All the points represented on the map above are part of Station 10. The results of the physical characterisation along the whole transect can be found figure 12. Following the eruption of New Late'iki (i.e., Metis Shoal; 19.18°S, 174.87°W) one month prior to the cruise (a submarine volcano that turned into an island; Plank et al., 2020), an additional substation "Proxnov" located further north of this site (15 km from LD 10-T5) was studied as part of LD 10.

3.1 Work at Station: summary

- At each station, the 'classical' CTD and the Trace Metal Rosette (TMR) were used to perform biogeochemical sampling and sample collection for the measurement of metals and metal species associated with specific organic matter. A total of 119 cast were made. Several measurements could be made directly on board, such as oxygen, total mercury, several tracers of hydrothermal sources (CO₂, CH₄, FeII and pH), the rest of the samples were analyzed onshore.
- Zooplankton and phytoplankton nets were made at each station (trio comprising 2 x 200 µm mesh nets and 1 x 100 µm mesh net); a surface net specific to the study of Trichodesmium was also deployed at each station.
- A 'marine snow catcher' was deployed at least once per station and will allow the characterization of the export pathway for organic material exported at different depths.
- Some microturbulence profiles could be realized before the loss of the VMP instrument during a recovery.
- Three drifting moorings were carried out at the 2 long stations (LD5 (5 days) & LD10 (4 days));, see Figure 2) with a series of instruments installed on the line (from surface to 1000 m depth) allowing both physical measurements and the collection of material exported for further biogeochemical, microbiological, molecular and image processing as the quantification of the remineralization of this material. In addition a drifting mooring was deployed on a shorter timescale (3 days) at SD 8 to deploy only the RESPIRE traps.
- One fixed mooring was installed at SD12 comprising several instruments to cover an annual cycle of exported material; this mooring was successfully recovered in november 2020 (TONGA RECUP <https://campagnes.flotteoceanographique.fr/campagnes/18001357/> on board R/V Alis).

- Sediment core sampling was carried out in 5 stations, both to characterize the chemical composition of recent sediments, its grain size distribution and mineralogy but also in collaboration with the project Pourquoi Pas les Abysses/ eDNAbyss (Sophie Arnaud - Haond (IFREMER)) to identify the genetic diversity characterizing the different provinces crossed.

- Multibeam echo sounder surveys were carried out over the 2 volcanoes targeted in our campaign in order to use the acoustic data for both a fine survey of the topography and anomalies in the water column for the visualization of possible plumes of hydrothermal fluids.

- In addition to these recurrent works at stations, we have continuously characterized the surface water and the lower atmosphere: three instruments permanently connected to the surface continuum of the Atalante (TSG) have made it possible to characterize plankton, its genetic diversity (in particular the diazotrophs organisms) and photosynthetic activity, primary and secondary aerosol emissions. Intensive monitoring was also performed on this surface continuum by discrete sampling along some part of the transect to measure primary production, nutrient concentrations.

- two minicosms experiments (8 x 300 L) were carried out (at LD5 and LD10) in a clean room container in order to test the impact of a gradient of hydrothermal fluids on surface planktonic communities. -

-Several other process experiments were performed (see below)

- Several autonomous instruments were launched during the TONGA cruise: 2 BG ARGO floats, 5 ARVOR floats (<https://fleetmonitoring.euro-argo.eu/dashboard?Status=Active,Inactive&Cruise=TONGA>) and 20 SVP buoys, that allowed to contextualize the work areas after our campaign.

- Supporting data. Throughout the campaign, we were assisted by our colleagues on land for the choice of volcano sites, mooring deployments, for the choice of launching of autonomous instruments and for the characterization of the dynamics of the zones studied (in particular with the help of the simulations using the Ariane model and the Software Package for an Adaptive Satellite-based Sampling for Ocean campaigns (SPASSO). The valuable help of our colleague Carla Scalabrin for the interpretation of multibeam echosounder survey data is also noteworthy.

- Communication. A special effort was made to communicate to general public during the campaign. A director (Hubert Bataille IRD, hubert.bataille@ird.fr) was on board and in collaboration with a colleague on land (Julia Uitz, LOV julia.uitz@imevmer.fr), short videos and tweets were made very regularly, relayed by institutes and various laboratories. A total of 41 tweets and 5 videos have been posted. A 26' was launched in October 2020 visible here: French Version <https://www.youtube.com/watch?v=e5kAd0i6Dck> and English Version: <https://www.youtube.com/watch?v=UeABf-cVR-k>, with dissemination on the websites of the various institutes (IRD, CNRS, IFREMER). All images posted on the twitter account are available by mentioning the copyright @Hubert_Bataille @ird_fr

The site and the logo were designed by Thomas Jessin for the project.

- Project website: <http://tonga-project.org/web/>
- Twitter account: <https://twitter.com/tongaproject>

- Outreach. In the framework of the MonOceanet Moi project, the two BG ARGO floats launched during TONGA have been adopted by students from 2 schools (one in Abu Dhabi and one in Nouméa).

<http://www.monoceanetmoi.com/web/index.php/fr/adopt-a-float>. This 'adoption' was the occasion for the TONGA Pls to initiate the two classroom about ocean science in general and TONGA project in particular.

Table 1. Correspondance between stations and the three types of CTDs performed during TONGA.

TYPE	CAST	Station LABEL	YEAR	MONTH	DAY	HOUR	MIN	LAT_DEG	LAT_MIN	LONG_DEG	LONG_MIN
CTD	2	SD 1	2019	11	3	0	36	-21	1.8	172	10.84
CTD	3	SD 1	2019	11	3	3	32	-21	1.46	172	10.36
CTD	4	SD 1	2019	11	3	8	30	-21	0.5	172	9.23
CTD	5	SD 2	2019	11	4	19	5	-20	32.25	175	48.71
CTD	6	SD 3	2019	11	6	16	8	-20	31.84	-179	31.67
CTD	7	SD 3	2019	11	6	21	11	-20	31.33	-179	31.42
CTD	8	SD 4	2019	11	7	19	13	-20	30.24	-177	8.25
CTD	9	SD 4	2019	11	7	21	50	-20	30.27	-177	8.32
CTD	10	LD 5 T1	2019	11	9	16	59	-21	9.55	-175	54.29
CTD	11	LD 5 T1	2019	11	11	21	58	-21	9.53	-175	54.28
CTD	12	LD 5 T1	2019	11	12	0	4	-21	9.54	-175	54.28
CTD	13	LD 5 T1	2019	11	12	3	34	-21	9.54	-175	54.26
CTD	15	LD 5 T2	2019	11	12	23	26	-21	9.52	-175	50.52
CTD	18	LD 5 T3	2019	11	13	8	53	-21	9.28	-175	45.73
CTD	19	SD 6	2019	11	15	19	43	-20	41.22	-174	22.8
CTD	20	SD 6	2019	11	16	0	12	-20	41.2	-174	22.69
CTD	21	SD 7	2019	11	16	17	0	-20	30	-172	0.01
CTD	22	SD 7	2019	11	16	22	23	-20	29.9	-171	59.79
CTD	23	SD 7	2019	11	16	23	34	-20	29.92	-171	59.82
CTD	24	SD 8	2019	11	18	17	32	-20	23.37	-166	25.81
CTD	25	SD 8	2019	11	19	20	5	-20	23.06	-166	25.72
CTD	26	SD 8	2019	11	21	5	16	-20	24.23	-166	35.88
CTD	27	SD 9	2019	11	25	7	13	-19	15.86	-174	53.63
CTD	28	LD 10 T5	2019	11	25	17	56	-19	25.52	-174	57.89
CTD	29	LD 10 T5	2019	11	25	19	7	-19	25.52	-174	57.88
CTD	30	LD 10 T5	2019	11	25	20	33	-19	25.52	-174	57.89
CTD	31	LD 10 T5	2019	11	25	21	10	-19	25.52	-174	57.89
CTD	34	LD 10 T1	2019	11	27	20	12	-19	33.6	-175	11.4
CTD	35	LD 10 T1	2019	11	27	21	19	-19	33.46	-175	11.38
CTD	36	SD 11	2019	11	29	2	14	-19	31.24	-177	3.07
CTD	37	SD 11	2019	11	29	3	49	-19	31.25	-177	3.12
CTD	38	SD 11	2019	11	29	4	18	-19	31.23	-177	3.11
CTD	39	SD 12	2019	11	29	19	55	-20	42.03	-177	51.23
CTD	40	SD 12	2019	11	30	0	21	-20	42.02	-177	51.22
CTD	41	SD 12	2019	11	30	0	55	-20	41.99	-177	51.23
TMR	2	SD 1	2019	11	2	23	23	-21	1.73	172	10.78
TMR	3	SD 1	2019	11	3	4	13	-21	1.39	172	10.29
TMR	4	SD 2	2019	11	4	18	16	-20	32.24	175	48.79
TMR	5	SD 2	2019	11	5	2	43	-20	32.62	175	48.65
TMR	6	SD 2	2019	11	5	4	45	-20	32.55	175	48.54
TMR	7	SD 3	2019	11	6	17	17	-20	31.53	-179	31.43
TMR	8	SD 3	2019	11	6	19	2	-20	31.49	-179	31.35
TMR	9	SD 4	2019	11	7	20	47	-20	30.19	-177	8.26
TMR	10	SD 4	2019	11	8	0	5	-20	30.25	-177	8.3
TMR	11	LD 5 T5	2019	11	9	15	6	-21	9.54	-175	54.29
TMR	12	LD 5 T5	2019	11	11	4	12	-21	9.26	-175	44.69
TMR	13	LD 5 T5	2019	11	11	19	16	-21	9.55	-175	54.28
TMR	14	LD 5 T1	2019	11	11	19	44	-21	9.5	-175	54.28
TMR	15	LD 5 T1	2019	11	12	19	47	-21	10.57	-175	56

TMR	16	LD 5 T2	2019	11	12	21	39	-21	9.52	-175	50.51
TMR	17	LD 5 T3	2019	11	13	8	7	-21	9.27	-175	45.74
TMR	18	LD 5 T4	2019	11	13	20	56	-21	9.29	-175	45.08
TMR	19	St 6	2019	11	15	21	2	-20	41.21	-174	22.72
TMR	20	St 6	2019	11	15	22	53	-20	41.21	-174	22.72
TMR	21	St 7	2019	11	16	18	45	-20	30.02	-171	59.93
TMR	22	St 8	2019	11	18	15	22	-20	23.37	-166	25.83
TMR	23	St 8	2019	11	19	19	23	-20	23.29	-166	25.79
TMR	24	St 8	2019	11	19	21	45	-20	23.06	-166	25.72
TMR	25	St 8	2019	11	19	22	51	-20	23.15	-166	25.92
TMR	26	St 8	2019	11	20	22	17	-20	24.44	-166	35.67
TMR	27	St 8	2019	11	21	17	6	-20	24.47	-166	41.5
TMR	28	LD 10 T1	2019	11	24	0	40	-19	24.83	-175	7.61
TMR	29	LD 10 T1	2019	11	24	6	49	-19	24.89	-175	7.59
TMR	30	LD 10 T2	2019	11	24	19	25	-19	24.96	-175	3.15
TMR	31	LD 10 T3	2019	11	26	6	7	-19	25.44	-174	58.97
TMR	32	LD 10 T5	2019	11	26	18	17	-19	25.5	-174	57.86
TMR	33	LD 10 T5	2019	11	26	20	10	-19	25.51	-174	57.89
TMR	35	St 11	2019	11	29	3	0	-19	31.28	-177	3.12
TMR	36	St 11	2019	11	29	6	19	-19	31.17	-177	3.15
TMR	37	St 12	2019	11	29	21	22	-20	42	-177	51.23
TWO	1	LD 5 T5	2019	11	9	4	11	-21	9.12	-175	44.45
TWO	2	LD 5 T5	2019	11	9	4	55	-21	9.19	-175	44.58
TWO	3	LD 5 T5	2019	11	9	5	32	-21	9.27	-175	44.66
TWO	4	LD 5 T5	2019	11	9	6	2	-21	9.27	-175	44.66
TWO	5	LD 5 T5	2019	11	9	6	26	-21	9.3	-175	44.73
TWO	6	LD 5 T5	2019	11	9	7	15	-21	9.39	-175	44.92
TWO	7	LD 5 T5	2019	11	10	19	30	-21	9.28	-175	44.67
TWO	8	LD 5 T5	2019	11	10	21	40	-21	9.26	-175	44.68
TWO	9	LD 5 T5	2019	11	10	23	39	-21	9.26	-175	44.68
TWO	10	LD 5 T5	2019	11	11	0	43	-21	9.27	-175	44.68
TWO	11	LD 5 T5	2019	11	11	2	20	-21	9.26	-175	44.69
TWO	12	LD 5 T5	2019	11	11	3	34	-21	9.26	-175	44.69
TWO	14	LD 5 T4	2019	11	13	19	47	-21	9.29	-175	45.08
TWO	16	LD 5 T4	2019	11	14	21	11	-21	9.28	-175	44.68
TWO	17	St 8	2019	11	20	20	17	-20	24.33	-166	35.57
TWO	18	St 8	2019	11	20	21	37	-20	24.61	-166	35.7
TWO	19	St 8	2019	11	21	2	42	-20	24.4	-166	35.82
TWO	20	St 8	2019	11	21	3	29	-20	24.33	-166	35.82
TWO	21	St 9	2019	11	23	6	4	-19	30.85	-173	37.78
TWO	22	LD 10 T5	2019	11	23	21	35	-19	25.14	-174	57.55
TWO	23	LD 10 T5	2019	11	23	22	41	-19	25.16	-174	57.54
TWO	24	LD 10 T1	2019	11	24	1	23	-19	25.05	-175	7.59
TWO	25	LD 10 T2	2019	11	24	18	2	-19	24.95	-175	3.17
TWO	26	LD 10 T2	2019	11	24	20	39	-19	24.96	-175	3.15
TWO	35	LD 10 T3	2019	11	26	1	16	-19	30.6	-174	58.76
TWO	36	LD 10 T3	2019	11	26	4	30	-19	25.36	-174	58.97
TWO	37	LD 10 T5	2019	11	26	19	18	-19	25.51	-174	57.89
TWO	38	LD 10 T5	2019	11	26	21	11	-19	25.51	-174	57.89

5. DETAILED WORK PERFORMED AT SEA AND PRELIMINARY RESULTS

Only the names of the people on board are mentioned in the following section. A table with all the collaborators on land is provided at the end of this document.

4.2 Physical environment

4.2.1 CTDs

(Vincent Taillandier, LOV)

Three underwater units (CTDs) have been deployed to acquire continuous vertical profiles of different types of parameters. The three systems collected pressure, temperature, salinity, and dissolved oxygen. Single sensors measured pH, Eh, and turbidity in order to identify anomalies related to hydrothermal plumes. Other sensors measured down-welling solar irradiance, fluorescence of Chlorophyll-a, beam transmission at 600 nm and nitrate concentration in order to characterize the phytoplankton dynamics in the water column. Other sensors measured a series of optical properties (Chl fluorescence at four emission wave lengths, CDOM, backscattering) in order to identify the phytoplankton biomass at the community level. A total of 119 casts has been performed during the cruise. This sampling strategy is complemented with the deployment of two Biogeochemical-Argo floats, that embarked a similar suite of sensors, that will extend the collection over seasonal even inter-annual timescales.

Table 2. Summary of the different casts performed during the TONGA Cruise and the associated sensors. TMC: 'Trace Metal Clean' rosette (24 x GoFlo bottles). CTD: 'classical CTD' (24 x Niskin bottles). TWO: small classical CTD with 12 x Niskin bottles.

	T,S,O2,FCHL	IOP/AOP,NO3	PH,ORP,TURBI
SD 0	TMC_001 1500m	CTD_001 (SUNA upcast only) 1500m	
SD 1	TMC_003 bottom	CTD_003 750m	
SDt 2	TMC_006 bottom	CTD_005 (no SUNA) 190m	
SD3	TMC_008 bottom	CTD_007 1800m	
SD 4	TMC_010 + CTD_009 bottom	CTD_008 1000m	
LD 5 PANAMAX	TMC_016 bottom	CTD_015 bottom	TWO_013 30m-bottom
SD 6	TMC_020 bottom	CTD_019 bottom	
SD 7	TMC_021 bottom	CTD_023 2000m	
SD 8	TMC_026 + CTD_026 bottom	TWO_020 2000m	TWO_020 2000m
SD 9		TWO_021 2000m	TWO_021 2000m
LD 10 NOVEMBER	TMC_034 (bad T1 values) bottom	CTD_027 800m	TWO_034 bottom
LD 10b		TWO_041 1950m	TWO_041 1950m
SD 11	TMC_036 (bad T1 values) bottom	CTD_038 1900m	
SD 12	TMC_037 (bad T1 values) bottom	CTD_041 1850m	

Large scale sampling: a selection of CTD casts at every oceanographic station documented variations of hydrology (T, S, O₂, NO₃) and biogeochemistry (CHL, IOP/AOP, pH, EH) along the 20°S parallel.

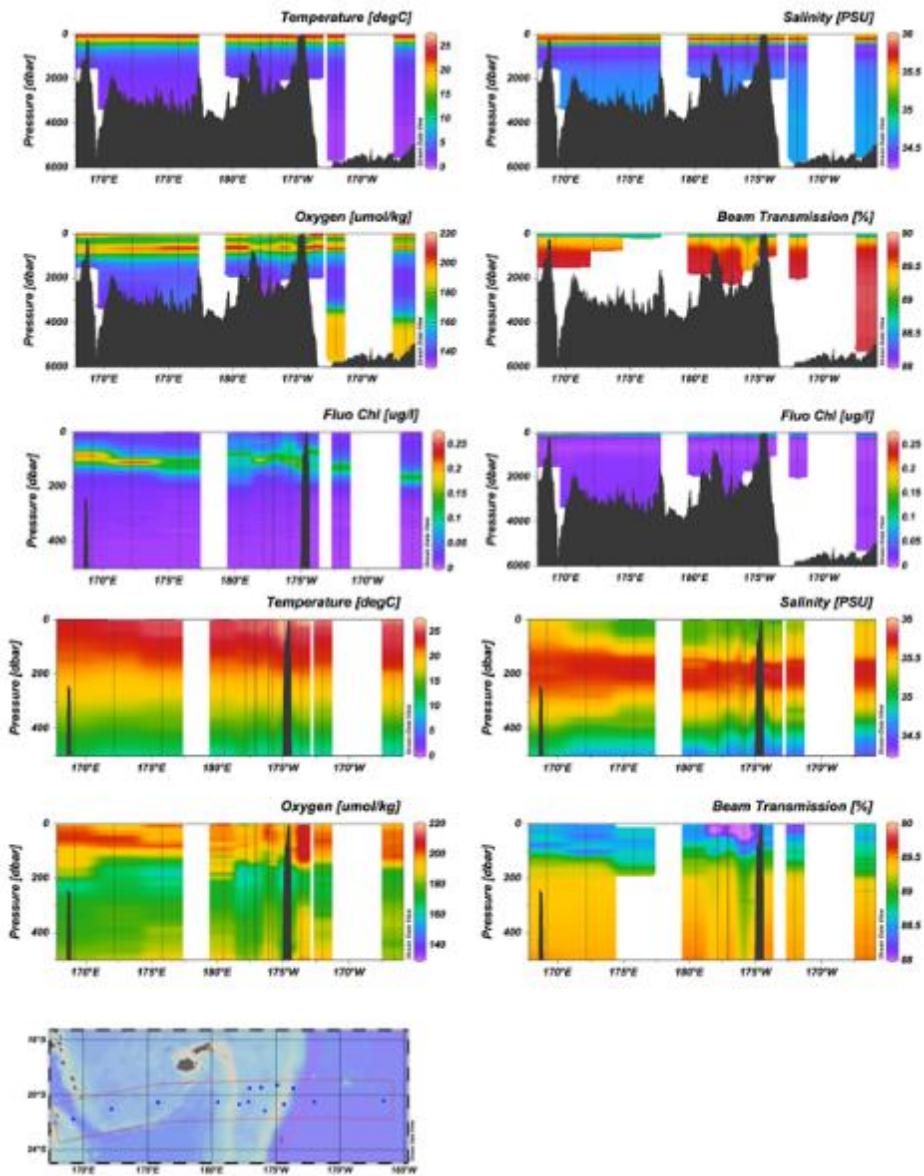


Figure 10. *Longitudinal evolution of 9 parameters measured by the sensors during a selection of casts performed during the west-east transect of the TONGA Cruise.*

Regional scale sampling: the area located of the Lau Basin between the Tonga volcanic arc and the Lau Arc provides a shallower basin in between the southern pacific gyre eastwards and the SEP productive area westwards. A more accurate survey has been performed over this basin, with a refinement towards the two hydrothermal sites under study.

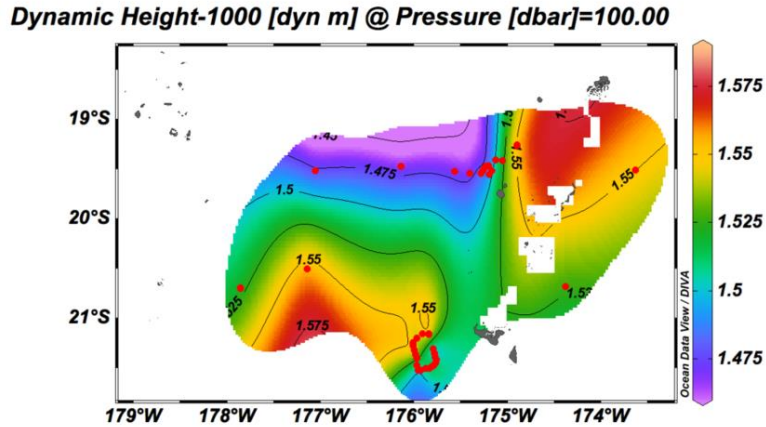


Figure 11. Dynamic height in the Lau basin from CTD and floats data

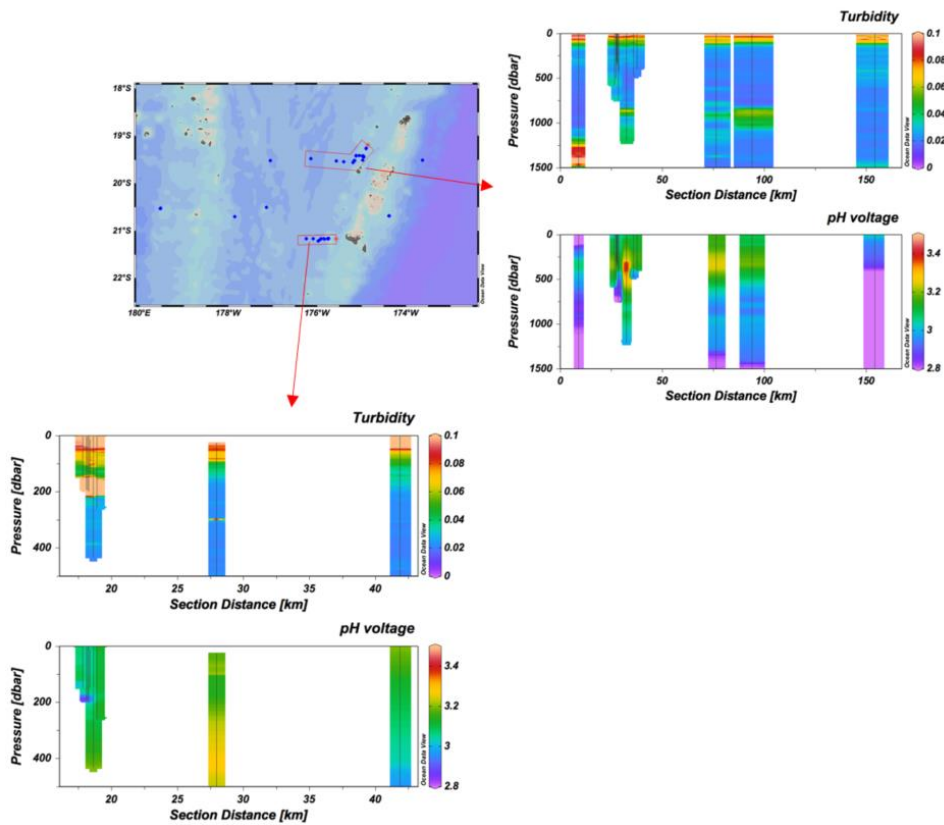


Figure 12. Representation of the intermediate stations where no sampling were performed and 'only' physical survey was allowed by CTD cast. As a result, we can provide a context to the evolution/transition between the volcanoes area and westward. (Upper figures: LD 10 environment; bottom figure: LD 5 environment).

4.2.2 Microturbulence measurements

(Jean-Michel Grisoni, IMEV (on board) and Pascale Bouruet-Aubertot and Yannis Cuypers (LOCEAN) (on land).

Turbulence measurements were performed with a vertical microstructure profiler that resolves the turbulent scales (~cm). The main purpose of the measurements in the context of TONGA is to infer turbulent diffusive fluxes of nutrients and chemical species. Turbulence is expected to be contrasted with a noticeable impact on vertical fluxes. From a physical point of view the main objective is to explain these contrasts with the identification of the dynamical processes responsible for the

onset of turbulence. **The VMP was unfortunately lost after a few profiles.** Nevertheless the data collected give evidence of a strong variability at LD 5 with enhanced turbulence for the last profiles above the volcano.

A first data-processing of these profiles has been performed, the interpretation needs further investigation with the joint analysis of CTD and ADCP data that provides the dynamical context.

An overview of the microstructure data is given in Figure 13 with vertical eddy diffusivity (K_z) and dissipation rate of turbulent kinetic energy (ϵ) zoomed in the 200m surface layer. The range of K_z values is within $[1 \times 10^{-6} - 4 \times 10^{-4}] \text{ m}^2 \cdot \text{s}^{-1}$ below 40m depth and with a mean value of $3.8 \times 10^{-5} \text{ m}^2 \cdot \text{s}^{-1}$. While K_z remains moderate, typically below $\sim 1 \times 10^{-5} \text{ m}^2 \cdot \text{s}^{-1}$, the last 4 profiles reveal an intensified turbulence, especially around 140m with K_z values intensified within at least an order of magnitude. This intensification is even stronger for ϵ , with values up to $1 \times 10^{-7} \text{ W} \cdot \text{kg}^{-1}$ to be compared with the mean value of $1.98 \times 10^{-8} \text{ W} \cdot \text{kg}^{-1}$ below 40m. The analysis of ship ADCP data gives evidence of a shear layer around 140m thus suggesting that shear instability possibly related with the volcano plume may be responsible for this layer of intensified turbulence.

Table 3. Position of the VMP profiles.

Date	N° CAST VPM	time start UTC	Time end UTC	LAT	LONG	N° ST	Depth sensor
07/11/2019	D026	00h45	01h40	-20°30.24'S	-177°8.24'W	ST4	720m
08/11/2019	D027	01h25	02h20	-21°09.55S	-175°54.29W	ST5	924m
11/11/2019	D028	03h50	04h00	-21°9.53'S	-175°54.28W	ST5	170m
11/11/2019	D029	04h01	04h11	-21°9.53'S	-175°54.28W	ST5	170m
11/11/2019	D030	04h12	04h21	-21°9.53'S	-175°54.28W	ST5	170m
11/11/2019	D031	04h21	04h30	-21°9.53'S	-175°54.28W	ST5	170m

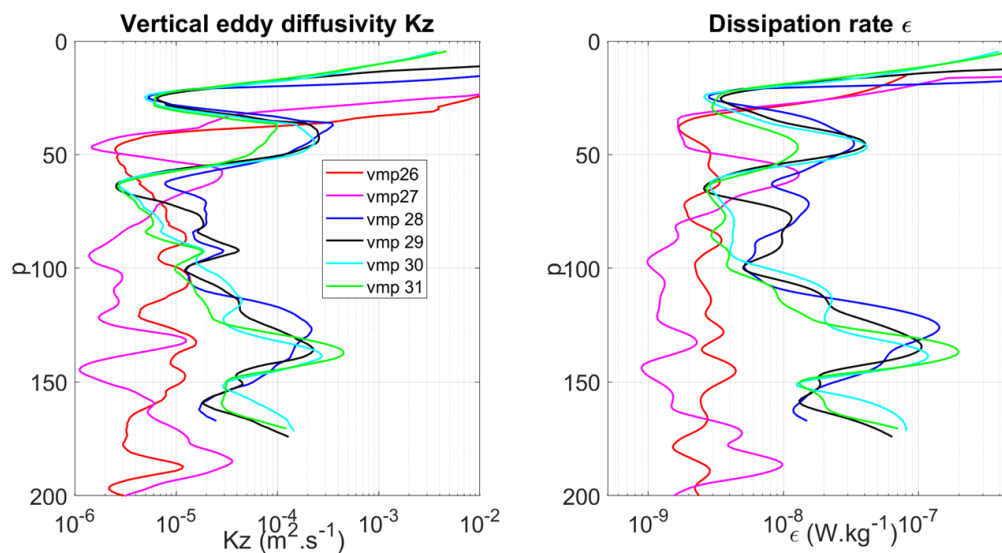


Figure 13. Vertical eddy diffusivity (K_z) and dissipation rate of turbulent kinetic energy (ϵ) obtained by the vertical microstructure profiler, zoomed in the 200m surface layer. Note that the 4 profiles vmp 28-31 were performed above Volcano 1 (LD5).

4.3 Stocks/diversity measurements (work at stations)

4.3.1 Chemical elements

4.3.1.1 Nutrients and core parameters

(Cathy Guigue, M I O)

Dissolved oxygen was measured on samples (0-bottom) on board on all the CTDs and some TMR in order to calibrate the O₂ sensors. Dissolved ammonia was measured on board (0-250 m) from samples taken from CTD. Samples for measurements of dissolved organic carbon (DOC), Fluorescent Organic Matter (FDOM) and Chromophoric Organic Matter (CDOM) have been collected in seawater and minicosms and will be analyzed back in the lab.

Table 4. Summary of the samples and analyses performed on board

Parameter	code of operation *	Where	Method
Dissolved oxygen (O ₂) in seawater for the calibration of the O ₂ sensor from the 24 bottles CTD.	Bottom CTD mainly TMC occasionally TOW when 24 btls CTD non possible	St test, St 3, St 4, St 5 (T1, T2, T5), St 6, St 7, St 8, St 10 (T1, T2, T3, T5), St 11, St 12. Calibrage optode ligne de mouillage.	Winkler Method <u>Acquired on board.</u>
Dissolved ammonia in seawater	Production CTD	St test, St 3, St 4, St 5 (T1, T2, T3 T5), St 6, St 7, St 8, St 10 (T1, T2, T3, T5), St 11, St 12.	Fluorometry <u>Acquired on board.</u>
Dissolved Organic Carbon (DOC) in seawater and minicosms	Bottom CTD mainly TOW when 24 btls CTD non possible	St 3, St 4, St 5 (T1, T2, T5), St 6, St 7, St 8, St 10 (T1, T2, T3, T5), St 11, St 12. For minicosms (see minicosm team report)	High Temperature Catalytic Oxidation (TOC-V 5000) Not on board.
Fluorescent Organic Matter (FDOM) in seawater and minicosms Chromophoric Organic Matter (CDOM) in seawater and minicosms	Bottom CTD mainly TOW when 24 btls CTD non possible	St 3, St 4, St 5 (T1, T2, T5), St 6, St 7, St 8, St 10 (T1, T2, T3, T5), St 11, St 12. For minicosms (see minicosm team report)	3D Fluorescence and absorbance Not on board.

Preliminary results.

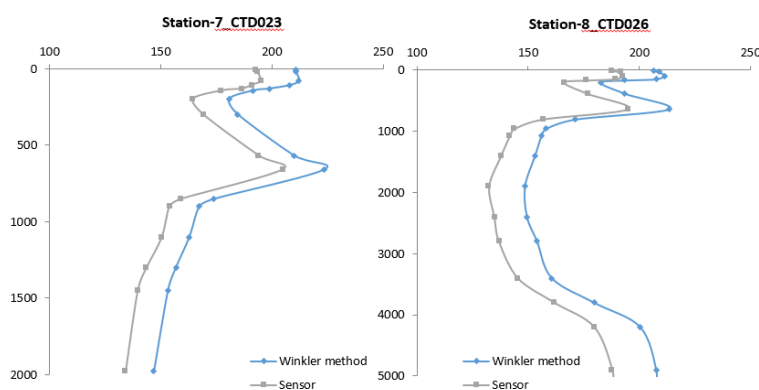


Figure 14. O₂ ($\mu\text{mol.kg}^{-1}$) measurements: comparison between discrete measurement (Winkler method on board) and O₂ sensor measurements. The sensor measurements will be calibrated thanks to the discrete measurements.

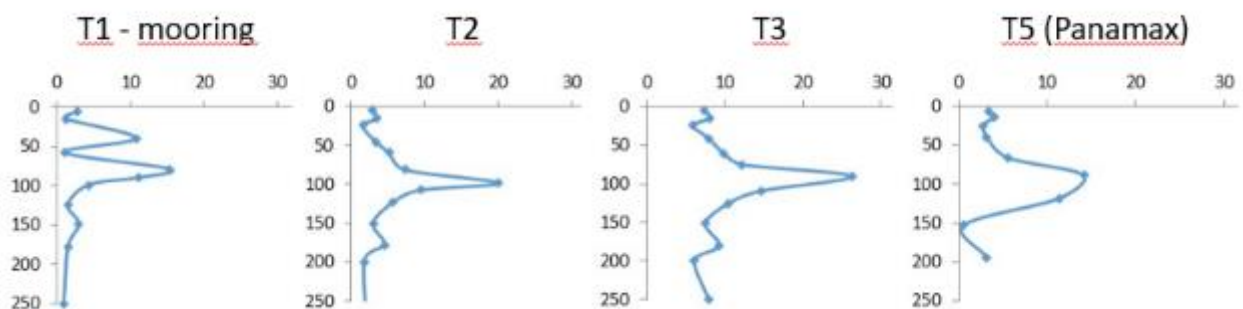


Figure 15. Evolution of ammonium concentrations (nM) along the transect between the mooring site of LD 5 and the Panamax site.

4.3.1.2 Metals

PI : Géraldine Sarthou (LEMAR). Other on-board participants: V. Arnone (Universidad de Las Palmas de Gran Canaria), D. Gonzalez-Santana (LEMAR), M. Bressac (IMAS), Guieu Cécile (LOV), Chloé Tilliette (LOV), Marie-Maëlle Desgranges (M I O), Catherine Gigue (M I O). On land participants: Planquette Hélène (LEMAR), Eva Bucciarelli (LEMAR), Whitby Hannah (LEMAR), Dulaquais Gabriel (LEMAR), François Lacan (LEGOS), Gonzalez Aridane G. (Universidad de Las Palmas de Gran Canaria), Mahieu, Leo (Univ. Liverpool), Salaün Pascal (Univ. Liverpool), Lars-Eric Heimbürger (M I O).

Characterization of metals was an important focus of the TONGA campaign and a large effort has been put to fulfill our objectives to better understand and quantify the biogeochemical cycle of metals and their sources in an area potentially influenced by shallow hydrothermal inputs. For that involvement, TONGA has been endorsed as a process study by the international program GEOTRACES and all the data acquired will be part of the database of that project, in link with the LEFE-CYBER data base.

Thus during TONGA, we studied their distributions in the dissolved and particulate phase (Fe, Mn, Cu, Co, Ni, Zn, Cd, Al, and Pb), their organic speciation (Fe and Cu), and their isotopic composition (Fe). In addition, a special attention was put on the short lived reduced Fe species, Fe(II), having an important role in the biological cycle. Indeed, hydrothermal vent sites are significant sources of Fe(II), and we identify the need to understand the present Fe(II) concentrations and the rate at which it converts to the insoluble Fe(III) phase. Finally, samples were collected to measure several species of mercury and Total Mercury and Dissolved Gaseous Mercury were directly analyzed on board.

Many laboratories are involved in all those measurements that were performed back to the labs.

Seawater were collected using a Trace Metal Clean Rosette (TMR, General Oceanics Inc. Model 1018 Intelligent Rosette), attached to a 6 mm Kevlar line. After collection, Go-Flo bottles were transferred into a clean container for sampling.



Figure 16. Trace Metal Rosette getting inside the new Clean Container where the sampling can be directly done (photo Hubert Bataille, IRD).

On each TMR cast, nutrient samples were taken to check potential leakage of the Go-Flo bottles. Analyses were performed back to the MIO laboratory.

Table 5. Comprehensive list of parameters measured from samples collected by the TMR at each station.

Station #	TMC Cast #	PTM	DTM	dFe	Fe Org Sp	Cu Org Sp	Fe isotopes	Humics A	Humics + thiois	Humics B	Fe binding	Thiols	DOM	Intercalibration	Nutrients	Fe(II)	pH	kFe	M kFe	dHg	tHg	DGM + MMHg	TM/Hg	Hg isotopes	Hg incub	DOC	Ammonium	O2
Test	1		X	X											X													
1	3	X	X	X											X						X	X	X	X				
2	6	X	X	X	X	X		X		X	X	X	X	X	X		X	X			X	X	X	X		X	X	
3	8	X	X	X	X	X		X		X	X	X	X	X	X		X	X			X	X	X	X				
4	10	X	X	X	X	X			X	X	X		X	X	X	X	X	X			X	X	X	X				
5 (T5)	11		X		X	X			X						X							X	X					
5 (T5)	12	X	X	X	X	X	X		X	X	X		X	X	X	X	X	X			X	X	X	X	X			
5 (T1)	14	X	X	X	X	X	X		X	X	X		X	X	X		X	X			X							
5 (T2)	16	X	X	X	X	X			X	X	X		X	X	X		X	X			X							
5 (T3)	17	X	X	X	X	X			X	X	X		X	X	X	X	X	X			X		X					
5 (T4)	18	X	X	X	X	X	X		X	X	X		X	X	X	X	X	X	X		X	X	X					
6	20	X	X	X	X	X			X	X	X		X	X	X		X	X			X	X	X					
7	21	X	X	X	X	X			X	X	X		X	X	X		X	X			X	X	X			X	X	
8	22		X		X	X			X						X						X		X					
8	25						X								X						X			X	X			
8	26	X	X	X	X	X			X	X	X		X	X	X	X	X	X	X		X	X	X				X	
10 (T1)	28		X		X	X			X						X						X		X					
10 (T1)	29	X	X	X	X	X			X	X	X		X	X	X		X	X			X	X	X					
10 (T2)	30	X	X	X	X	X			X	X	X		X	X	X	X	X	X			X	X	X					
10 (T3)	31	X	X	X	X	X			X	X	X		X	X	X	X	X	X			X	X	X					
10 (T5)	33	X	X	X	X	X			X	X	X		X	X	X	X	X	X			X	X	X					
10 (Prox-Nov)	34	X	X	X	X	X			X	X	X		X	X	X	X	X	X	X		X	X	X					
11	36	X	X	X	X	X			X	X	X		X	X	X		X	X			X	X	X					
12	37	X	X	X	X	X			X	X	X		X	X	X		X	X			X	X	X					

Details on the parameters to be measured:

- Dissolved trace metal concentrations (dTM)

Dissolved trace metals (Mn, Co, Ni, Cu, Zn, Cd and Pb) were filtered on-line through 0.45 µm using a polyethersulfone filter (Supor®). All samples were acidified within 24 h of collection with ultrapure hydrochloric acid (HCl, Merck, 0.2%, final pH 1.7).

Dissolved trace metals will be analysed using a preconcentration system SeaFAST coupled to a high resolution magnetic sector field inductively coupled mass spectrometer (HR-ICP-MS, Element XR) method following Tonnard et al. (2019), in the shore-based LEMAR laboratory.

- Dissolved iron (dFe)

Dissolved Fe samples were filtered on-line through 0.45 µm using a polyethersulfone filter (Supor®). All samples were acidified within 24 h of collection with ultrapure hydrochloric acid (HCl, Merck, 0.2%, final pH 1.7). They will be analysed by FIA with chemiluminescence detection (Obata et al., 1993) in the shore-based LOV laboratory.

- Iron redox speciation: Fe(II) and **and Fe(II) oxidation kinetics**

All samples were collected using a Trace Metal Clean Rosette (TMR, General Oceanics Inc. Model 1018 Intelligent Rosette), attached to a 6 mm Kevlar line. They were collected unfiltered and poured into trace-metal clean LDPE bottles. Samples for Fe(II) were collected in 60 mL bottles, kFe samples in 125mL bottles and extra water was collected in 1L bottles for multi-parametric kFe determination. Fe(II) concentrations were immediately measured on board, while samples for Fe(II) oxidation kinetics were frozen at -20°C and will be analyzed back at the QUIMA laboratory in the Universidad de las Palmas de GC. Dissolved Fe(II) was filtered in-line (0.2µm filter) and pre-concentrated for 180 seconds in a 8-HQ column (modified from Ussher et al. (2009) SOP for dissolved Fe(II) and King (1991)). Iron(II) oxidation kinetics samples will be measured on land by DIA-CL using a FeLUME system (King 1995).

- Organic speciation of Cu and Fe (Fe org sp and Cu org sp)

Samples for organic speciation of Fe were filtered on-line through 0.45 µm using a polyethersulfone filter (Supor®) and immediately frozen at -20°C. They will be analysed in the shore-based laboratory (Univ. Liverpool, UK) by a newly developed method of cathodic stripping voltammetry (Mahieu et al., in prep.).

Samples for organic speciation of Cu were filtered on-line through 0.45 µm using a polyethersulfone filter (Supor®) and immediately frozen at -20°C. They will be analysed in the shore-based laboratory (Univ. de Las Palmas de Gran Canaria) by cathodic stripping voltammetry (Campos and van den Berg, 1994).

- Fe isotopes

Sample for Fe isotopic composition were filtered on-line through 0.2 µm filter cartridges (SARTOBRAN® 300, Sartorius). All samples were acidified within 24 h of collection with ultrapure hydrochloric acid. The Fe isotopic compositions will be measured back to the shore-based laboratory (LEGOS, Toulouse, France) as described in Lacan et al. (2008 and 2010). Basically, after iron preconcentration and purification, the Fe isotopic composition will be measured with a multi-collector ICPMS.

- Humic substances and thiols (Humics A&B, thiols, Fe binding)

Samples for humic substances and thiols were filtered on-line through 0.45 µm using a polyethersulfone filter (Supor®) and immediately frozen at -20°C. The formers will be analysed in the shore-based laboratory (Univ. Liverpool, UK) by cathodic stripping voltammetry of their complexes with copper, as described by Whitby and van den Berg (2015). Voltammetric detection of iron-humic complexes directly will also be performed following Abualhaja et al. (2015). Thiols concentrations will be analysed following Leal et al. (1999).

- Dissolved organic matter (DOM)

Samples for DOM were filtered on-line through 0.45 µm using a polyethersulfone filter (Supor®). All samples were acidified within 24 h of collection with ultrapure hydrochloric acid (HCl, Merck, 0.1%, final pH 2.3) and immediately frozen at -20°C. They will be analysed back to the shored-based laboratory (LEMAR) using size-exclusion chromatography (Dulaquais et al., 2018).

- Particulate trace metals (pTM)

Particulate trace metal samples were taken from the filtration through 0.45 µm using a polyethersulfone filter (Supor®). All filters will be digested and analyzed back in LEMAR by SF-ICP-MS following Planquette and Sherrell (2012) method. Acetic acid leaches (Berger et al., 2008) will also be undertaken in order to assess the bioavailable fraction. A subset of samples will also be dedicated for SEM imaging.

- Mercury (*Total Mercury (THg), Dissolved Mercury(dHg), Dissolved Gaseous Mercury (DGM)/Methylmercury (MMHg), Total methylmercury (TMeHg), Hg isotopes*).

Our objectives were to determine Hg speciation and isotopy in the water column as well as in the hydrothermal fluids. Total Hg and DGM were analysed onboard. TMeHg, MMHg and Hg isotopes will be analysed back in the lab (MIO). In addition to seawater collected at the 12 stations, incubations were carried out at 3 stations (2 volcanoes and 1 mooring station) and sediments samples (sediment cores) at 4 stations. Rainwater, Phytoplankton and seawater sampling from minicosms and RESPIRE were also taken. THg has also been measured onboard on CTD Tow-yo. Overall THg datas range from 0,4 pM up to 20 pM. The highest THg concentrations were measured in areas with physico chemistry anomalies that can potentially come from hydrothermal fluids. THg concentrations in rainwater range from 18 pM to 103 pM.

- Intercalibration

Samples for intercalibration (dFe, dTM, Fe and Cu organic speciation, DGM, MMHg, and TMeHg) were taken at 2 different stations (St 8, cast 26 and St. 12 cast 37) following the GEOTRACES protocol.

(several of those species will also be measured in the samples from the minicosms experiment (see that section for details).

Preliminary results.

Most of the samples will be analysed back to the different laboratories. Measurements will be carried out back to the different home laboratories: LEMAR (Brest, France), LOV (Villefranche/mer), LEGOS (Toulouse, France), University of Liverpool (UK), Universidad de Las Palmas de Gran Canaria (Spain), M I O (Marseille, France).

We present here the differences observed among the filters sampled for the determination of the particulate metals that illustrate well the diversity of the amount and type of collected particles. Figure 17 compares those filters at the two volcano stations (LD 5 and LD 10), and at the oligotrophic station (SD 8 in the gyre).

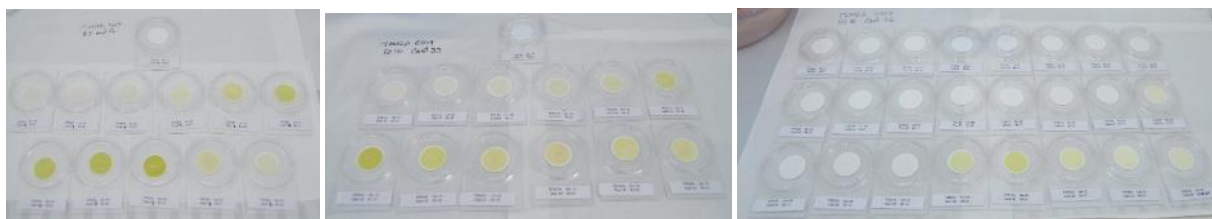


Figure 17. Filters taken at: (left) LD 5 (volcano 1), cast 17, (center) LD 10, cast 33, (right) SD 8 (gyre), cast 26

Results for total mercury (Marie-Maëlle Desgranges, M I O). On the profiles of stations 1 to 12, THg values range from 0.4 pM to a maximum of 20 pM. The highest values (>3pM) are obtained in areas of physico-chemical anomalies that could be hydrothermal plumes. On station 1 to 3 from West to East, a strong and high THg signal (4pM<THg<7pM) is measured at 700 m, 550 m and 250 m respectively. Tow-yo CTD strategy allowed to detect high THg concentrations (from 10 pM to 20 pM) at both volcano stations at the maximum acoustic signal and ProxNov station. THg water of rain water range from 18 pM to 103 pM from West to East.

4.3.1.3 Gases: Methane in the water column

(for O₂, see specific section 4.4.1.1)

(Cédric Boulard (PI) et Jean-Philippe Gac) (on board). On land participants: Laurence Garczarek, Estelle Bigeard, (UMR7144/Roscoff)

Methane (CH₄) is the second greenhouse gas after CO₂ with a radiative power 20 to 30 times more effective than CO₂ on a 100-yr period. At the global scale, oceans are considered as a minor source of CH₄ but marine contribution has proven difficult to quantify with great certainty due to the scarcity of data available and the inability to capture the spatiotemporal dynamics of CH₄ emissions. In the open ocean, CH₄ is supersaturated relative to atmospheric concentrations, which is known as the ocean methane paradox. Several mechanisms have been proposed to explain this paradox but there is still a lack of data on the different ways of CH₄ production, especially in the mixed layer, as well as on the optimal environmental conditions. The objectives of the study are 1) to evaluate the spatiotemporal dynamics of CH₄ concentrations in the mixed layer, 2) to track the sources of CH₄ and 3) to identify the planktonic populations and the metabolic ways of CH₄ production.

During the TONGA cruise, we carried out water sampling for the measurement of methane concentrations (on board and on shore using a gas chromatograph) and the stable carbon isotopic signature of the dissolved CH₄ as well as CO₂ and DIC in the mixed layer.

Samples for CH₄ measurements and $\delta^{13}\text{C-DIC/CH}_4$ in the mixed layer were taken on all 0-400m classic CTD-rosette casts at 5, 15, 25, 50, above DCM, in the DCM and below DCM water depth in coordination with the sampling for metagenomics, metatranscriptomics and metabarcoding.

The technique for CH₄ determination on board is based on headspace extraction followed by GC analysis. The onboard GC was fitted with an HID detector allowing the detection of permanent gases at less than 0.1 ppmV detection limits. On shore, the duplicates will be analysed using the same technique but with another detector to confirm the data obtained on board.

CH₄ and CO₂ δ¹³C and CH₄ δH will be analyzed using coupled GC – Isotope Mass Ratio Spectroscopy (GC-IRMS) available at the IUEM (Brest). The carbon isotopic signature will allow the determination of the source of CH₄ as well as to evaluate the biogeochemical processes, i.e. mixing, consumption or production.

Table 6. Summary of the sampling performed during TONGA for CH₄ concentrations and δ¹³C-DIC analysis.

Date	CTD number	Station	Max depth	Parameters
01/11/2019	CTD-1	Test	4800	18xCH ₄ , Li/Sr
	PROD			6xδ ¹³ C
03/11/2019	CTD-2	Station 1	3623	18xCH ₄ , Li/Sr
	PROD			6xδ ¹³ C
06/11/2019	CTD-6	Station 3	1912	27xCH ₄ , Li/Sr
	PROD			10xδ ¹³ C
06/11/2019	CTD-7	Station 3	1912	15xCH ₄ , Li/Sr
	DEEP			5xδ ¹³ C
07/11/2019	CTD-8	Station 4	2400	47xCH ₄ , Li/Sr
	PROD			9xδ ¹³ C
11/11/2019	CTD-11	Station 5	2094	21xCH ₄ , Li/Sr
	PROD	Mooring J2		7xδ ¹³ C
12/11/2019	CTD-15	Station 5.5	1678	24xCH ₄ , Li/Sr
	DEEP	T2		12xδ ¹³ C
12/11/2019	CTD-16	Station 5	2373	8xCH ₄ , Li/Sr
		"Vincent"		4xδ ¹³ C
13/11/2019	CTD-18	Station 5	2373	14xCH ₄ , Li/Sr
	PROD	T3		7xδ ¹³ C
16/11/2019	CTD-20	Station 6	1038	14xCH ₄ , Li/Sr
	PROD			7xδ ¹³ C
16/11/2019	CTD-21	Station 7	2700	14xCH ₄ , Li/Sr
	PROD			7xδ ¹³ C
21/11/2019	TWO-17	Station 8	5382	16xCH ₄ , Li/Sr
		Gyre		8xδ ¹³ C
25/11/2019	CTD-28	Station 10	303	14xCH ₄ , Li/Sr
	PROD	Simone		7xδ ¹³ C
27/11/2019	CTD-34	Station 10	1926	14xCH ₄ , Li/Sr
	PROD	Mooring		7xδ ¹³ C
28/11/2019	CTD-36	Station 11	2540	14xCH ₄ , Li/Sr
				7xδ ¹³ C
29/11/2019	CTD-39	Station 12	1978	14xCH ₄ , Li/Sr
	PROD			7xδ ¹³ C

Preliminary results: First results indicate a systematic oversaturation of the mixed layer (150 to 300%) along the TONGA cruise track. CH₄ maximum occurs in the DCM.

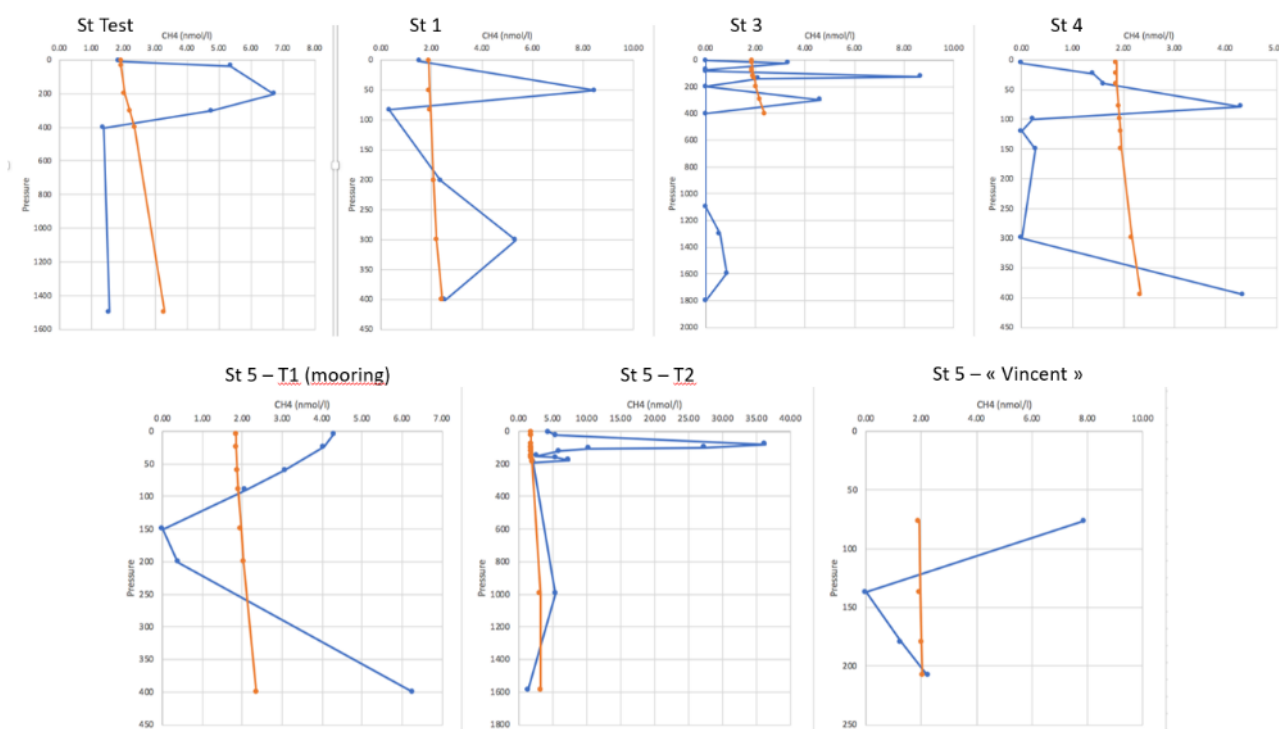


Figure 18. Vertical profiles of CH₄ concentrations (nmol.l⁻¹) for the first 7 stations during the TONGA cruise. The red line indicates the saturation concentration of CH₄ relative to atmospheric concentrations.

4.3.1.4 Physical and Chemical tracing of hydrothermal plumes

(Cédric Boulard AD2M, Vincent Taillandier LOV et al.)

An important phase of the characterisation of the hydrothermal fluids was done thanks to the deployment of a small frame CTD-rosette fitted with 12 NISKIN bottles and various in situ physical and chemical sensors to detect the presence of chemical and physical/optical anomalies related to hydrothermal activity in the water column. Several physical and chemical tracers were used: conductivity, temperature, turbidity, redox potential (Eh), pH, CH₄, and ³He (this last parameter will be determined back in the lab). Hydrothermal tracers can be detectable some hundreds of meters above and a few kilometers around any given vent source.

All operations were conducted using a 12-Niskin bottle rosette frame onto which were mounted 2 Turbidimeters (Seapoint Turbidity Meters), 1 pH sensor (AMT GmbH) and 1 Eh sensor (AMT GmbH), as well as an altimeter for seafloor detection. Note that pH and Eh sensors were acquired through the LEFE action 'MEMESTRA' and belong to UMR 7144 (Station Biologique de Roscoff). The full CTD-rosette package was provided by the DT-INSU (Parc océanographique hauturier), which also provided the assistance for interfacing Eh and pH sensors on the CTD-rosette. All sensors were interfaced to a SBE9+ (Seabird Electronics). The rosette frame was hung on the coaxial seacable using a shackle, while connection between the ship's cable and the CTD-rosette was realized par the ship's engineers. The other end of the seacable was connected to the SBE11+ deck unit interfaced to a PC. Seasave Software provided by Seabird Electronics was used for real-time data acquisition and display of the down- and upcasts data. **Niskin bottles were fired during upcasts at different levels in the water column, whenever an anomaly (T, S, turbidity and Eh) appeared on the screen.**

The CTD-rosette was deployed in 'pseudo'-tow ways, either as vertical casts or as towed casts ('tow-yos' at 1,5 kn max). During vertical casts, the CTD-rosette was lowered in the water column at a speed of 1 m/sec or less to the deepest point. There, the depths for water sampling were chosen based on turbidity and Eh anomalies displayed on the screen. Bottles were fired on the way up step by step.

Tow-yos consisted in lowering and raising the CTD-rosette between a constant set depth and a few meters above the seafloor while the ship moved along a transect at a maximum speed of 0.4 knot.

Physico-chemical characteristics of the water column as well as the sample bottle files were extracted using SBE-processing software, producing .cnv files, which are available on the cruise's hard drive. Note that for these specific operations, CTD casts were named TWO-XX (XX being the cast number).

Samples were taken from the Niskin bottles for the analysis of dissolved gases (CO₂, CH₄), Helium isotopes and other relevant parameters. A preliminary analysis of dissolved CO₂ and CH₄ was carried out on board using a gas chromatograph.

Table 7. Sample collection and data available for the plume survey

Date	TWO number	Start position	Max depth	Parameters
09/11/2019	TWO-1	-21.15196	111	36xCH ₄ , Li/Sr
	Volcano 1	-175.7408		12xδ ¹³ C
				3x He
09/11/2019	TWO-3	-21.15454	160	27x CH ₄ , Li/Sr
	Volcano 1	-175.7444		9xδ ¹³ C
	Panamax			1x He
09/11/2019	TWO-5	-21.1552	160	30xCH ₄ , Li/Sr
	Volcano 1	-175.74584		10xδ ¹³ C
				3x He
09/11/2019	TWO-6	-21.15802	210	36xCH ₄ , Li/Sr
	Volcano 1	-175.7515		12xδ ¹³ C
				2x He
11/11/2019	TWO-10	-21.15442	202	33xCH ₄ , Li/Sr
	Volcano 1	-175.74468		11xδ ¹³ C
				3x He
13/11/2019	TWO-14	-21.15482	254	16xCH ₄ , Li/Sr
	Volcano 1	-175.7513		8xδ ¹³ C
				1x He
24/11/2019	TWO-22	-19.41898	580	6xCH ₄ , Li/Sr
	Volcano 2	-174.95908		3xδ ¹³ C
				0x He

24/11/2019	TWO-25		1237	24xCH ₄ , Li/Sr
	Volcano 2			12xδ ¹³ C
				0x He
24/11/2019	TWO-26	-19.416	1204	10xCH ₄ , Li/Sr
	Volcano 2	-175.05248		5xδ ¹³ C
				1x He
24/11/2019	TWO-27	-19.44414	430	8xCH ₄ , Li/Sr
	VS1	-174.95692		4xδ ¹³ C
				1x He
24/11/2019	TWO-28	-19.44252	343	8xCH ₄ , Li/Sr
	VS2	-174.94788		4xδ ¹³ C
				1x He
24/11/2019	TWO-29	-19.43376	364	8xCH ₄ , Li/Sr
	VS4	-174.95622		4xδ ¹³ C
				1x He
25/11/2019	TWO-30	-19.42518	280?	8xCH ₄ , Li/Sr
	VS5	-174.96482		4xδ ¹³ C
	Maximone			1x He
25/11/2019	TWO-32	-19.41942	300?	8xCH ₄ , Li/Sr
	VS8	-174.95806		4xδ ¹³ C
				1x He
25/11/2019	TWO-34	-19.26961	1640	20xCH ₄ , Li/Sr
	November 5.7	-174.89144		10xδ ¹³ C
				1x He

The position of the TWO above the volcano at LD 10 are represented below :

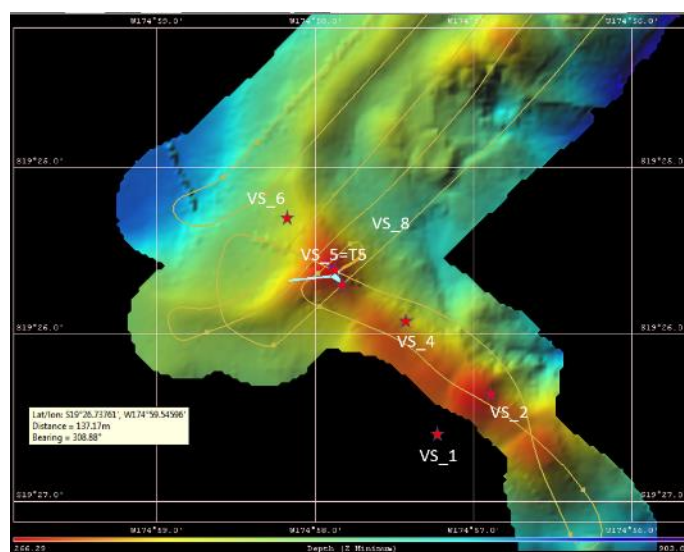


Figure 19. *Bathymetry and TOW stations performed during the cruise to determine the T5 point of the LD 10. The TOW stations reported in table 6 are reported on that map.*

Preliminary conclusions on volcanoes surveys:

LD 5. Shallow hydrothermal activity has been confirmed at volcano 1 (LD5-T5) with a strong enrichment in volatiles (CO₂, H₂S) as well as FeII in the water samples. The presence of numerous echoes indicates the presence of several sources which might be of black smoker type. The enrichment in volatiles is typical of hydrothermal fluids from arc volcanoes.

LD 10. In that volcano area, shallow hydrothermal circulation appears to have stopped, likely due to the recent eruption of the Metis-Shoal Volcano ("November" on our map). However, further exploration showed the presence of hydrothermal plumes below 1000m depth close to Metis.

Example at LD 5 - T5 (Volcano 1): clear presence of a shallow hydrothermal source.

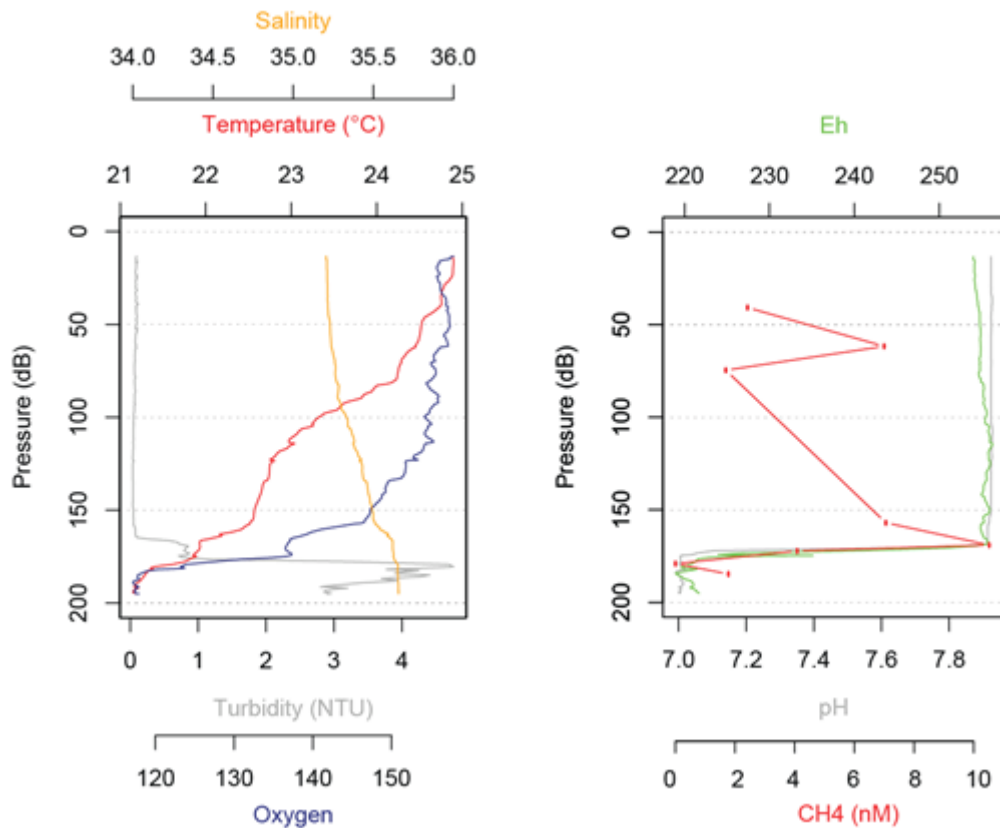


Figure 20. Vertical profiles of Temperature, salinity, turbidity, oxygen, pH, Eh and CH₄ above Volcano 1 (LD5- T5), in the strongest acoustic anomaly. **The turbidity anomaly at 170m depth correlated to Eh, pH and CH₄ anomalies indicates the presence of a hydrothermal source in the vicinity. CO₂ concentrations (not showed) were also very strong (GC detector got saturated), while discrete pH measurement confirmed a pH of 6.5 (a strong H₂S smell was also noticed in the water samples). Note a CH₄ anomaly at 60m water depth, which is not related to hydrothermal activity but is correlated to the DCM (see section 4.2.1.3).**

Example at LD10-T5 (Volcano Simone): discontinuous acoustic echoes and physical anomalies might indicate a less active hydrothermal circulation, controlled by the strong volcanic activity of the close Metis-shoal volcano.

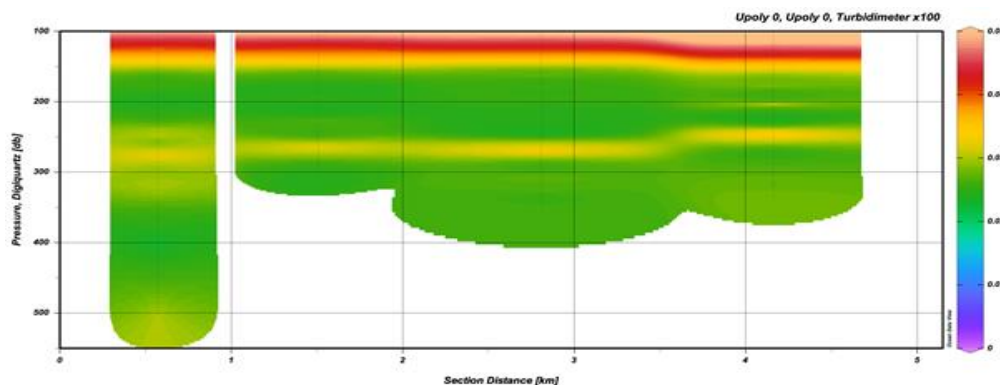


Figure 21. Turbidity section at LD10-T5 above Volcano Simone during the tow-yo like operation (TWO27 to TWO32), showing a light anomaly at 260 to 310m water depth. Further exploration of the area to find the source was unsuccessful. It appears to be widespread above the entire area. There was no correlation with CH₄, pH or Eh anomalies. This questions the origin of this anomaly, which might be the consequence of the recent eruption of the Metis-Shoal Volcano in October/November 2019 less than 10 nm from volcano Volcano Simone.

Temporal survey above LD10-T5. Here, the small CTD have been positioned right above the maximum acoustic anomaly and during 1h30, the parameters have been continuously recorded allowing to record the hydrothermal activity at very high

spatial and temporal resolution. The modification of seawater properties near by / temporary to a source emission has been caught to document the thermohaline processes that settled the hydrothermal plume before its dispersion.

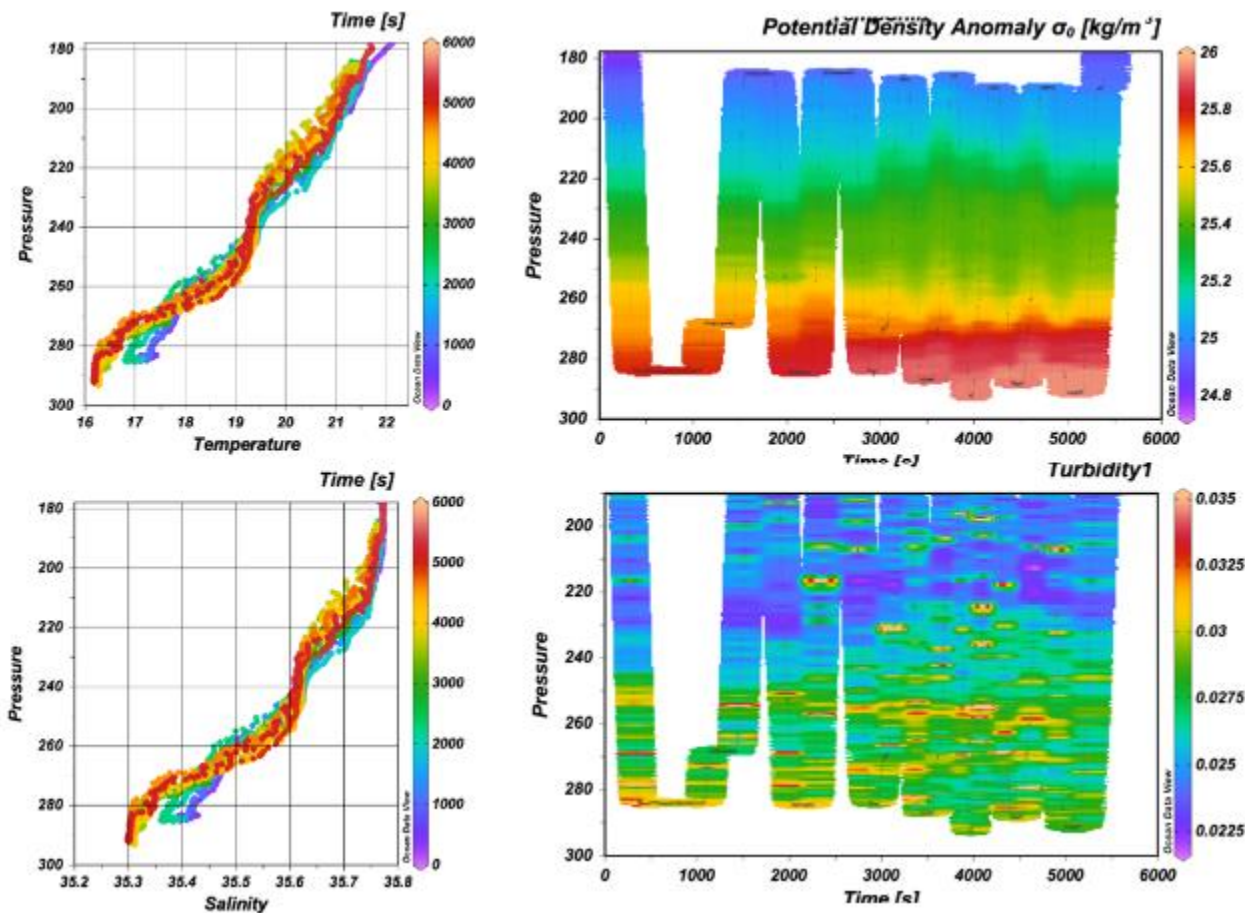


Figure 22. Temporal variability in salinity, temperature, turbidity and potential density anomaly recorded by the instruments with a fixed position of the rosette right above the main acoustic anomaly at Simone volcano (LD 10-T5).

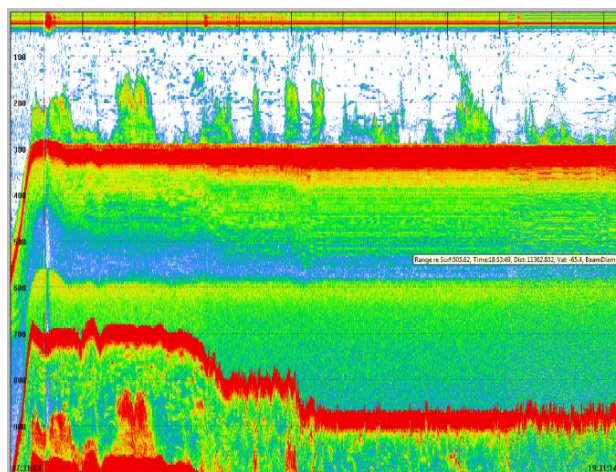


Figure 23. Print screen of the outputs of the EK60 during the time series at LD 10- T5 depicting the sporadic character of the acoustic anomaly (the boat has a fixed position).

The role of the recent eruption of the Metis Shoal volcano (with the formation of an island, see figure below) is certainly very important to explain the different observation that we were able to make above and in the vicinity of Volcano Simone. For

that reason, we decided to get as close as possible to the Metis Shoal, still showing some activity. We couldn't approach too close for obvious security reason. We have done 1 CTD profile at that station called 'NOVPROX' and 1 TMR profile.

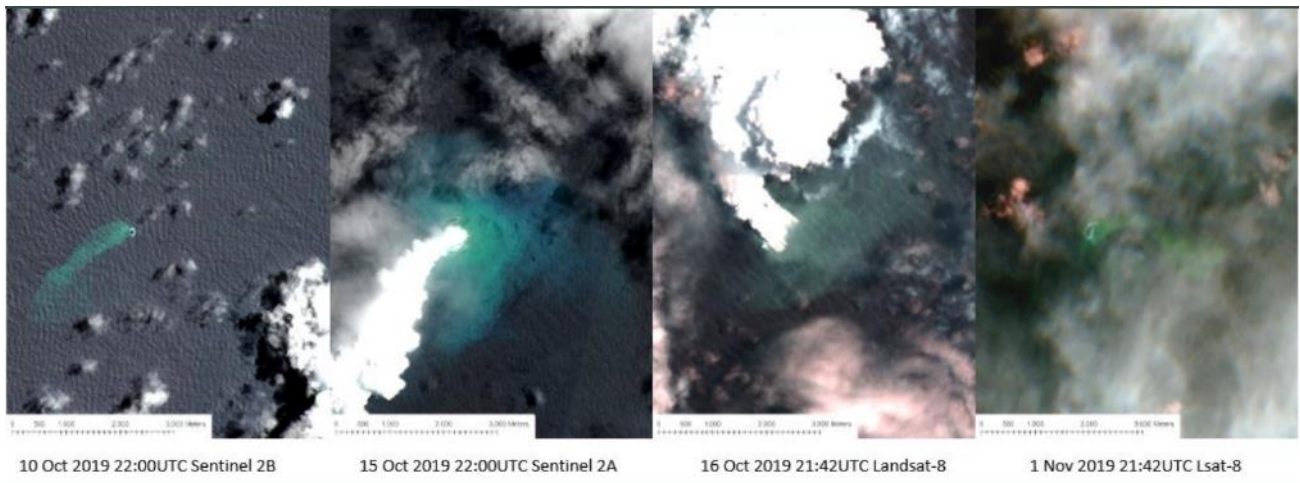


Figure 24. Satellite imagery showing the eruption of the Metis Shoal eruption that started mid-october 2019. By Nov 1 an elongated island has appeared at the main focus of activity. (source @geonet). The island formed was visible from board and sporadic emissions has been seen when we had the chance to approach the site on November 27 2019.

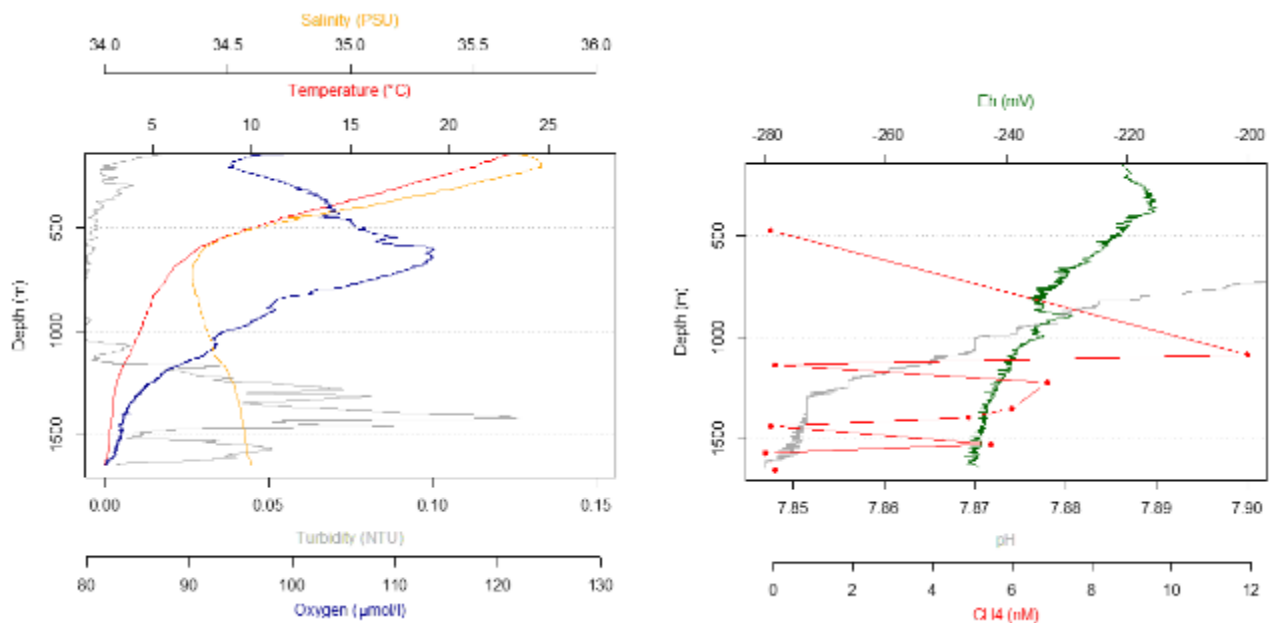


Figure 25. Vertical profiles of Temperature, salinity, turbidity, oxygen, pH, Eh and CH_4 above the station called 'NOVPROX', 5.7 miles south of the Metis Volcano that erupted on 16th of Oct. 2019. The same small turbidity anomaly was found at 270m water depth with no anomaly of CH_4 , Eh or pH, confirming that it cannot be from hydrothermal origin. However, strong turbidity anomalies correlated to CH_4 anomalies were found at 1100m, 1400 and 1500 water depth, which indicate the presence of hydrothermal activity nearby, and possibly at least 3 deep hydrothermal sources.

4.3.2 Diversity within the planktonic communities

(Estelle Bigeard (AD2M) and Mathilde Ferrieux (AD2M) on board; Roscoff team on land).

The diversity within the planktonic communities was investigated by using a combination of metaomics approaches. The link between in situ CH_4 concentration and the marine communities (genomes) was also investigated.

Table 8. Parameters to be measured

Parameter	code of operation *	Where	Method
Flow cytometry samples	CTD production	All stations (SD1 to 12, LD 5-T1-T5, LD10-T1-T5) + rain samples (2 samples)	Fixation with gluta and DMSO at 12 depths.
MetaTranscriptomics	CTD production	All stations (SD1 to 12, LD 5-T1-T5, LD10-T1-T5)	20L filtration on 2 size fractions (3µm and 0.2µm) within the 15minutes after the sampling time at 1 depth at station Type 1, up to 4 depths at V1 and MAXIMONE, ST10-T5
MetaGenomics	CTD production	All stations (SD1 to 12, LD 5-T1-T5, LD10-T1-T5)	20L filtration on 3 size fractions (3µm, 0.2µm, 30kDa) at 1 depth at station Type 1, up to 4 depths at V1 and Simone
MetaBarcode (3 size fractions)	CTD production	All stations (SD1 to 12, LD 5-T1-T5, LD10-T1-T5)	5L filtration on 3 size fractions (3µm, 0.2µm, 30kDa) at 6 depths
Culture isolates	CTD production	SD06, SD07, SD08, LD 5-T5, LD 10- T5, SD11, SD12	Enrichment experiments using different media

4.3.3 Essential traits of Plankton and elemental (iron, Lithium) concentrations and quotas

Plankton nets have been done at each station and many parameters will be measured both to identify the natural assemblage both for phytoplankton and zooplankton but also to measure a number of chemical elements to characterize metal quotas in the contrasted environments visited, for example.

Table 9. Recap of the plankton nets samples.

stations	sampling time (local)	
	local	UTC
3	1:00 PM	1:00 AM
4	2:00 PM	2:00 AM
5 t1	2:00 PM	2:00 AM
5 t2	1:00 PM	1:00 AM
5 t4	5.30 pm	5.30 am
6	9.30 am	9.30 pm
7	11.00 am	11.00 pm
8	2.30 pm	02.30 am
10 t5	10.30 am	10.30 pm
10 t3	5.30 pm	5.30 am
10 t1	1.15 pm	1.15 am
11	1.50 pm	1.50 am
12	2.30 pm	2.30 am

Recap of work to be done on samples:

- **zooplankton:**

Work to be performed by Dr. Lavenia Ratnarajah, University of Liverpool. Each station, between 50 ml up to 400 ml of sample collected was filtered on board by Chloé Tilliette and freeze. Those samples have been send to Lavy and she will do the following: (1) Identify the zooplankton collected ; (2). Measure trace metals and P, N and C in these zooplankton (and if there's any faecal pellet as well) by size class ; (3) Compare the stoichiometry in the zooplankton with other stoichiometry acquired by other groups on board.

- **Phytoplankton:**

Work to be performed by Karine Leblanc, MIO. Analyses will include taxonomy, state of cells, and C biomass estimates for key plankton functional groups (diatoms, microplanktonic diazotrophs, dinoflagellates, rhizaria). This work is linked with the sampling performed using other tools (Marine Snow catcher, bottlenet, traps, see section 4.5.3. The overall aim is to describe via the use of different collecting devices the planktonic community from the surface layer to deep layers, to try to link the surface phytoplankton community to the deep C export. We collected microplankton in the surface layer using a phytoplankton net (35 µm mesh size) and we deployed a bottle-net (20 µm mesh size) for deep layer particle concentration at all short and long study sites. In parallel, samples were collected both from marine snow catcher and gel traps, in order to determine the contribution of microplankton, in particular siliceous organisms, to the sinking particle flux.

- **Phytoplankton and Zooplankton:**

Work to be performed by Nathalie Vigier, LOV. Lithium concentrations of hot hydrothermal fluids are two orders of magnitude higher than in seawater. Similarly as for other trace metals (such as copper), lithium can act as an essential element at low level but can be toxic at high levels. Our team has recently shown that lithium isotopes measured in marine organisms are sensitive to environmental parameters and metabolic activity (Thibon et al., 2023). Yet there is no measurements of Li concentration, nor of Li isotopes for phytoplanktonic and zooplanktonic species. Based on the Tonga sampling strategy, we want to explore the possibility to measure lithium and its isotopes in the natural planktonic biomass collected along a gradient between seawater and a hot volcanic fluid. Thus, at each station, Chloé Tilliette (LOV) took both an aliquote of the zooplankton net and of the phytoplankton net that were filtered and dried (15 samples). The filters were then stored at ambient temperature. In addition, 4 filters were also recovered from 10 L of waters filtration along the gradient between SW and the hydrothermal fluid (200m). Finally, during the minicosms binary mixing experiments, small filters were collected for lithium. Back to the lab, Nathalie Vigier, Fanny Thibon and Lucas Weppe will do the following analysis: sequential leaching, Li concentrations, Li purification in clean lab and Li isotope measurements when possible results will be compared to similar measurements performed in the filtered waters by Valerie Chavagnac (GET) and our team, and interpreted with regards to the other biological and environmental data.

Work to be performed by Fabien Lombard, LOV. Phyto and zooplankton response to various nutrients and metallic inputs could be highly variable and ranging from toxicity to enhancement of growing ability. All in one, profound changes on phyto and zooplanktonic assemblages are awaited within the contrasted environments sampled during the TONGA cruise. By the mean of Quantitative Imaging Methods, we will study the full community of plankton and its variation in some essential traits (size, shape, coloniality etc). Samples from each station were preserved for their analysis back in the lab (the Flowcam for the microplankton compartment and the ZooScan for the mesoplankton compartment). The plankton images using these two methods will be analyzed using ecotaxa software. The results will be analyzed in view of the environmental data acquired simultaneously (using multivariate analysis methods). The results obtained at stations will also be analysed with regard to the results obtained during manipulations in mesocosms (see specific section).

4.3.4 Phytoplankton communities and bio-optics at stations

(Celine Dimier (IMEV), Vincent Taillandier (LOV))

An optical package (Eco FLBB CD (fChl, bbp, fCDOM and C-Rover); Eco 3X1M sensor) is mounted on CTD-rosette devices to acquire optical data simultaneously to discrete biogeochemical and diversity measurements (Phytofloat protocole). These measurements are accompanied by discrete sampling (3 depths) of seawater from the Niskin bottles for POC, flow cytometry, polarized microscopy and optical microscopy. In addition, samples for pigment determination are taken at 12 depths to measure chlorophyll biomass and analyze phytoplankton diversity. This database will serve to develop regional and global transfer functions through which it will be possible to convert optical observations from BGC-Argo floats into phytoplankton diversity information.

Table 10. Work performed on board regarding phytoplankton communities and bio-optics

Parameter	code of operation *	Where	Method
Pigment	Discrete sampling on rosette cast (10-12 depths)	SD1 (ctd#2), SD2 (ctd#5), SD3 (ctd#6), SD4 (ctd#8), LD5 (tow#10, 12, 14, ctd#9,11,15,18,), SD6 (ctd#20), SD7 (ctd#21), SD8 (ctd#25), LD10 (tow#24, 26, 28), SD11 (ctd#36), SD12 (ctd#39)	HPLC - Lab - Villefranche
PIC/POC	Phytofloat: discrete sampling on rosette cast (3 depths)	SD1 (ctd#2), SD2 (ctd#5), SD3 (ctd#6), SD4 (ctd#8), LD5 (ctd#9,11 ; tow#12), SD6 (ctd#20), SD8 (ctd#25), LD10 (tow#24), SD11 (ctd#36)	CHN analyzer - Lab - Villefranche
Microscopy lugol	Phytofloat: discrete sampling on rosette cast (3 depths)	Idem as PIC/POC	Microscopy - Lab Villefranche
Microscopy nanoplankton	Phytofloat: discrete sampling on rosette cast (3 depths)	Idem as PIC/POC	Microscopy - Lab Villefranche
Cytometry	Phytofloat: discrete sampling on rosette cast (3 depths)	Idem as PIC/POC	Flow cytometry - Lab Roscoff
Nutrients (for Sandra Nunige)	Discrete samples on rosette cast	SD3 (ctd#7), SD4 (ctd#9), LD5 (ctd#10,12,15,18 Tow#12,14), SD6 (ctd#19), SD7 (ctd#23), SD8 (ctd#26), LD10 (tow#25,26,37; ctd#33), SD11(ctd#38), SD12 (ctd#41)	Lab - Marseille- for Sandra Nunige
Silicates	Discrete samples on rosette cast	Idem as nutrients	Lab - Marseille- for Sandra Nunige
Delta 15NO3 et delta 15DON (Angie Knapp)	Discrete samples on rosette cast	SD2 (ctd#6), SD3 (ctd#7), SD4 (ctd#9), LD5 (tow#12,14, 18; ctd#10), SD6 (ctd#19), SD7 (ctd#23), SD8 (ctd#26), LD10 (tow#37; ctd#33), SD12 (ctd#41)	

4.4 Fluxes measurements, processes studies at stations

4.4.1 Heterotrophic prokaryotic production

(France van Wambeke, MIO)

The heterotrophic prokaryotic production was determined vertically within the euphotic zone and horizontally through the TONGA gradients expected (Iron, P, N). From bacterial growth efficiency, a bacterial carbon demand could be determined and compared to primary production fluxes and used to determine the metabolic balance of the microbial system. From heterotrophic prokaryotic production, heterotrophic bacterial P and N demand could be calculated and compared with nitrogen fixers and sources of available P (diffusion regeneration through phosphatase activity).

Table 11. Recap sampling for Heterotrophic prokaryotic production

Parameter	code of operation *	Where	Method
Heterotrophic prokaryotic production (BP) ng C l ⁻¹ h ⁻¹	CTD "prod" 10 layers between 0 and 200m	SD1, SD2, SD3, SD4, LD5 (T1, T2, T3, T5), SD7, SD8, LD 10 (T1, T2, T3, T5), SD11, SD12	3H leucine technique combined with the centrifuge method
Heterotrophic prokaryotic production (BP) ng C l ⁻¹ h ⁻¹	Minicosm (see processes studies)	Minicosm exp at LD 5 & LD 10	
Heterotrophic prokaryotic production (BP) ng C l ⁻¹ h ⁻¹	Participation to DOP experiment (see Processes studies)	SD 8 and LD 5-T5	
Heterotrophic prokaryotic production (BP) ng C l ⁻¹ h ⁻¹	Marine snow catcher at volcanos sites and SD8	Suspended, slow sinking and fast sinking fractions	

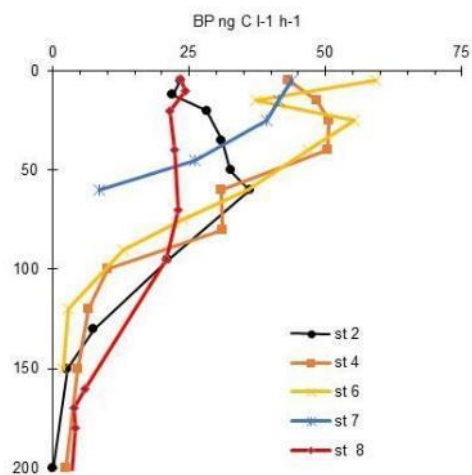


Figure 26. Selected vertical profiles of heterotrophic prokaryotic production

4.4.2 Primary production and N₂ Fixation rates

(MIO: Sophie Bonnet, Olivier Grosso, Caroline Lory, Mar Benavides, Univ. Haifa: Ilana Berman-Frank, IMEV: Jean-Michel Grisoni)

Primary production, N₂ fixation and Fe uptake rates have been quantified over the photic layer and across hydrothermal/trophic gradients. Samples for the identification and quantification of the major groups of diazotrophs by microscopy and qPCR and illumina sequencing have also been taken. Finally samples for C, N, and Fe intracellular quotas have been collected.

Table 12. Recap sampling for Primary production and N₂ Fixation rates

Parameter	code of operation *	Where	Method
¹⁵ N ₂ + ¹³ C fixation	TMC	SD1-SD11	Stable isotope labeling (13, 15N2)
Diazotroph quantification/characterization	TMC	SD1-SD11	Epifluorescence microscopy
nifH gene abundance	TMC	SD1-SD11	qPCR
nifH and Fe/P stress genes	TMC	SD1-SD11	RT-PCR
Oxygen productions	TMC	SD1-SD11	Optods
Fe uptake rates	TMC	SD1-SD12	Radioactive isotope labeling (⁵⁵ Fe)
N, P, Fe intracellular composition of <i>Crocospaera</i>	TMC	SD 1, 2, 3, 4, 7, 8, 11 and 12. LD 5 & LD 10	sorting in cytometry and ICP-MS analyses for metal concentration and C and N quotas
Trace metals composition of Trichome sections	TMC Phytoplankton Net	SD 3, 7, 8, 11 and 12. LD 5 & LD 10	synchrotron x-ray fluorescence (SXRF)

Preliminary results. Some microscope images are available, showing high concentrations of diazotrophs (*Trichodesmium* and *Crocospaera*) in the photic layer.

Initial observations of *Trichodesmium* morphologies along the cruise transect revealed mostly single filament and very small colonies (tufts) of *Trichodesmium* spp. Throughout the cruise transect at least two species of *Trichodesmium* were identified – *T. erythraeum*, *T. contortum*, and a third genus which belongs to the *Trichodesmium* cluster – *Katagnymene*. The only station where many colonies were observed was SD. 11 where surface *Trichodesmium* slicks were identified from deck (figure 27) and sampled with nets.



Figure 27. The CTD at the surface at SD11 where a strong bloom of *Trichodesmium* was visible (photo: C. Guieu).

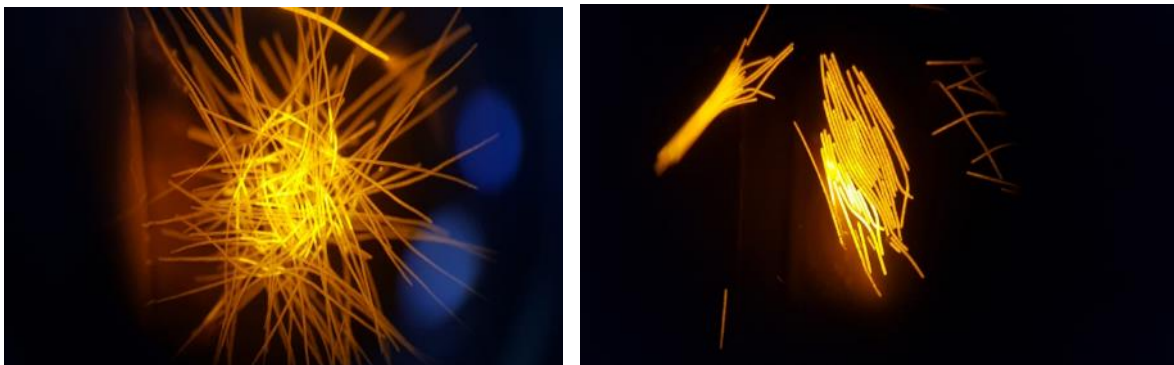


Figure 28. *Trichodesmium* colonies under epifluorescence microscopy at station Volcano 2 (Photo: S. Bonnet)

4.4.3 Phosphate availability and microbial P cycle

(Elvira Pulido Villena, MIO)

The microbial acquisition of dissolved organic phosphorus (DOP) through alkaline phosphatase (AP) ecto-enzymes might be controlled by Fe availability due to a recently discovered Fe co-factor in one of the most widely distributed AP family, the PhoX (Yong et al. 2014, Browning et al. 2017). In the framework of TONGA we propose:

- to examine the microbial DOP acquisition and the bioavailable P pool across a longitudinal gradient in phosphate and Fe concentrations
- to study the link between Fe and P cycle under the influence of hydrothermal sources vs. under oligotrophic conditions

For this purpose, we have performed onboard measurements of AP activities in the euphotic layer at most stations visited during the TONGA cruise. In addition we have sampled for lab measurements of a number of parameters allowing to characterize the phosphorus pool: phosphate, DOP, bioavailable fraction of DOP (AP-DOP) and particulate organic phosphorus.

Table 13. Recap sampling for microbial P cycle

Parameter	code of operation *	Where	Method
Alkaline Phosphatase nmol P L-1 h-1	CTD "prod" Minicosm Bottle experiments Marine Snow Catcher Respire traps	SD1, SD2, SD3, SD4, LD5 (T1, T2, T3, T5), SD7, SD8, LD 10 (T1, T2, T3, T5), SD11, SD12	Microplate spectrofluorimetry Fluorogenic substrate MUF-P
Phospho-diesterase activity nmol P L-1 h-1	CTD "prod" Bottle experiments Marine Snow Catcher Respire traps	SD1, SD2, SD3, SD4, LD5-T5, SD7, SD8, LD- 10-T5, SD11, SD12	Microplate spectrofluorimetry Fluorogenic substrate bis MUF-P
Aminopeptidase activity nmol leu L-1 h-1	CTD "prod" Minicosms Bottle experiments Marine Snow Catcher Respire traps	SD1, SD2, SD3, SD4, LD5-T5, SD7, SD8, LD 10- T5, SD11, SD12	Microplate spectrofluorimetry Fluorogenic substrate MCA- leucine
Betaglucosidase activity nmol glucose L-1 h-1	CTD "prod" Bottle experiments Marine Snow Catcher Respire traps	SD1, SD2, SD3, SD4, LD5-T5, SD7, SD8, LD 10- T5, SD11, SD12	Microplate spectrofluorimetry fluorogenic substrate MUF - Beta D glucoside
Phosphate concentration nM	CTD "prod" Minicosm (see Processes studies section) Participation to DOP experiment (see Processes Studies section)	SD1, SD2, SD3, SD4, LD5 (T1, T2, T3, T5), SD7, SD8, LD 10 (T1, T2, T3, T5), SD11, SD12	LWCC-CFA (not acquired on board)
Bioavailable fraction of DOP nM	CTD "prod" Minicosm (see Processes studies section) Participation to DOP experiment (see Processes studies section)	SD1, SD2, SD3, SD4, LD5 (T1, T2, T3, T5), SD7, SD8, LD 10 (T1, T2, T3, T5), SD11, SD12	Sample incubation with purified alkaline phosphatase (performed on board) LWCC-CFA analysis (not acquired on board)
DOP μ M	CTD "prod" Minicosm (see Processes studies section) Participation to Mar DOP experiment (see Processes studies section)	SD1, SD2, SD3, SD4, LD5 (T1, T2, T3, T5), SD7, SD8, LD 10 (T1, T2, T3, T5), SD11, SD12	Not acquired on board
POP μ M	CTD "prod"	SD1, SD2, SD3, SD4, LD5 (T1, T2, T3, T5), SD7, SD8, LD 10 (T1, T2, T3, T5), SD11, SD12	On board filtration of 1.2 L seawater. Analysis not conducted on board.
Nutrients (N, P)	CTD "prod" (Elvira) CTD "0-bottom" (Céline) TMC 0-bottom (Géraldine)	SD1, SD2, SD3, SD4, LD5 (T1, T2, T3, T5), SD7, SD8, LD 10 (T1, T2, T3, T5), SD11, SD12	Not acquired on board

4.5 Characterization of export pathways

4.5.1 Export at 200 m and 1000 m on short time scale close to the shallow volcanoes

(Cécile Guieu (LOV), Nagib Bairi (MIO), Guillaume de Lièges (IMEV))

At LD 5 and LD 10, PPS5 sediment traps have been deployed on the drifting mooring line respectively during 5 days and 4 days. PPS5 are large structure allowing the collection of exported material thanks to a 1 m² surface collection. The rotation of the plateau allows to collect this exported material on a pre defined time scale. It was 24h integration time at station 5 and 23h integration time at station 10.



Figure 29. The 2 PPS5 to be deployed at the long station during TONGA. The bottles that collect the material are at the base of the structure.

The collected material (preserved in situ with 2% formaldehyde solution) will be processed by Cellule Pieges at IMEV in Villefranche. Swimmers will be removed and likely the zooplankton will be identified if enough plankton is recovered (using zooscan technique). Then, the samples will be freeze-dried, the mass will be weighted to get the mass flux. Several aliquots of this material will then be used to determine: total C, POC, PIC, total N, PON. After acid digestion, a series of metals will be determined in order to get the metal fluxes at different depths and locations. Biogenic and lithogenic silicates will also be determined.

Table 14. Sediment traps samples from PPS5 devices during TONGA.

LD 5 T1 (mooring site)		LD 10 T1 (mooring site)	
200 m	1000 m	200 m	1000 m
No sample : engine of the rotating plate suffered a water leak and was destroyed	5 samples x 24 h	4 samples x 23 h	4 samples x 23 h

4.5.2 Mesopelagic remineralization of sinking particles

PI : Matthieu Bressac (LOV). Other participants: MIO: Sophie Bonnet, Mar Benavides, Elvira Pulido-Villena, France Van Wambeke, Catherine Guigue, Marie-Maëlle Desgranges. LOV: Cécile Guieu. IMEV: Céline Dimier, LEMAR: Géraldine Sarthou, David Gonzales Santana, Veronica Arnone. Not onboard: Hélène Planquette, Hannah Whitby.

The main goal of this experiment project was to investigate the mesopelagic remineralization of sinking particles and the associated regeneration of trace elements within water masses impacted or not by shallow hydrothermal inputs. RESPIRE and TM-RESPIRE traps were deployed on a free-drifting mooring line, along with other instruments, to collect sinking particles within the upper mesopelagic (150-300 m) and incubate them at in situ pressure and temperature conditions. Bacterial remineralization rates and the associated release of trace elements within the dissolved phase were quantified.

Table 15. Recap for RESPIRE traps deployment

Parameter	code of operation *	Where	Method
Bacterial remineralization of sinking particles ($\text{mmol O}_2 \text{ m}^{-2} \text{ d}^{-1}$)	RESPIRE traps deployed on a free-drifting mooring line	LD5, SD8, LD 10	O ₂ time-series measured within the incubation chamber of the RESPIRE traps
Release of dissolved trace elements during the bacterial degradation of sinking particles. Collaborator: Géraldine Sarthou.	TM-RESPIRE traps deployed on a free-drifting mooring line	LD5, SD8, LD 10	NA
Vertical flux of particulate organic carbon (POC). Collaborator: Céline Dimier.	RESPIRE and TM-RESPIRE traps deployed on a free-drifting mooring line	LD5, SD8, LD 10	NA
Release of dissolved organic carbon (DOC) during bacterial degradation of sinking particles. Collaborator: Catherine Guigue.	RESPIRE traps deployed on a free-drifting mooring line	LD5, SD8, LD 10	NA
Activity of heterotrophic bacteria attached to sinking particles (bacterial production and enzymatic activities). Collaborators: Elvira Pulido-Villena and France Van Wambeke.	RESPIRE traps deployed on a free-drifting mooring line	LD5, SD8, LD 10	NA
Genomics (heterotrophic bacteria attached to sinking particles). Collaborators: Sophie Bonnet and Mar Benavides.	RESPIRE traps deployed on a free-drifting mooring line	LD5, SD8, LD 10	NA
Microscopy (sinking particles). Collaborators: Sophie Bonnet and Mar Benavides.	RESPIRE traps deployed on a free-drifting mooring line	LD5, SD8, LD 10	NA
Vertical flux of particulate trace elements. Collaborator: H�el�ene Planquette (not onboard).	TM-RESPIRE traps deployed on a free-drifting mooring line	LD5, SD8, LD 10	NA
Release of humic substances, thiols, copper- and Fe-binding ligands during the bacterial degradation of sinking particles. Collaborators: Veronica Arnone and Hannah Whitby (not onboard).	TM-RESPIRE traps deployed on a free-drifting mooring line	LD5, SD8, LD 10	NA
Release of mercury and methylmercury during the bacterial remineralization of sinking particles. Collaborators: Marie-Ma�elle Desgranges	TM-RESPIRE traps deployed on a free-drifting mooring line	LD5, SD8, LD 10	NA

Preliminary results show the remineralization rates obtained with the RESPIRE traps deployed at three different depths (~170-290 m) at the SD 8 and LD10. At the SD 8 site, the remineralization rates decreased with depth, ranging from 8.6 $\text{mmol O}_2 \text{ m}^{-3} \text{ d}^{-1}$ at 170 m depth to 2.7 $\text{mmol O}_2 \text{ m}^{-3} \text{ d}^{-1}$ at 275 m depth. Interestingly, an opposite pattern was observed at LD 10 with remineralization rates, unexpectedly low considering the productivity in surface, increasing with depth (from 3.9 $\text{mmol O}_2 \text{ m}^{-3} \text{ d}^{-1}$ at 168 m to 9.45 $\text{mmol O}_2 \text{ m}^{-3} \text{ d}^{-1}$ at 288 m). However, these remineralization rates still need to be normalized by the particulate organic carbon fluxes captured by the RESPIRE traps (onshore analysis), if we are to fully understand the mesopelagic remineralization at these two contrasting biogeochemical sites.

Remarks:

- Due to an issue with the Arduino program, the oxygen time-series measured within the incubation chambers of the RESPIRE were not recorded at LD 5.

- Black particles were observed within the incubation chamber of the RESPIRE traps at SD8 and LD10. The origin of these particles is still unclear but additional investigations (e.g. electronic microscopy) should allow us determining their origin.

4.5.3 Biogeochemical and microbial characterization of export material and fluxes across Fe/hydrothermal gradients

MIO: Sophie Bonnet, Mar Benavides, Nagib Baihri, Elvira Pulido-Villena, France Van-Wambeke. Univ Haifa: Ilana Berman-Frank.

On a global scale, N₂ fixation by diazotrophic organisms provides the main external source of N to the ocean (Gruber, 2004). The new N brought by the diazotrophs is a new production route, therefore for the export of material outside the euphotic layer through an alternative biological pump called the 'N₂-primed Prokaryotic Carbon Pump' (Karl et al., 2003).

The studies that we published in the context of VAHINE projects (ANR JCJC S. Bonnet) and OUTPACE (ANR PIs: T. Moutin, S. Bonnet) demonstrated in situ the link between nitrogen fixation and export carbon (eg Berthelot et al., 2016, Bonnet et al., 2016, Caffin et al., 2018). However, the export pathways of nitrogen / carbon from the diazotrophy out of the euphotic layer are at this little documented, and on a very small number of diazotrophic organisms, which often compromises their representation in biogeochemical models (Gimenez et al., 2016).

With the aim of characterizing the role of diazotrophs in vertical export fluxes, we used different approaches and equipment to recover sinking material from the mesopelagic layer:

- 1) Marine Snow Catcher (MSC): The MSC was deployed at 200 m on all short duration stations, and at 3 depth horizons (170, 270 and 1000 m) on the two volcano stations and the gyre stations.
- 2) Bottlenet: The bottlenet was casted from 2000 to 200 m at 9 short duration stations. Blanks (bottlenet closed) were regularly performed between 200 and 0 m.
- 3) Acrylic traps: Three 4-tube sets of acrylic traps were deployed at 170, 270 and 1000 m at the 2 mooring stations. Each 4-tube set consisted of: 1 tube for 'omics analyses (filled with RNA later), 1 tube for biogeochemical analyses (containing formalin), 1 tube for particle visual characterization (containing an acrylamide gel, Collab: F. Le Moigne), and 1 tube for microbial analyses (which contained ¹³C+¹⁵N₂ label for the second deployment).



Figure 30. Acrylic traps deployed at long stations 5 and 10 during TONGA

Table 16. Summary of the samples collected in the different devices and parameters to be measured.

Parameter	code of operation	Where	Method
Sinking particle characterization	MSC	SD1-SD11, LD 5 – T1, LD 10- T1	POC concentrations nifH gene abundance Flow cytometry Microscopy counts TEP concentration Enzymatic activities Bacterial production
Mesopelagic community characterization	Bottlenet	SD3, SD4, LD5, SD7, SD8, LD10, SD11, SD11bis, SD12	Microscopy counts Calcifying and silicifying plankton counts Scanning electron microscopy Cell viability N ₂ fixation Nitrogenase immunolabeling POC/PON concentrations BSi/LSi concentrations nifH gene abundance flow cytometry Pigments Fatty acids
Export flux characterization	Acrylic traps	LD5 – T1, LD10 – T1	Omics Particle visual characterization POC/PON/POP/PIC concentrations Pigments BSi/LSi concentrations Flow cytometry Microscopy counts nifH gene abundance nitrogenase immunolabeling N ₂ fixation (nanoSIMS on filter and on resin-embedded particles) TEP concentrations TEP visualization Calcifying and silicifying plankton counts Scanning electron microscopy

Preliminary results

Our first observation is the presence of high quantities of phytoplankton (mainly diazotrophs) in sediments traps, up to 1000 m, at both mooring station (2 volcanos). Figures 32 show images from the three traps (170 m, 270 m, 1000 m) showing the export of diazotrophs and transparent exopolymeric particles that form a sticky matrix to which other particles and organisms attach. This enlarges the total particle size and mass and results subsequently in enhanced export to depth. As seen from Figure 32 not only large phytoplankton and diazotrophs such as *Trichodesmium* individual filaments and/or colonies are exported but also small (2-6 micrometer diameter) unicellular phytoplankton, mainly the diazotroph *Crocospaera*, under the form of cluster of tens/hundreds/thousands cells imbedded in sticky matrixes. The same observation has been done at almost all stations (excluding SD 8) in the Marine snow catcher samples (fast sinking fraction).

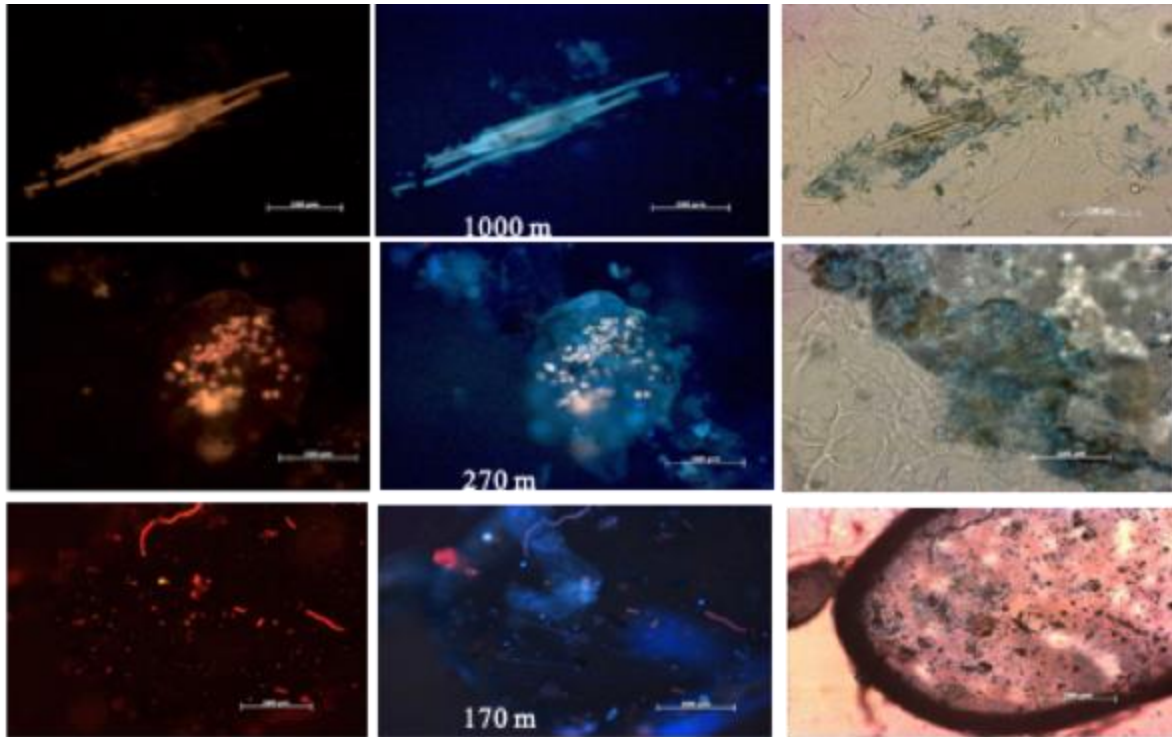


Figure 31. Diazotroph export in sediment traps at 170m, 270m, and 1000 m from LD 10.. Each trio of slides shows an identical image viewed with a phycoerythrin filter (left panels), PDMPO filter (middle), white light (right panels) to highlight staining by Alcian Blue for transparent exopolymeric particles (TEP) seen in blue shades. Both right and middle panels illustrate the organic matrix surrounding many of the particles in the traps. Visualized on the left panels are phycoerythrin containing cyanobacteria identified as *Trichodesmium* at 1000 m, *Crocospaera*-and *Synechococcus* like ecotypes at 270 m and a combination of all at 170m. Slides are representative images from these depths. All three traps contained each of the described organisms.

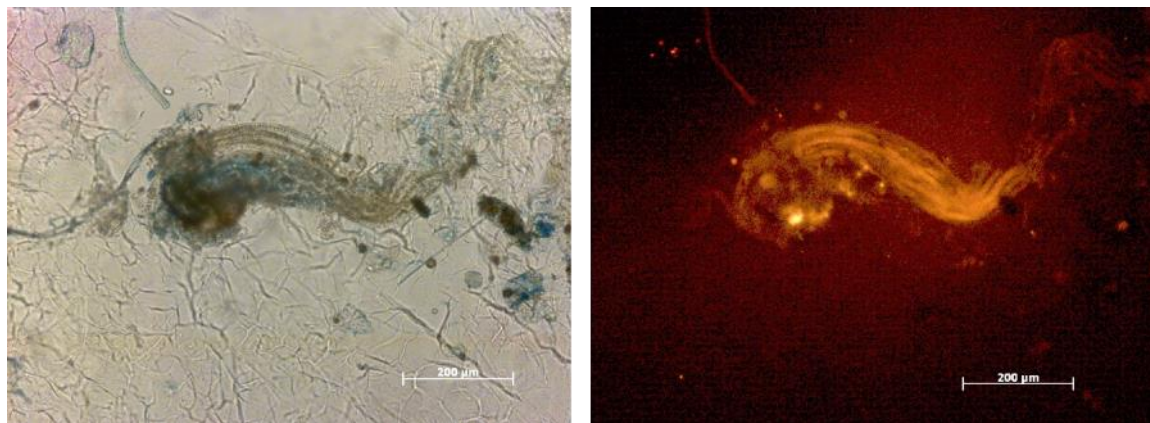


Figure 32. Diazotroph export in sediment traps at 270m at LD 10. Slide on the right viewed with a phycoerythrin filter displays cyanobacteria identified as *Trichodesmium* filamentous colonies and unicellular *Crocospaera*-and *Synechococcus* like ecotypes. Left slide under white light highlights staining by Alcian Blue for transparent exopolymeric particles (TEP) seen in blue shades showing the carbohydrate organic matrix surrounding many of the particles in the traps.

4.5.4 Study of export at 200 m and 1000 m the annual time scale

LOV: Cécile Guieu, MIO: Sophie Bonnet, Marie-Maëlle Desgrandes, Nagib Bairi, IMEV: Guillaume de Liège

A fixed mooring line has been deployed at station 12 and will be collecting data/samples for a full annual cycle (recovery R/V Alis Nov. 2020 during the TONGA RECUP leg) to study the seasonal variability of export and the contribution of diazotrophy to such fluxes.

The position of the mooring was carefully decided according to several criteria: to be far enough from the shallow volcanoes to integrate at the regional scale the effect of the likely fertilisation from the fluids and (2) to be located in an area where the dynamic is not too strong (this was obtained from the simulations using the Ariane modelling). **The position is: 20°42.408S / 177°52.128 W**

It has been instrumented with 2 Technicap PPS5 (1 m² collecting area) sediment trap and inclinometer (NKE S2IP) at depths of ~200 m (below the photic layer) and 1,000 m (seafloor depth ~1,500 m), CTD sensors (Sea-Bird SBE 37) and current meters (Nortek Aquadopp). The total mass and C, N, P fluxes will be determined. Trace metal will be measured in the exported material and metal fluxes will be derived. Using this ⁸¹⁵N budget, we will determine what fraction of export production was supported by N₂ fixation during the deployment and how it correlates this with surface chlorophyll data, POC fluxes and ARGO data. The swimmers will be picked from the bulk samples and characterized (zooscan).

The fixed mooring line has also been instrumented below the 200 m-depth trap with 2 automatic sequential passive samplers (THOE) recently developed and patented by AEL (N. Caledonia) and Technicap (France). The chelating resins (DGT) chosen for this study binds the following metals : Al, As, Cd, Co, Cr, Cu, Fe, Mn, Ni, Pb, Zn (Sampler 1), and, Hg and MMHg (Sampler 2) respectively, that will trace hydrothermal inputs during the one-year period of deployment and will be used for the interpretation of POC exports and remineralization fluxes, together with surface chlorophyll a concentrations (satellite data), CTD and currents data, in addition to data acquired by the ARGO floats data.



Figure 33. *A THOE instrument installed on the TONGA fixed mooring.*

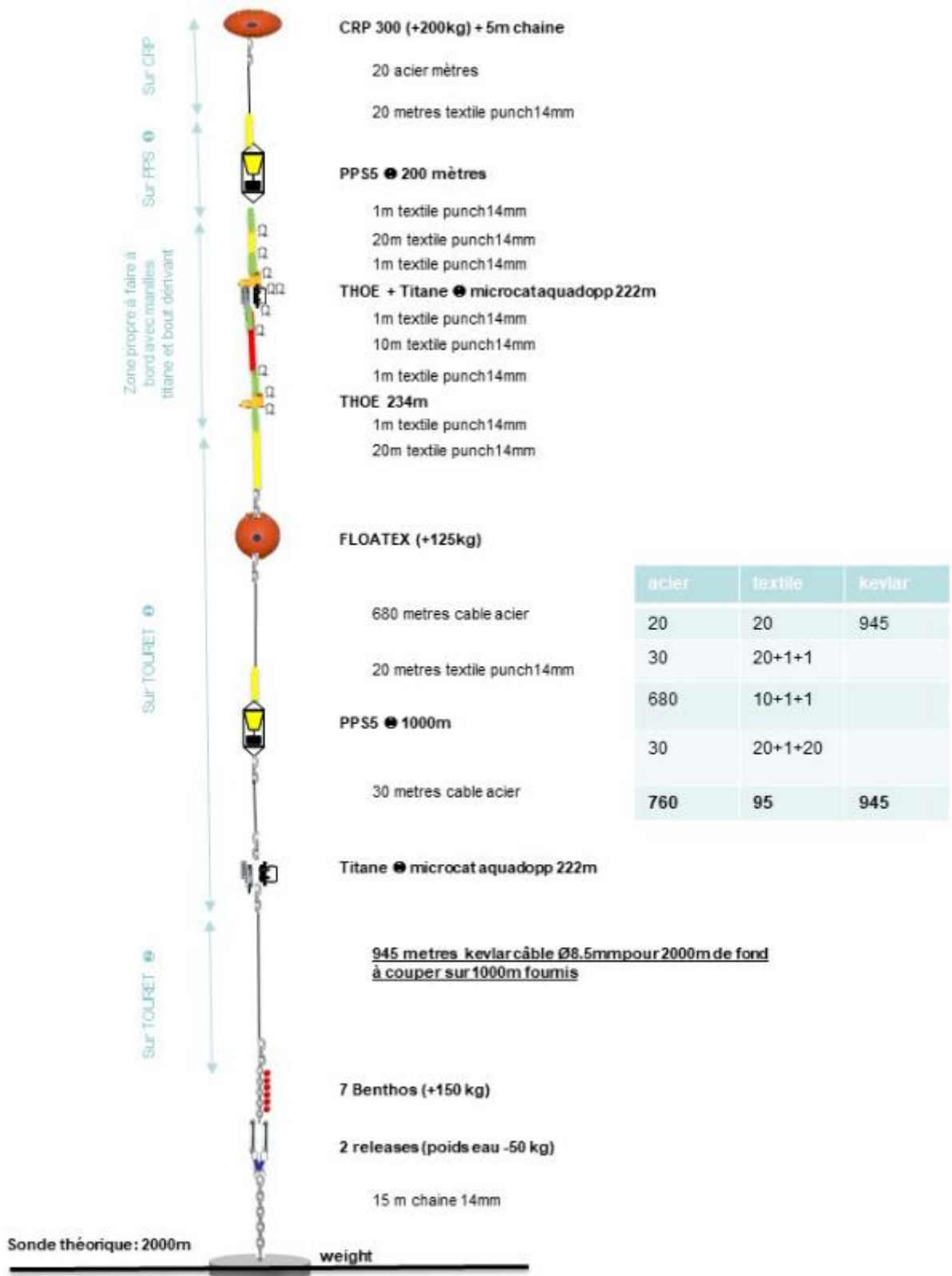


Figure 34. Design of the fixed mooring.

4.6 Stocks, diversity and processes in the sediment

LOV: Cécile Guieu, AD2M: Cédric Boulard, Jean-Philippe Gac, MIO: Olivier Grosso.

The impact of shallow volcanoes was investigated from the atmosphere down to the sediments. Sediments cores were sampled at six locations: SD 2 and SD 8 being the most distant from the Tonga Arc and the shallow volcanoes, LD 5-T1 and LD- 10-T1 being likely the most impacted, and SD 12 because it is the site where the fixed mooring was launched. In addition, cores were also performed at SD 4 but this was unsuccessful.



Figure 35. Launching of the Octopus Multicorer at night (left). Slicing a core (right).

Table 17. Summary of the collected cores.

stations	Lat	Long	depth m	Collecte
SD2	20° 32.640'S	175° 48.660'E	3410	2 cores
SD4	20° 29.750'S	177° 8.300'O	2192	did not work
LD5	21°12.201'S	175° 58.1080'O	2140	1 core
SD8	20°23.335'S	166°25.65'O	5326	2 cores
LD10	19°34.169'S	175°12.69'O	1940	6 cores
SD12	20°41.441'S	177°51.405'O	1930	8 cores



Figure 36. Position of the sediment cores performed during Tonga. (station 4 was unsuccessful): three very contrasted area have been sampled.

Sediments have been aliquoted on the first 20 cm and frozen and will be characterized for:

- DNA content (Coll. Sophie Arnaud Haond, Ifremer, Projet Pourquoi Pas les Abysses/ eDNAbyss) to investigate diversity in very contrasted environments of this unexplored region.

- total metal concentrations and grain size distribution (LOV), Hg concentrations (MIO)

- aliquots will be used in incubation experiments to better understand the effect particles have on the Fe(II) oxidation rates (LEMAR).

4.7 Underway work

4.7.1 Atmosphere

LISA: Karine Desboeufs, Lucie Beillard, LAMP: Karine Sellegri)

The chemical composition of the air (gas + aerosols), as well as the size and number distribution of aerosols from embryonic size (1nm) were continuously monitored in the lower atmosphere during the campaign (PEGASUS container laboratory, figure 37). These measurements are conditioned by a favorable starboard wind that is not impacted by the fumes from the boat. Aerosols sampling have been also performed on filters installed at the front of the boat on the look-out less subject to contamination from the Atalante. The height of the boundary layer and the actinic flux were also measured (instrument installed on bridge E). Rain samples were taken. At LD 10, as the Metis Shoal volcano was still active (emissions visible from the bridge), a short transect to the NW (downwind) could be done toward the still active volcano where the boat stayed few hours during the night.

Finally, measurements of primary aerosol emissions (chemical and biological) were also carried out at the air-sea interface (on the seawater surface underway).



Figure 37. View of the PEGASUS container laboratory for the monitoring of the composition/physical characterisation of the lower atmosphere: this was continuously performed during TONGA.

Table 18. Summary of the atmospheric sampling during TONGA

Parameter	when	Where	Method
Gaseous and particulate composition	Continuous routine measures	Atmospheric underway	PEGASUS

Incident radiation	Discrete routine measures	Atmospheric underway	Radiometer
Boundary layer	Continuous routine measures	Atmospheric underway	Lidar
Primary marine aerosol emissions		Surface seawater underway (see next section)	

Preliminary results. Atmospheric monitoring was done continuously throughout the campaign. The measurements are very intermittent due to the presence of smoke from the boat that can be filtered from the database, i.e. finally, we estimate that around 30% of the data are usable. The consequence is that we do not have continuous measurements over a full day and many measurements at night only (Figure 38: example of size distribution of the marine aerosol, and pollution peaks of the boat superimposed for November 03). 7 rains were collected. A layer of aerosols was observed at altitude around 2000m around the Metis-Shoal volcano.

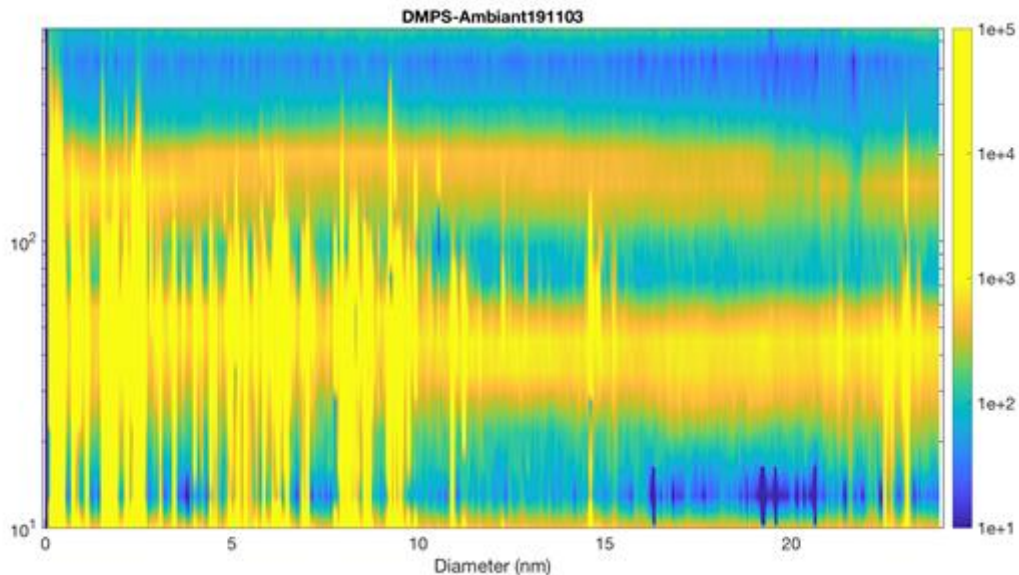


Figure 38. *Size distribution of the pristine marine aerosol superimposed with polluted aerosols emitted by the boat (concentration greater than 500 parts / cm³, scale in orange to yellow).*

Another objective of the atmospheric team was to work on aerosols emissions from the sea to the atmosphere. The goal was to identify if the gases emitted by the phytoplankton are precursors of nanoparticles in the atmosphere, in particular those emitted by species favored by hydrothermal sources. In parallel, the characteristics of sea spray generated from the seawater underway (see below) were compared with those of the ambient atmosphere, in order to test the parametrization of existing sources.

For that purpose, measurement of the size distribution of the aerosol from the embryonic size (1nm) as well as the chemical composition of the particle embryos in ambient atmosphere (in Pegasus) was performed. Until the power outage that occurred on November 12, the analysis of the chemical composition of neutral embryos could be performed. After that date, the analysis of the chemical composition of naturally charged embryos in negative mode was performed (as the outage damaged the neutralization part of our instrument). Also, as soon as conditions were favorable (wind from starboard), the measurement of the size distribution of the aerosol over the size range 10-500 nm and sampling of a filter for the measurement of glaciogenic nucleus in the ambient atmosphere was performed.

4.7.2 Surface waters underway

The surface continuous measurements by inline sensors (TSG and FRRF) provided continuous measurements of temperature and salinity along the track of the ship.

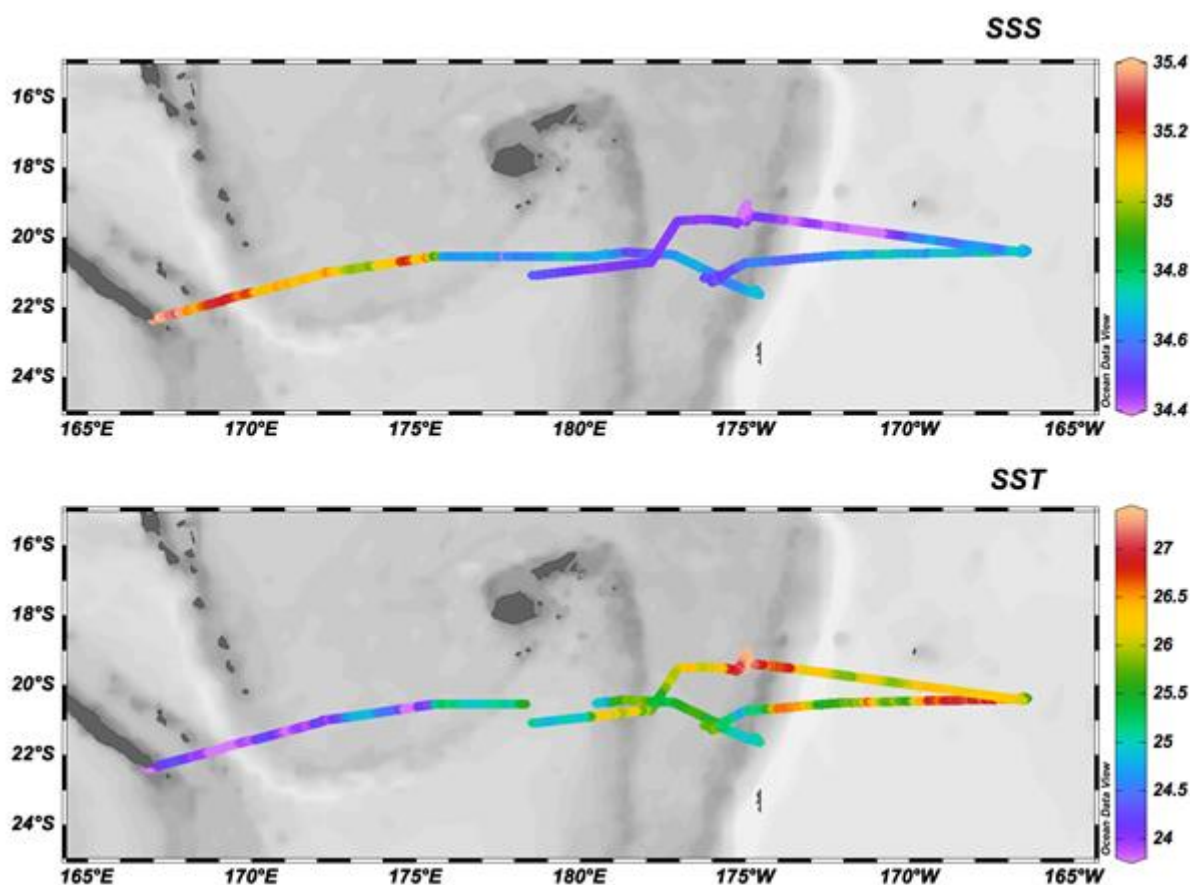


Figure 39. Sea surface salinity and sea surface temperature continuously measurement during TONGA. Although the figure cannot represent a synoptic view of the S and T pattern during the whole campaign (in particular because of the observed warming between beginning and end of the 37 days campaign), important and rapid changes were observed in the sea surface characteristics. (Figure Vincent Taillandier).

Several instruments have been plugged to the sea surface underway in order to get continuous measurements (or high frequency discrete measurements) to determine:

- (1) The role of fine scale dynamics in structuring diazotrophic activity and diversity
- (2) The high spatio-temporal characterization of photosynthetic activity
- (3) How biological activity impact marine emissions

4.7.2.1 Role of fine scale dynamics in structuring diazotrophic activity & diversity

MIO: Mar Benavides, France Van Wambeke, Sophie Bonnet, Olivier Grosso, Caroline Lory.

Dinitrogen (N₂) fixation by diazotrophic plankton provides the greatest external source of nitrogen to the oceans. The energy and nutritional resources that limit N₂ fixation in are geographically distributed by global ocean circulation. Superimposed on this large scale, smaller flow instabilities such as submesoscale (0.1-10 km, hours/days) and mesoscale (10-100 km, weeks/months) structures (collectively named “fine scale”) mix seawater parcels altering natural resource gradients. While these structures can be depicted by satellite data, their effect on microbial community structure and their ecological

interactions requires sampling in situ. Unfortunately, the usual spatiotemporal resolution of oceanographic cruises does not resolve the fine scale. During the TONGA cruise we targeted fine scale structures. These structures were selected thanks to the daily reports of satellite images (provided by the SPASSO team, see Physical and environmental context during TONGA campaign) for sea surface temperature, chlorophyll, geostrophic velocity, as well as Lagrangian parameters including FSLE and Okubo-Weiss.

Plankton biomass was sampled at high-resolution using the OCE-5, an automated device that obtains samples every ~20 min as the ship navigates. Biomass will be later extracted to obtain DNA samples. Different diazotroph groups will be enumerated using quantitative polymerase chain reaction (qPCR) assays. On two selected surveys, other measurements were included including: N₂ fixation rates, flow cytometry and microscopy counts, RNA, bacterial production and nutrient concentrations.

Table 19. Recap of underway sampling for diazotrophy vs fine scale dynamics

Parameter	code of operation *	Where	Method
nifH gene abundance	OCE-5	Transects shown on Fig. 40	qPCR
Diazotroph characterization	Underway		Microscopy counts
Diazotroph gene expression	Underway		RT-PCR
Bacteria and picoplankton quantification	Underway		Flow cytometry
Nutrient concentrations	Underway		Colorimetric analyses
Bacterial production	Underway		³ H-Leu uptake

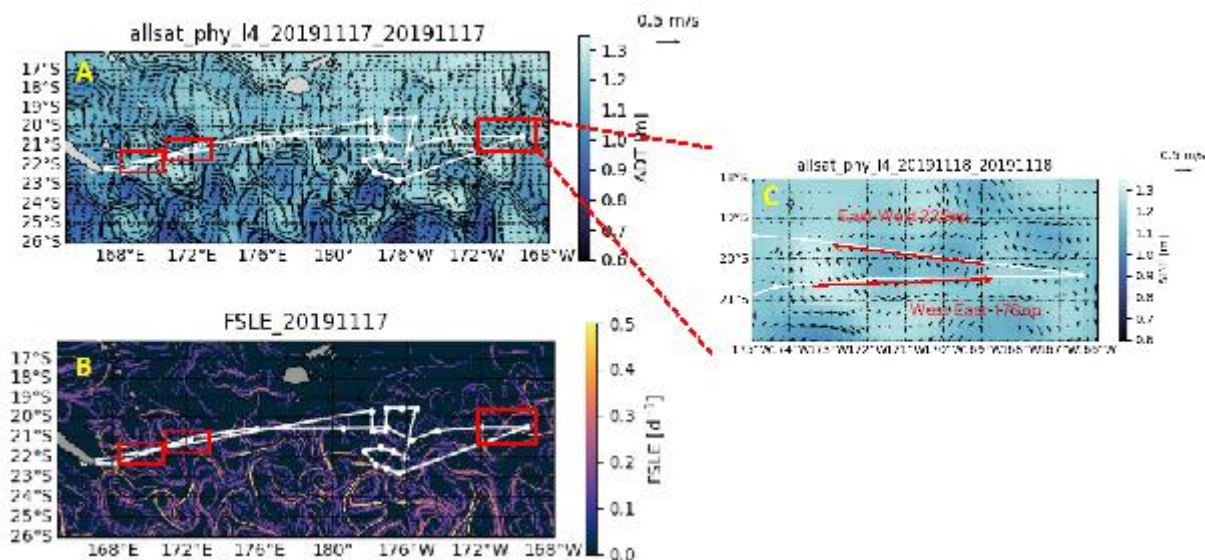


Figure 40. Location of the three structures targeted for high frequency sampling. (A) geostrophic velocities, (B) Finite Space Lyapunov Exponent parameter -depicts fronts-, (C) zoom-in of the third structure sampled. This structure was sampled twice: west-to-east on its southern flank, and east-to-west on its northern flank.

4.7.2.2 High spatio-temporal characterization of photosynthetic activity

Haifa Univ: Ilana Berman-Frank.

Fluorescence has been used to assess changes in the abundance of phytoplankton since the 1960s. Recent technological advances have also allowed a more focused investigation of photophysiology of phytoplankton via different fluorescence measuring platforms. One such widely available one that has been used for the past 20 years has been fast repetition rate fluorometry (Kolber et al. 1998), which builds on an earlier pump and probe technique and delivers a rapid chain of flashes of ~ 27500 imolphotons $m^{-2} s^{-1}$ over a period of 150-400 is to obtain F_m . This method allows simultaneous, single turnover (ST) of most PSII reaction centres and an assessment of various parameters related to electron transport and photochemistry through the photosynthetic electron transport chain of photosystem II. Many studies have shown these parameters are affected by the ecophysiological status of the phytoplankton and can inform us regarding lack of nutrient availability (i.e. changes in P, Fe, N), diel cycles, effects of changing irradiance etc. Here we used the Frrf in continuous mode throughout the cruise track using surface water pumped into the ship continuously.

Table 20. Recap underway photosynthetic activity

Parameter	code of operation	Where	Method
Fv/Fm, Photosynthetic efficiency of PSII,	Underway surface	throughout the sampling period of the fronts according to Transects shown above	Continuous underway measurement using FASTACT Frrf
Photosynthetic parameters related to electron transfer of PSII			
Chlorophyll concentration		Took discrete samples along the cruise track	Chlorophyll extraction and in-vitro measurement

4.7.2.3 How biological activity impacts marine emissions

LAMP: Karine Sellegri

The objective was to characterize the marine emissions emitted in the form of spray in the subtropical pacific zone is to determine how marine biology influences them. In particular in the context of TONGA, a more targeted objective was to determine how hydrothermal emissions modify the biogeochemical characteristics of water in relation to spray emissions. The adopted strategy was to characterize in parallel the emissions and the properties of the surface underway with a significant temporal resolution in order to accumulate statistics in the two compartments and thus to be able to derive relations in between them. The characterization of marine spray emissions conducted in recent cruises revealed a linear relationship between the nanoplankton and the number of spray particles emitted. One working hypothesis is that this relationship is linked to the presence of organic compounds of lipidic nature which lower the surface tension of water.

Spray emissions were generated by bubbling from the surface underway and their concentration, distribution in sub- and super-micron size were satisfactory measured continuously over the entire campaign from 01 November to 01 December. Their chemical composition, as well as their content in glaciogenic nuclei, will be analyzed in the laboratory (from filter sampled daily (samples integrated over 24 hours). In parallel, seawater from the underway were also analyzed for:

- surface tension (immediate measurement on board) of surface continuous water samples as a function of the temperature carried out 4 times a day (8h, 12h, 16h, 20h).
- flow cytometry (to be done at AD2M, Roscoff), with a frequency of 4 samples per day.
- concentration of inorganic and organic compounds by mass spectrometry and (2) the content in glaciogenic nuclei.

Preliminary results. The seaspray concentrations varied from 500 to 3000 particles per cm^3 with minima obtained in the most oligotrophic zone of the campaign (SD 8), but also in the heart of the zone of intense hydrothermal activity. The link with

photosynthetic efficiency measurements and Chl-a performed on the surface continuum, as well as the flow cytometry measurements, will make it possible to analyze the causes of this variability.

4.8 Process Studies

4.8.1 Mixing experiments in minicosms

LOV: Frédéric Gazeau, Chloé Tilliette, Cécile Guieu. IMEV Jean-Michel Grisoni, Guillaume De Liège, Céline Dimier. MIO: Sophie Bonnet, Mar Benavides, Caroline Lory, Olivier Grosso, France Van Wambeke, Catherine Guigue, Marie-Maëlle Desgranges, Elvira Pulido-Villena. AD2M: Estelle Bigeard, Mathilde Ferrieux. LEMAR Géraldine Sarthou, David Gonzales Santana. QUIMA: Veronica Arnone. University of Haifa: Ilana Berman-Frank.

During the TONGA campaign, the potential link between hydrothermal, metal concentrations (including iron) and biological processes was studied by conducting mixing experiments in a clean container equipped with eight climate reactors designed at LOV (Figure 41). Two mixing experiments between hydrothermal fluid and surface water were conducted during LD 5 and LD 10 to monitor the biological response for different mixing scenarios. Surface water and bottom water were pumped with a clean, high-speed peristaltic pump to avoid disturbing communities. However, during the second experiment, due to the reduction of the volumes of bottom water to be added, we collected the 'volcano end-member' using the CTD.

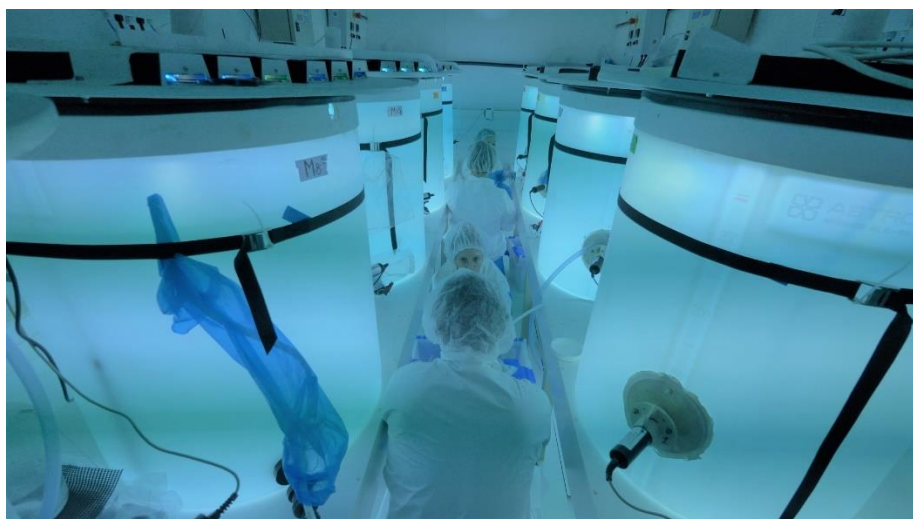


Figure 41. *Inside the clean container during the mixing experiment at LD 5. (Photo Hubert Bataille)*

For these two experiments that lasted about ten days each, the objective was to study the impact of hydrothermal vents on the composition and functioning of surface planktonic communities. Many parameters and processes have been studied, only a small proportion of which have been directly measured on board.

Both experiments lasted over ten days during which many parameters and processes were measured (see list below). During the first experiment (11/11/2019 - 20/11/2019), the hydrothermal water additions (filtered on 10 μm) were 0, 5, 10, 15, 20, 25, 30 and 40 liters for a total of 275 litres inside each minicosm at the beginning of the experiment. During the second experiment (23/11/2019 - 02/12/2019), we decided to reduce the volumes added in order to follow the gradient: 0, 1, 2, 5, 10, 20, 30 and 40 liters. The sampling times were for the two experiments: T0 (before mixing), T + 12 h, + 24 h, + 48 h, + 96 h, + 144 h, + 192 h (+ 216 h for site V1).

Table 21. Summary of the parameters to be measured in the samples from the two mixing experiments performed in minicosms

Parameter	Where	Method
Irradiance	LD 5, LD 10	Capteurs PAR (continu)
Température	LD 5, LD 10	Thermomètres (continu)
Alcalinité totale (A_T)	LD 5, LD 10	Titration potentiométrique
pH_T	LD 5, LD 10	Spectrophotométrie (à bord)
POC / PON (incluant ^{13}C)	LD 5, LD 10	Analyse élémentaire et isotopique (EA-IRMS)
^{13}C -DIC	LD 5, LD 10	Analyse isotopique (EA-IRMS)
Chlorophylle a	LD 5, LD 10	
Pigments	LD 5, LD 10	HPLC
DIN-DON (nano)	LD 5, LD 10	Spectrophotométrie (fibre optique)
DFe	LD 5, LD 10	FIA
δ^7Li MOP	LD 5, LD 10	MC-ICP-MS
δ^7Li eau	LD 5, LD 10	MC-ICP-MS
NH_4	LD 5, LD 10	Fluorométrie (à bord)
Bulk $^{15}N_2$ fixation	LD 5, LD 10	Analyse isotopique (EA-IRMS)
Cell-specific $^{15}N_2$ fixation	LD 5, LD 10	NanoSIMS
Diazotroph abundance	LD 5, LD 10	qPCR
Diazotroph diversity	LD 5, LD 10	nifH amplicon sequencing
Production prokaryotique hétérotrophe	LD 5, LD 10	Leucine tritiée (à bord)
Activité alcaline phosphatase et aminopeptidase (total)	LD 5, LD 10	(à bord)
DIP, DOP, AP-DOP (Nano)	LD 5, LD 10	Spectrophotométrie (fibre optique)
Sels nutritifs	LD 5, LD 10	Autoanalyseur
Abondances phytoplancton, bactéries et virus	LD 5, LD 10	Cytométrie en flux
Abondances flagellés hétérotrophes	LD 5, LD 10	Cytométrie en flux
Diversité phytoplancton, bactéries et virus (metaB)	LD 5, LD 10	Metabarcoding
Abondance microautotrophes et microhétérotrophes	LD 5, LD 10	Microscopie
Métaux trace dissous	LD 5, LD 10	ICP-MS
Spéciation cuivre organique	LD 5, LD 10	
Spéciation fer organique	LD 5, LD 10	
Thiols	LD 5, LD 10	
Substances humiques	LD 5, LD 10	
dFe(II)	LD 5, LD 10	
DOM	LD 5, LD 10	
Fe(II) oxidation kinetics	LD 5, LD 10	
DOC	LD 5, LD 10	Analyseur TOC
FDOM/CDOM	LD 5, LD 10	
O_2 metabolism (O_2/Ar)	LD 5, LD 10	Membrane inlet mass spectrometer (à bord)
Abondance mésozooplancton	LD 5, LD 10	Zooscan
Pièges à sédiment	LD 5, LD 10	Analyse élémentaire

Preliminary results

Both experiments went as expected without any problem. Only few results are available at this time but the pH and chlorophyll data obtained onboard suggest the presence of an acid plume at the LD 5 – T5 site (~ 6.4) probably containing toxic elements for community development. This toxic effect seems to subside at the end of the experiment with stimulation of chlorophyll growth after 5 days of experience.

The bottom water collected at the LD 10-T5 site appears clearly less acidic (~ 7.7) with a fertilizing effect observed more quickly.

The analysis of the many parameters for which we have sampled will allow us to confirm or not these first results.

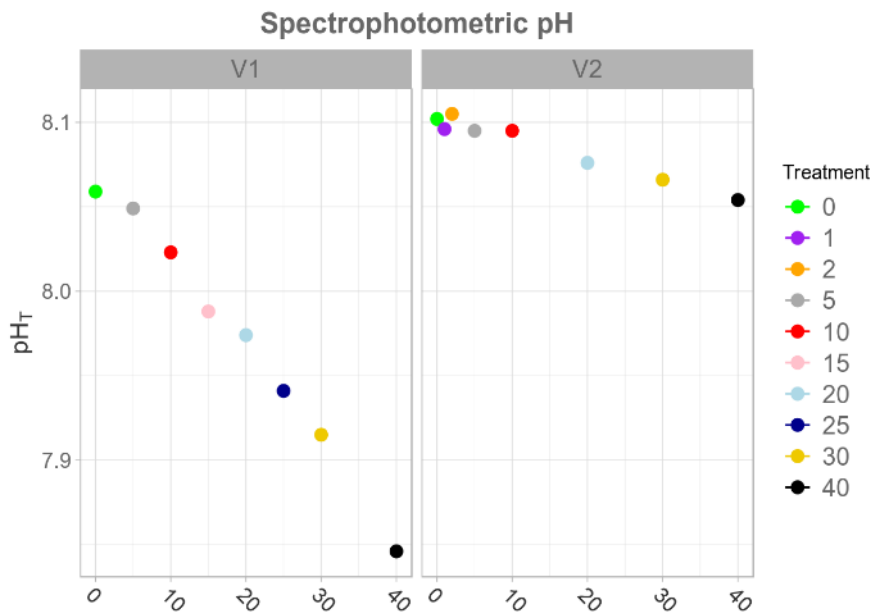


Figure 42. pH levels in the various minicosms after 12 h depending on the volume of bottom water added. (left: mixing surface seawater with hydrothermal end-member from LD 5 -T5; right: mixing surface seawater with bottom water collected at LD 10-T5. The legend corresponds to the volumes of bottom water added (in liters in the whole minicosm (total volume = 275 litres)).

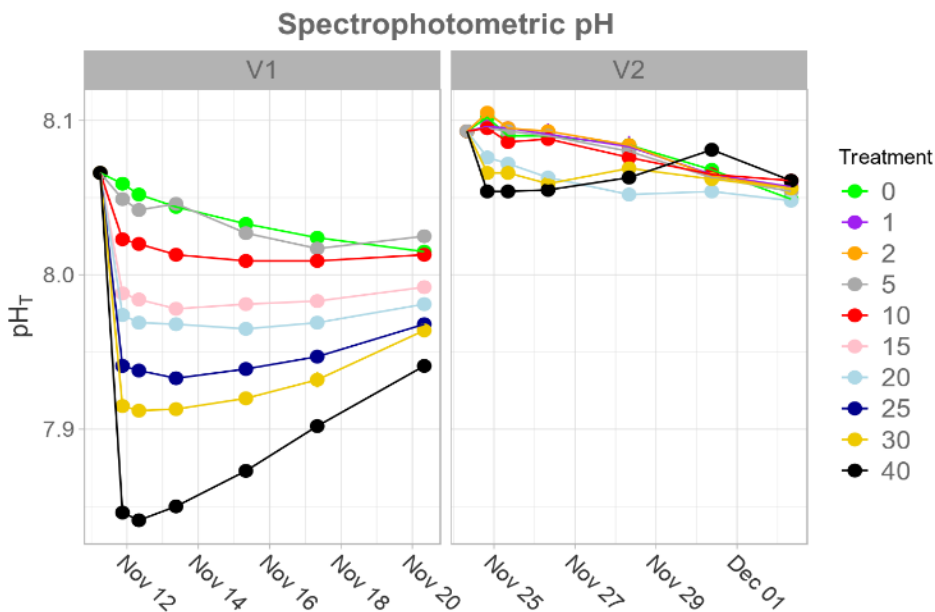


Figure 43. Evolution of pH in the two experiments (left: mixing surface seawater with hydrothermal end-member from LD5-T5; right: mixing surface seawater with bottom water collected at LD 10-T5. The legend corresponds to the volumes of bottom water added (in

liters in the whole minicosm (total volume = 275 litres)).

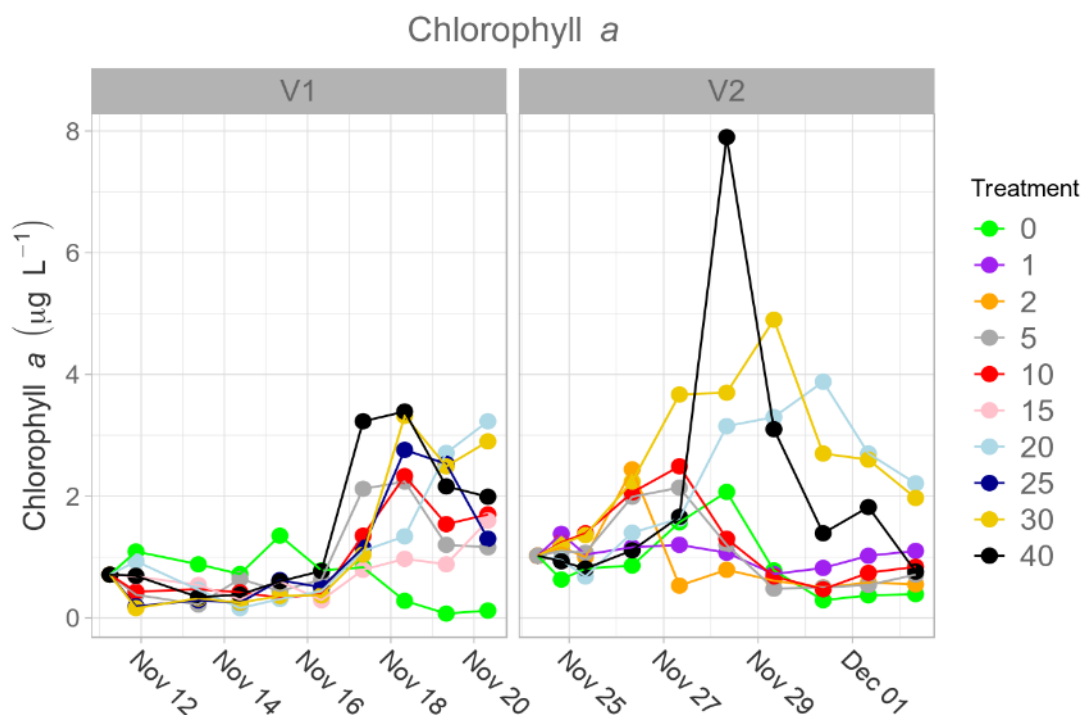


Figure 44. Evolution of the [Chla] in the two experiment (left: mixing surface seawater with hydrothermal end-member from LD5-T5; (right: mixing surface seawater with bottom water collected at LD10-T5. The legend corresponds to the volumes of bottom water added (in liters in the whole minicosm (total volume = 275 litres)).

4.8.2 Effect of different DOP molecules on N_2 fixation, DOP acquisition, gene expression and methane production

MIO: Mar Benavides, Elvira Pulido-Villena, France Van-Wambeke. AD2M: Cédric Boulart, Jean-Philippe Gac.

Mixotrophy (the dual use of inorganic and organic sources) is clearly emerging as the rule rather than as the exception in marine photosynthetic plankton nutrition. While non-photosynthetic diazotrophs are thought to rely on dissolved organic matter (DOM) for their growth, the use and potential benefits of DOM compounds other than DOP in cyanobacterial diazotrophs (their 'mixotrophic potential') remains poorly understood.

Trichodesmium has the genetic capacity to metabolize dissolved organic phosphorus (DOP) compounds such as phosphomonoesters and phosphonates, which allows it to grow in phosphate-depleted regions. Other diazotrophs such as *Crocospaera watsonii* can use phosphomonoesters but not phosphonates, reducing their phosphorus-acquisition resources to some extent.

Marine DOP is composed of phosphoesters (C-O-P bonds), phosphonates (C-P bonds) and phosphoanhydrides (P-O-P bonds). While the use both phosphoesters and phosphonates has been tested on diazotrophs, here we test for the first time the effect of phosphoanhydrides, benefiting from the P-rich and P-poor areas visited by the TONGA cruise.

Table 22. Parameters to be measured at the 2 stations tested

Parameter	code of operation	Where	Method
-----------	-------------------	-------	--------

15N2 + 13C fixation	Classic rosette	LD5 and SD8	Stable isotope labeling (IRMS and nanoSIMS)
nifH gene abundance	Classic rosette	LD5 and SD8	qPCR
Methane production	Classic rosette	LD5 and SD8	Gas chromatography
Methane genes	Classic rosette	LD5 and SD8	Transcriptomics?
Ecto Enzymatic activities	Classic rosette	LD5 and SD8	Fluorogenic substrates
Bacterial production	Classic rosette	LD5 and SD8	3H-Leu uptake
DIP/AP-DOP concentrations nM	Classic rosette	LD5 and SD8	LWCC-CFA technique
Bacteria and picoplankton abundance	Classic rosette	LD5 and SD8	Flow cytometry

Preliminary results

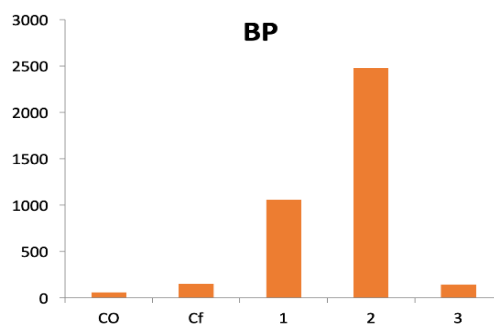


Figure 45. *Heterotrophic prokaryotic production at station LD5 (pmol C L⁻¹ h⁻¹). C0=time zero, Cf=control (incubated 48h), 1=ATP additions, 2=AMP additions, 3=3polyP additions.*

4.8.3 Impacts of P and Fe availability on colony formation in *Trichodesmium* spp.

Univ Haifa: Ilana Berman-Frank. MIO: Sophie Bonnet, Mar Benavides

The diazotrophic *Trichodesmium* spp., extremely important in the eastern tropical Pacific Ocean, exhibit two basic morphologies: a free-living, single filament (trichome) composed of tens of cells with similar phenotypical morphologies and spherical or fusiform colonies termed “puffs” and “tufts” (or “rafts”), respectively. Colony sizes vary considerably and range between ~ 50 to 200 trichomes per colony. In *Trichodesmium*, trichomes are typically considered an “organismic unit” as the chains of cells are surrounded by joint periplasmic membrane and cytoplasm.

Trichodesmium have many physiological strategies to increase nutrient acquisition and assimilation in their oligotrophic niche. The morphological type may also aid in these efforts. Colonial morphologies enhance buoyancy regulation (in *Trichodesmium* gas vesicles and carbohydrate ballasting are common) and enable nutrient mining from depth. Surface colonies take-up, store, and dissolve iron oxides and aeolian dust. Resident communities of holobionts/epibionts additionally facilitate nutrients for the colonies, while large colony sizes may deter the copepod grazers that ingest *Trichodesmium*

Here we examined the transformation from single trichomes to colonial morphologies.

Table 23. Recap of the operations performed

Parameter	code of operation	Where	Method
-----------	-------------------	-------	--------

Colony versus filament morphology	TMR-PROD/Classic Rosette	All stations Depth profiles	Microscopy
Colony versus filament morphology	Surface nets	Stations where <i>Trichodesmium</i> abundant	Microscopy, RNA, proteomics on <i>Trichodesmium</i>
Colony versus filament morphology	Underway sampling from surface	Along station transects	Microscopy, RNA, proteomics on <i>Trichodesmium</i>
nifH gene abundance	Classic rosette		qPCR
Dissolved P and Fe	TMR	Stations near volcanoes Panamax & Simone (Station 8)	
Experiments to test effect of enrichment of Fe and P on morphological shape of <i>Trichodesmium</i>	Specific experiment On surface slick populations	SD 11	Microscopy, RNA, proteomics on <i>Trichodesmium</i>
Effect of removing Fe (DFOB) on morphological shape of <i>Trichodesmium</i>	Specific experiment	LD5 & LD10	Microscopy, RNA, proteomics on <i>Trichodesmium</i>

Preliminary results

Initial observations of *Trichodesmium* morphologies along the cruise transect revealed mostly single filaments and very small colonies (tufts) of *Trichodesmium* spp. Throughout the cruise transect at least two species of *Trichodesmium* were identified – *T. erythraeum*, *T. contortum*, and a third genus which belongs to the *Trichodesmium* cluster – *Katagnymene*. The only station where many colonies were observed was SD. 11 where surface *Trichodesmium* slicks were identified from deck and sampled with nets.

In this last station an enrichment experiment with Fe-EDTA and PO_4 . After 24 h with either Fe or P additions microscopic observations revealed (qualitatively at this stage) more free filaments and smaller colonies or colonies that appeared to be less compact with filaments looser within the colonies.



Figure 46. *Trichodesmium* after 24 h enrichment with Fe-EDTA and with PO_4 . Left panel control – no additions, middle panel + Fe, right panel + PO_4

4.9 Autonomous instruments launched during TONGA.

LOV: Vincent Taillandier, IMEV: Guillaume De Liege

Several autonomous instruments were launched during the TONGA cruise: 2 BG ARGO floats, 5 ARVOR floats and 20 SVP buoys, all active and allowing to contextualize the work areas after our campaign. These data will be completed by all the parameters acquired on board during the campaign, namely the ADCP data but also the trajectories given by the drifting moorings at 3 stations. These deployments have been assisted by Antoine Poteau (LOV) for the BG ARGO floats, and by Noé Poffa (Ifremer) (Argo profiling floats)

4.9.1 BGC ARGO and ARVOR floats

All the BGC Argo and ARVOR floats that have been all successfully deployed can be find here: <https://fleetmonitoring.euro-argo.eu/dashboard> : search for “tonga” to display the position of the floats, the following screen will allow to localize the floats and the profiles

Table 24. Update (**nov 2023**) of the 2 BGC Argo and the 5 ARVOR floats launched during the TONGA cruise between Nov 9 and Dec 1, 2019.

7 floats

A	WMO	Float S/N PTT	Float	Last Tx	Last cycle	Battery	Launch date	Cruise
	6903025	P41306-16FR002 lovbio109b	PROVOR_III	28/02/2022 22:44:00	209	9.8	09/11/2019	TONGA
	6903024	P41306-16FR001 lovbio108b	PROVOR_III	26/03/2023 23:06:00	408	5.3	24/11/2019	TONGA
	6902989	AI2600-19FR005 880238	ARVOR	05/08/2023 02:51:34	161	9.2	29/11/2019	TONGA
	6902927	AI2600-18FR018 651475	ARVOR	10/11/2023 02:45:30	170	9.3	01/12/2019	TONGA
	6902986	AI2600-19FR002 850575	ARVOR	12/11/2023 07:42:30	171	9.3	23/11/2019	TONGA
	6902988	AI2600-19FR004 880937	ARVOR	16/11/2023 02:48:30	171	9.2	27/11/2019	TONGA
	6902985	AI2600-19FR001 860692	ARVOR	16/11/2023 12:47:30	176	9.4	14/11/2019	TONGA

The positions and trajectories (nov 2023):

BGC-ARGO	ARVOR	ARVOR	ARVOR	BGC-ARGO	ARVOR	ARVOR
LD5-T1	LD5-T5	SD9	LD10-T5	LD10-T1	SD 11	SD 12

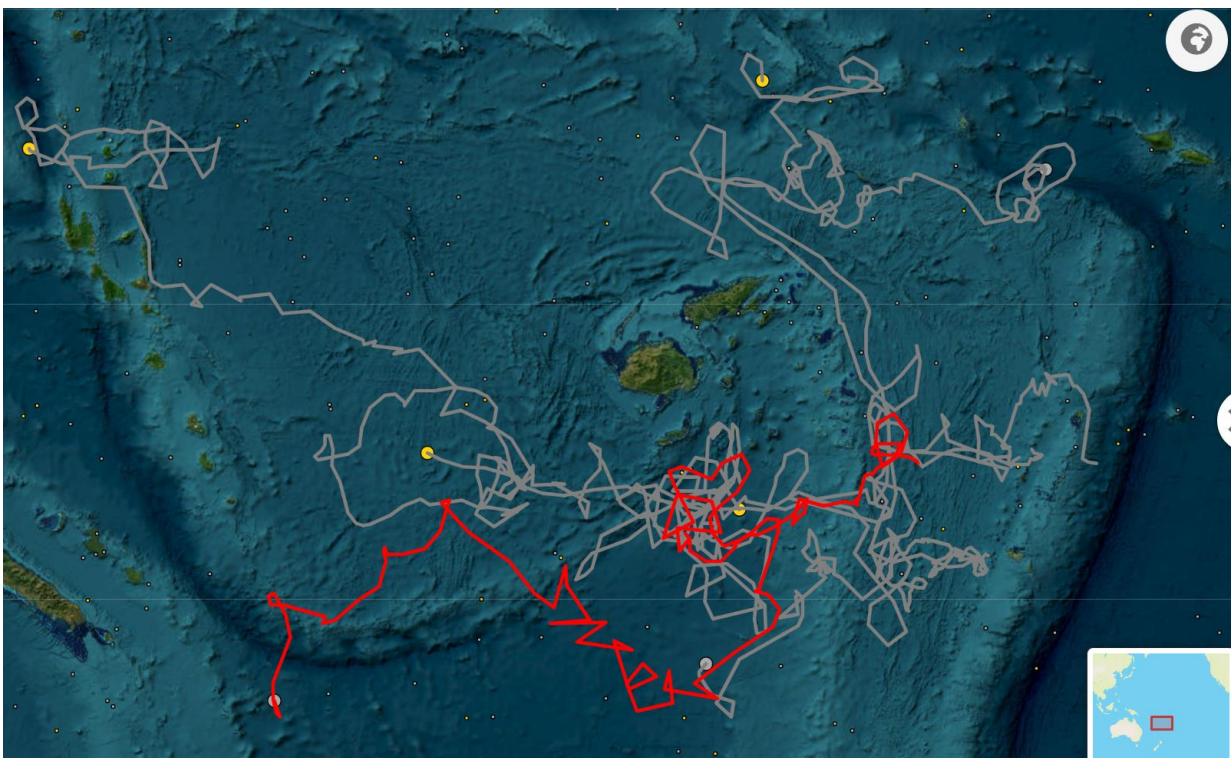
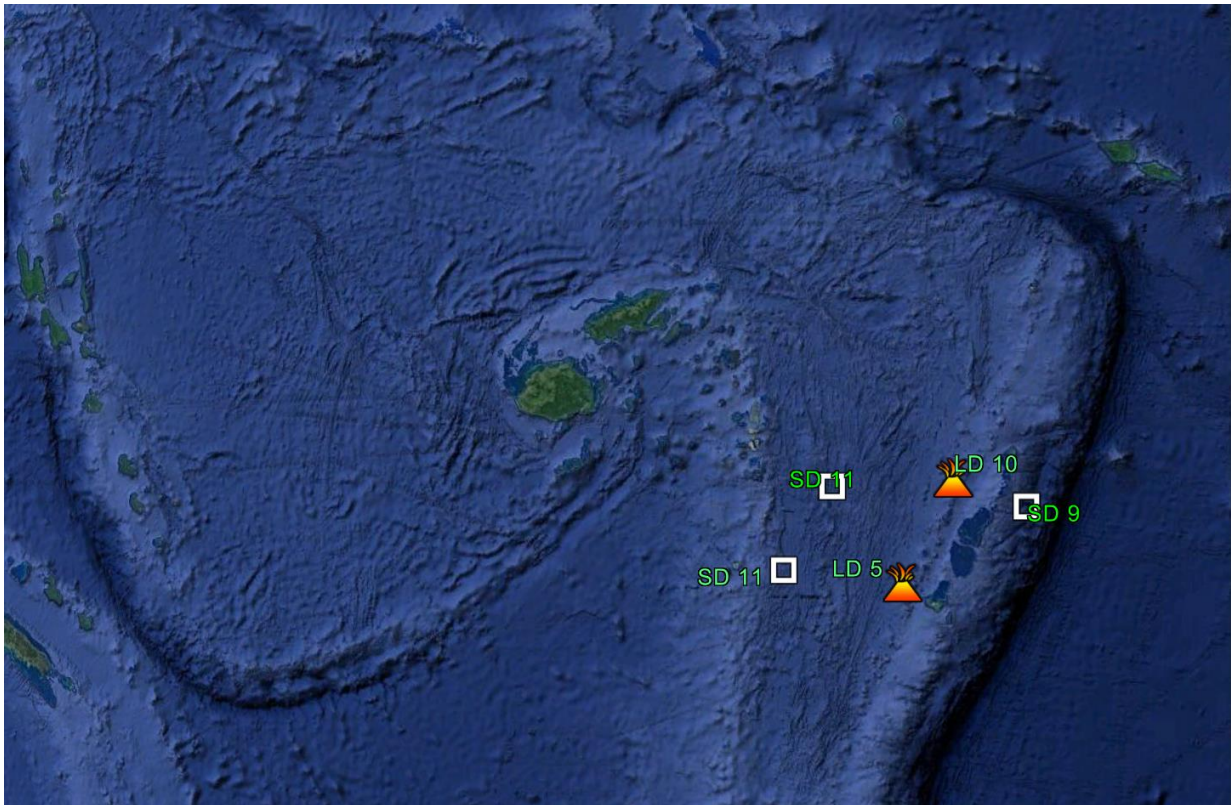


Figure 47. (top) Initial position of the five ARVOR (T and S sensors) and two BGC-Argo profiling floats equipped with the same optical package as the CTD-rosette (Phytofloat protocole) have been launched in the two hydrothermal sites explored during the TONGA cruise (LD 5 and LD 10). (bottom) As in Nov 2023, 4 ARVOR are still profiling, the figure shows the trajectories of the floats since December 2019.

4.9.2 SVP buoys

A total of 20 buoys have been launched: 5 at each of the three mooring sites and 5 above PANAMAX (volcano1)

Table 25. Summary of the position and time of deployment of the 20 buoys during TONGA.

Launching time : UTC	9/11/19 between 21h22 and 21h30	14/11/19 between 21h33 and 21h39	23/11/19 between 23h19 and 23h27	01/12/19 between 01H56 and 01H59
Launching time : local time	10/11 between 9h22 and 9h30	15/11/19 between 9h33 and 9h39	24/11/19 between 11h19 and 11h27	1/12/19 between 13h56 and 13h59
Launching location	SD 5 (drifting mooring). Position : between 21°09,59S 175°54,25 W & 21°09,7S 175°53,6W	LD 5 (PANAMAX) position 21°09,3S ; 175°44,66W & 21°09,54S ; 175°44,76W	LD 10 (drifting mooring site) 19°25,16s ; 174°57,61w & 19°25,13S ; 174°57,85W	SD 12 (fixed mooring site) between 20°43,23S ; 177°52,00W and 20°43,08S ; 177°52,53W
Vessel speed	From 2 to 7 knts	2 knts	1.5 knts	From 1 to 5 knts
SVP's number (reference to be find at the CORIOLIS web site)	6511780	66028220	300234067242660	300234067242600
	7016130	66029030	300234067243670	300234067240620
	6515820	66028240	300234067243620	300234067242630
	6511803	66028250	300234067242810	300234067240670
	6518780	66028270	300234067242750	300234067241780

All the trajectories and present position of the 20 bouys deployed during TONGA can be found on the CORIOLIS web site <http://www.coriolis.eu.org/Data-Products/Data-Delivery/Data-selection>.

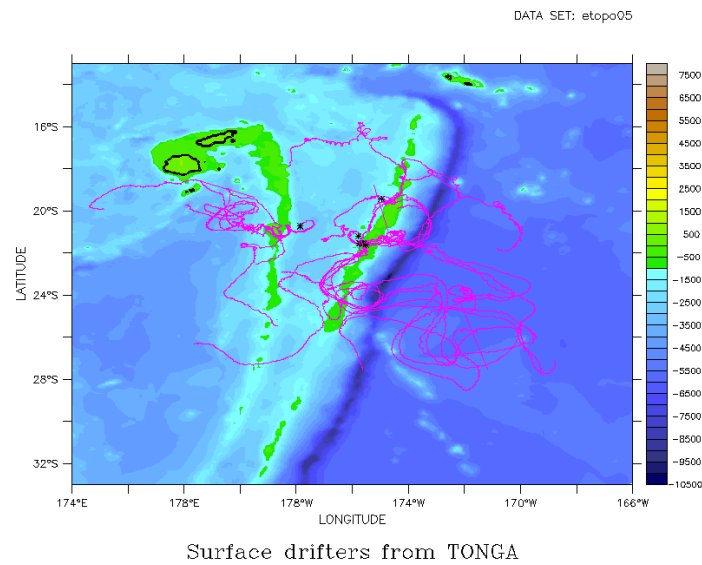


Figure 48. Position of drifters as recorded on March 4, 2020.

In addition to these buoys, we also have the trajectories of the drifting moorings that will help us to interpret the results obtained from those deployments.

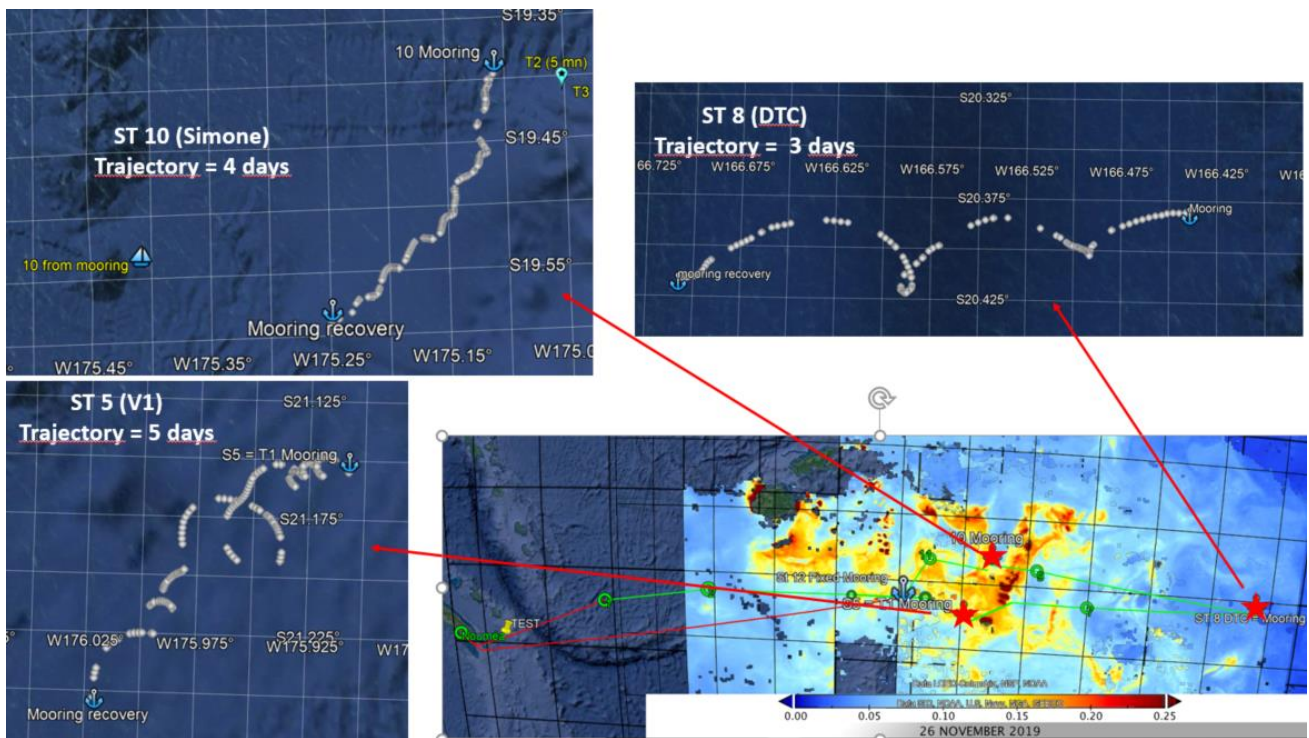


Figure 49. Location of the drifting mooring during their 3 to 5 days deployment, superimposed to the Chla satellite image of Nov 26/2019.

4.10 Supporting data

The team onboard was daily assisted by scientists on-land to find the best area to investigate the TONGA objectives. Physicists (Christophe Maes and Nicolas Grima, LOPS ; Anne Petrenko and Stephanie Barrillon, M i O) assisted the team onboard with the dynamics of the visited water masses to adjust the sampling strategy and to decide the best area to deploy the various autonomous instruments. Geologists (Bernard Pelletier (IRD), Julien Collot (DIMENC NC), Martin Patriat (IFREMER) & Olivier Hyvernaud (LDG PF) helped to target the shallow volcanoes providing bathymetry and indications of activity. Carla Scalabrin (IFREMER) interpreted the multibeam data.

4.10.1 Ariane simulations

One specific task dedicated to the team on land was to provide during the cruise some model simulations that will inform the vessel's team about the structure of the dispersion of a shallow volcanic emission. For that purpose, the LOPS team sent us regularly and for different targeted positions, the plume detection in « near real time » as a function of time after the particles from the fluid have been artificially put into the dynamic system at a given time. That was done for different depths. Two examples of working figures provided during the cruise are given below.

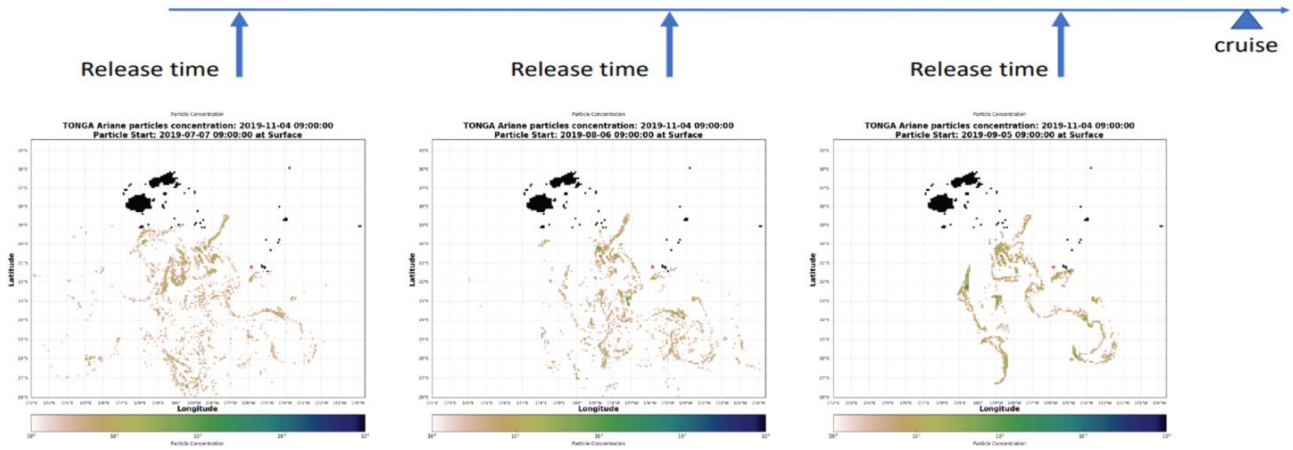


Figure 50. View of the particles concentrations at Surface on the 4 Nov 2019 with a release from V1 (red star) on 7 July (left), on 6 August (center) and 5 September (right)

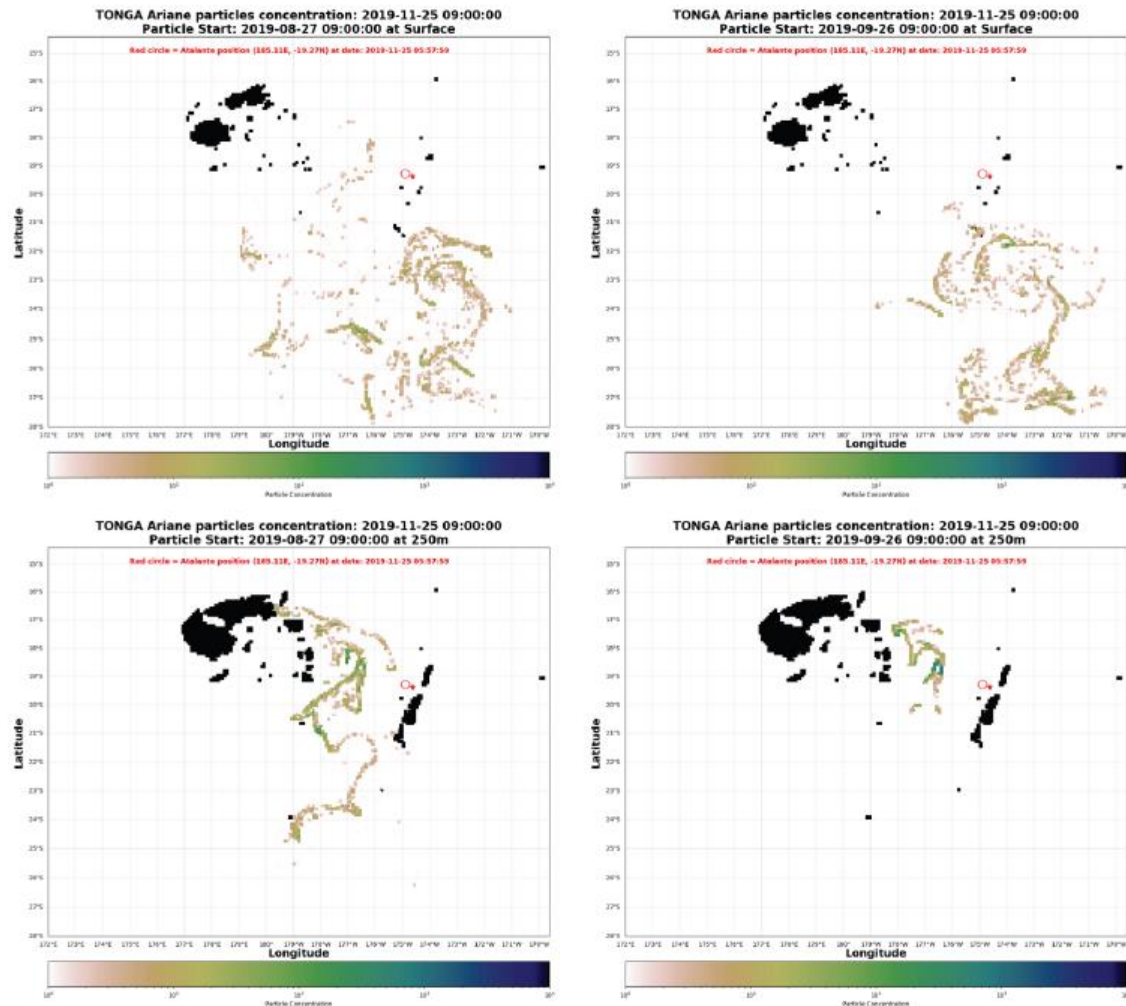


Figure 51. View of the particles concentrations at surface (top) and at 250 m (bottom) on the 25 Nov 2019 with a release from Simone (red star) on 27 August (left), and on 26 Sept (right).

These analyses help us to interpret the data acquired onboard and will be extremely useful to interpret the fate of the anomalies generated by the fluids at different time and space scale. Also, the simulation will be improved by additional

dynamics characterization acquired during the cruise (and later on, thanks to the autonomous floats and surface buoys). An intriguing aspect will be to match those simulations with the ocean color data (chl-a) observations from satellite. Indeed, the satellite views available during the campaign show clearly the dispersion of the Chla toward the east of the TONGA Arc, as also shown in the Ariane simulation. The question remains to interpret these increased Chla concentrations: either related to transport of Chla-rich filaments from the Lau Basin and/or caused by the diffusion of fertilizing fluids causing local blooming (one example is given below).

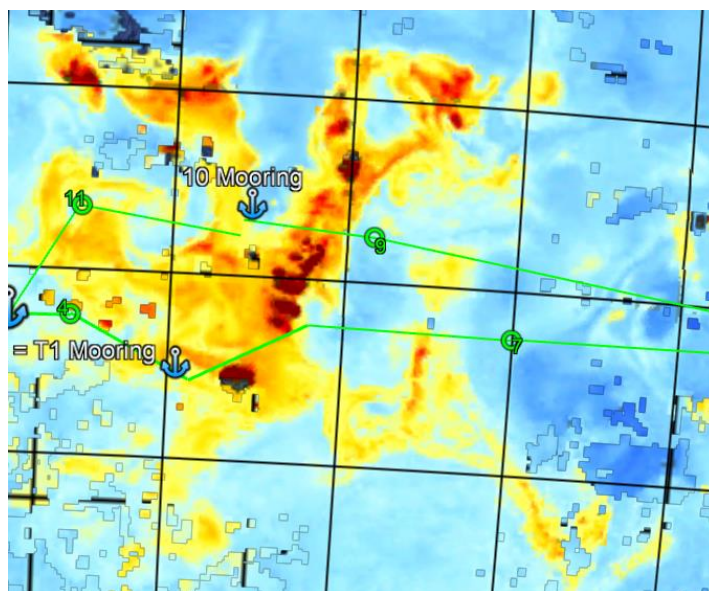


Figure 52. *Chla concentrations of the 26 Nov. showing high Chla concentrations in the Fe-poor region east of the TONGA Arc.*

4.10.2 SPASSO

The SPASSO (Software Package for an Adaptive Satellite-based Sampling for Ocean campaigns <https://spasso.mio.osupytheas.fr/>) exploited several satellite datasets in order to help the sampling strategy by providing analysis of near-real time data : the surface ocean circulation, its dynamics (fronts, small scale eddies), its chlorophyll concentrations as well as its temperature. All the figures can be accessed via the following web site : <https://spasso.mio.osupytheas.fr/TONGA>.

During TONGA, we used the following daily and near-real time datasets: (1) altimetry data from the Global Ocean AVISO; the altimetry-derived currents were then processed by SPASSO to derive Eulerian and Lagrangian diagnostics of ocean circulation: Okubo-Weiss parameter, kinetic energy, particle longitudinal and meridional advection, Finite Size Lyapunov Exponent (FSLEs); (2) the Global Ocean - Sea Surface Temperature Multi-sensor Observations (level 3 with 0.1° resolution and level 4 with 0.25° resolution and (3) the chlorophyll concentration (level 3 with a resolution of 4 km, multi satellite ACRI product) provided by [CMEMS - Copernicus Marine Environment Monitoring Service](#).

6. REFERENCES IN THE TEXT

- Abualhija, M. M., Whitby, H., & van den Berg, C. M. (2015). Competition between copper and iron for humic ligands in estuarine waters. *Marine Chemistry*, 172, 46-56.
- Berger, C. J., Lippiatt, S. M., Lawrence, M. G., & Bruland, K. W. (2008). Application of a chemical leach technique for estimating labile particulate aluminum, iron, and manganese in the Columbia River plume and coastal waters off Oregon and Washington. *Journal of Geophysical Research: Oceans*, 113(C2).
- Berthelot, H., Bonnet, S., Grosso, O., Cornet, V., & Barani, A. (2016). Transfer of diazotroph-derived nitrogen towards non-diazotrophic planktonic communities: a comparative study between *Trichodesmium erythraeum*, *Crocospaera watsonii* and *Cyanothece* sp. *Biogeosciences*, 13(13), 4005-4021.
- Bonnet, S., Berthelot, H., Turk-Kubo, K., Cornet-Barthaux, V., Fawcett, S., Berman-Frank, I., ... & Capone, D. G. (2016). Diazotroph derived nitrogen supports diatom growth in the South West Pacific: A quantitative study using nanoSIMS. *Limnology and Oceanography*, 61(5), 1549-1562
- Browning, T. J., Achterberg, E. P., Yong, J. C., Rapp, I., Utermann, C., Engel, A., & Moore, C. M. (2017). Iron limitation of microbial phosphorus acquisition in the tropical North Atlantic. *Nature communications*, 8(1), 15465.
- Caffin, M., Berthelot, H., Cornet-Barthaux, V., Barani, A., & Bonnet, S. (2018). Transfer of diazotroph-derived nitrogen to the planktonic food web across gradients of N₂ fixation activity and diversity in the western tropical South Pacific Ocean. *Biogeosciences*, 15(12), 3795-3810
- Dulaquais, G., Waeles, M., Gerringa, L. J., Middag, R., Rijkenberg, M. J., & Riso, R. (2018). The biogeochemistry of electroactive humic substances and its connection to iron chemistry in the North East Atlantic and the Western Mediterranean Sea. *Journal of Geophysical Research: Oceans*, 123(8), 5481-5499.
- Gimenez, A., Baklouti, M., Bonnet, S., & Moutin, T. (2016). Biogeochemical fluxes and fate of diazotroph-derived nitrogen in the food web after a phosphate enrichment: modeling of the VAHINE mesocosms experiment. *Biogeosciences*, 13(17), 5103-5120.
- Gruber, N. (2004). The dynamics of the marine nitrogen cycle and its influence on atmospheric CO₂ variations. In *The ocean carbon cycle and climate* (pp. 97-148). Springer Netherlands.
- Guieu, C., Bonnet, S., Petrenko, C., Menkes, C., Chavagnac, V., Desboeufs, & K., Moutin, Iron from a submarine source impacts the productive layer of the Western Tropical South Pacific (WTSP), *Nature Sci. Rep.*, 8 (1), 9075, 2018. (et communiqué de presse <https://archives.cnrs.fr/insu/article/1943>)
- Karl et al. *Ocean Biogeochem.*, Springer, 2003
- King, D. W., Lin, J., & Kester, D. R. (1991). Spectrophotometric determination of iron (II) in seawater at nanomolar concentrations. *Analytica Chimica Acta*, 247(1), 125-132.
- King, D. W., Lounsbury, H. A., & Millero, F. J. (1995). Rates and mechanism of Fe (II) oxidation at nanomolar total iron concentrations. *Environmental science & technology*, 29(3), 818-824
- Kolber, Z. S., Prášil, O., & Falkowski, P. G. (1998). Measurements of variable chlorophyll fluorescence using fast repetition rate techniques: defining methodology and experimental protocols. *Biochimica et Biophysica Acta (BBA)-Bioenergetics*, 1367(1-3), 88-106
- Lacan, F., Radic, A., Jeandel, C., Poitrasson, F., Sarthou, G., Pradoux, C., & Freyrier, R. (2008). Measurement of the isotopic composition of dissolved iron in the open ocean. *Geophysical Research Letters*, 35(24).
- Lacan, F., Radic, A., Labatut, M., Jeandel, C., Poitrasson, F., Sarthou, G., ... & Freyrier, R. (2010). High-precision determination of the isotopic composition of dissolved iron in iron depleted seawater by double spike multicollector-ICPMS. *Analytical chemistry*, 82(17), 7103-7111.
- Leal, M. F. C., Vasconcelos, M. T. S. D., and van den Berg, C. M. G. (1999). Copperinduced release of complexing ligands similar to thiols by *emiliania huxleyi* in seawater cultures. *Limnol. Oceanogr.* 44, 1750–1762. doi: 10.4319/lo.1999.44.7.1750
- Lucia, M., Campos, A., & Van den Berg, C. M. (1994). Determination of copper complexation in sea water by cathodic stripping voltammetry and ligand competition with salicylaldehyde. *Analytica Chimica Acta*, 284(3), 481-496.
- Massoth, G., Baker, E., Worthington, T., Lupton, J., De Ronde, C., Arculus, R., ... & Lebon, G. (2007). Multiple hydrothermal sources along the south Tonga arc and Valu Fa Ridge. *Geochemistry, Geophysics, Geosystems*, 8(11)
- Obata, H., Karatani, H., & Nakayama, E. (1993). Automated determination of iron in seawater by chelating resin concentration and chemiluminescence detection. *Analytical Chemistry*, 65(11), 1524–1528. <https://doi.org/10.1021/ac00059a007>

Planquette, H., & Sherrell, R. M. (2012). Sampling for particulate trace element determination using water sampling bottles: methodology and comparison to in situ pumps. *Limnology and Oceanography: Methods*, 10(5), 367-388.

Thibon et al., in prep?

Ussher, S. J., Milne, A., Landing, W. M., Attiq-ur-Rehman, K., Séguret, M. J., Holland, T., ... & Worsfold, P. J. (2009). Investigation of iron (III) reduction and trace metal interferences in the determination of dissolved iron in seawater using flow injection with luminol chemiluminescence detection. *Analytica chimica acta*, 652(1-2), 259-265.

Whitby, H., & van den Berg, C. M. (2015). Evidence for copper-binding humic substances in seawater. *Marine Chemistry*, 173, 282-290.

Yong, S. C., Roversi, P., Lillington, J., Rodriguez, F., Krehenbrink, M., Zeldin, O. B., ... & Berks, B. C. (2014). A complex iron-calcium cofactor catalyzing phosphotransfer chemistry. *Science*, 345(6201), 1170-1173.

7. ANNEXE 1: PARTICIPANTS ON BOARD

	Last name	First name	Expertise	Role on board	Labo
1	Guieu	Cécile	biogeochemistry	Chef scientist, minicosms experiments, sediment cores, sediment traps	LOV/ IMEV, CNRS
2	Bonnet	Sophie	biogeochemistry	Chef scientist, supervision of diazotrophy team work	M I O/ AMU, IRD
3	Gazeau	Fredéric	biogeochemistry	Mixing experiments in minicosms	LOV/ IMEV, CNRS
4	Taillandier	Vincent	biogeochemistry /physics	CTDs responsible	LOV/ IMEV, CNRS
5	Tilliette	Chloé	biogeochemistry	Mixing experiments in minicosms	LOV/ IMEV, CNRS
6	Dimier	Céline	biogeochemistry	Pigments, phytoplankton	LOV/ IMEV, CNRS
7	Grisoni	Jean Michel	instrumentation, mouillages	turbulence, moorings, in support for the diazotrophy team	LOV/ IMEV, CNRS
8	De Liège	Guillaume	instrumentation, mouillages	Mooring (responsible), CTD team	LOV/ IMEV, SU
9	Pulido-Villena	Elvira	biogeochemistry	Nutrients and processes experiments	M I O/ AMU, CNRS
10	Grosso	Olivier	biogeochemistry	Diazotrophy team, O ₂	M I O/ AMU, CNRS
11	van Wambeke	France	biogeochemistry	Microbiology, processes experiments	M I O/ AMU, CNRS
12	Bhairy	Nagib	biogeochemistry, mouillages	Moorings, responsible for deployments of : plankton nets, marine snow catcher ; CTD team	M I O/ AMU, CNRS
13	Lory	Caroline	biogeochemistry	Diazotrophy team	M I O/ AMU
14	Benavides	Mar	biogeochemistry	Diazotrophy team, organic matter	M I O/ AMU, IRD
15	Desgranges	Marie	biogeochemistry	Mercury	M I O/ AMU
16	Guigne	Cathy	biogeochemistry	Core parameters (nutrients, DOC, O ₂ etc.)	M I O/ AMU, CNRS
17	Gac	Jean-Philippe	geochemistry	Gases and tracing hydrothermal fluids	AD2M, CNRS
18	Boulart	Cédric	geochemistry	Gases and tracing hydrothermal fluids	AD2M, CNRS
19	Bigéard	Estelle	biology	Virus	AD2M, CNRS
20	Ferrieux	Mathilde	biology	Plankton diversity	AD2M, CNRS
21	Sellegri	Karine	Atmopsheric chemistry	Marine aerosols emissions	LAMP, CNRS
22	Bressac	Matthieu	biogeochemistry	Trace metals, export, in situ processes	University of Tasmania
23	Barman Frank	Ilana	biogeochemistry	Nitrogen cycle	University of Haifa

24	Sarthou	Géraldine	chemistry	Responsible for Trace Metal team	LEMAR
25	Gonzalez Santana	David	chemistry	Trace Metal team and on board measure of Fell	LEMAR
26	Amone	Veronica	chemistry	Trace Metal team	Universidad de Las Palmas de Gran Canaria
27	Desboeufs	Karine	Atmpsheric chemistry	Responsible for atmospheric measurements	LISA
28	Beillard	Lucie	Atmpsheric chemistry	atmospheric measurements in PEGASUS	LISA
29	Bataille	Hubert	Movie maker	Video, photos and link with Julia Uitz to feed the twitter account	IRD

8. ANNEXE 2: PARTICIPANTS ON LAND

Lasname	Firstname	Position	Laboratory
Pelletier	Bernard	Senior scientist	UMR Géoazur (UNS, OCA, CNRS, IRD), Centre IRD de Nouméa, New Caledonia
Baudoux	Anne-Claire	Research Scientist	AD2M Adaptation et Diversité en Milieu Marin, CNRS, Sorbonne Université, Station biologique de Roscoff
de Vargas	Colomban	Senior scientist	
De Vargas	Colomban	Senior scientist	
Gachenot	Martin	Engineer	
Garczarek	Laurence	Senior scientist	
Jeanthon	Christian	Senior Scientist	
Le Gall	Florence	Engineer	
Marie	Dominique	Senior scientist	
Not	Fabrice	Senior Scientist	
Probert	Ian	Research Engineer	
Ratin	Morgane	Engineer	
Simon	Nathalie	Associate professor	
Vaulot	Daniel	Senior scientist	
Fernandez	Jean-Michel	Research scientist	Analytical & Environmental laboratory (AEL/LEA), Nouméa, New Caledonia
Meyer	David	Postdoctoral researcher	Department of Marine Chemistry, Leibniz Institute for Baltic Sea research (IOW), Rostock, Germany
Prien	Ralf	Senior scientist	
Paparella	Francesco	Associate professor	Division of Sciences and Mathematics, New York University Abu Dhabi, Abu Dhabi, UAE
De Saint Léger	Emmanuel	Engineer	Division Technique de l'INSU - UPS855, CNRS-INSU, Plouzané
Dissard	Delphine	Research scientist	ENTROPIE (IRD, Université de la Réunion, CNRS), Nouméa, New Caledonia
Menkes	Christophe	Senior scientist	
Knapp	Angela	Professor	Florida State University (FSU), Tallahassee, FL
Arnaud-Haond	Sophie	Research scientist	Ifremer, UMR Marbec, Sète
Leblond	Nathalie	Engineer	Institut de la Mer de Villefranche, CNRS, Villefranche sur Mer
Scheurle	Carolyn	Engineer	
Cabrol	Lea	Research scientist	Institut Méditerranéen d'Océanologie, M.I.O, CNRS, IRD, Aix-Marseille Université, Toulon Université, Marseille
Dufour	Aurélié	Engineer	
Heimbürger-Boavida	Lars-Eric	Research scientist	
Le Moigne	Frédéric	Research scientist	
Lefèvre	Dominique	Research scientist	
Nunige	Sandra	Engineer	
Petrenko	Anne	Assistant professor	
Mazoyer	Camille	Engineer	

Tamburini	Christian	Senior scientist	
Boyd	Philip	Senior scientist	Institute for Marine and Antarctic Studies (IMAS)
Patriat	Martin	Senior scientist	Laboratoire Aléas géologiques et Dynamique sédimentaire, IFREMER, Plouzané
Dulaquais	Gabriel	Assistant Professor	Laboratoire des Sciences de l'Environnement Marin, LEMAR, CNRS, Univ Brest, IRD, Ifremer, Plouzané
Lorrain	Anne	Research scientist	
Planquette	Hélène	Research scientist	
Whitby	Hannah	Postdoctoral researcher	
Chaffron	Samuel	Research scientist	Laboratoire des Sciences du Numérique de Nantes (LS2N)
Lacan	François	Senior Scientist	Laboratoire d'Etude en Géophysique et Océanographie Spatiales LEGOS, CNRS, CNES, IRD, Université de Toulouse
Jeandel	Catherine	Senior Scientist	
Branchereau	Quentin	Outreach professional	Laboratoire d'Océanographie de Villefranche, LOV, CNRS, Sorbonne Université, Villefranche sur Mer
Lombard	Fabien	Assistant professor	
Montanes	Maryline	Engineer	
Uitz	Julia	Research scientist	
Vigier	Nathalie	Senior scientist	
Bouruet-Aubertot	Pascale	Senior scientist	Laboratoire d'Océanographie et du Climat, LOCEAN, Sorbonne Université, Paris
Cuypers	Yannis	Research Scientist	
Grima	Nicolas	Engineer	Laboratoire d'Océanographie Physique et Spatiale, CNRS, Univ Brest, IRD, Ifremer, Plouzané
Maes	Christophe	Senior scientist	
Chavagnac	Valérie	Senior scientist	Laboratoire Géosciences Environnement Toulouse, GET, CNRS, UPS, IRD, Toulouse University
Destrigneville	Christine	Associate professor	
Point	David	Research scientist	
Chevallier	Servanne	Engineer	Laboratoire Interuniversitaire des Systèmes Atmosphériques -LISA, CNRS, Université de Paris, UPEC, Paris
Doussin	Jean-François	Professor	
Feron	Anaïs	Engineer	
Gaimoz	Cécile	Engineer	
Journet	Emilie	Assistant professor	
Michoud	Vincent	Assistant Professor	
Triquet	Sylvain	LISA	
Berman-Frank	Ilana	Professor	Leon H. Charney School of Marine Sciences, Department of Marine Biology, University of Haifa, Israel
Diruit	Wendy	Engineer	OSU Ecce Terra, CNRS, Paris
Schmechtig	Catherine	Engineer	
Gonzalez	Aridane	PhD student	QUIMA, IOCAG, Instituto de Oceanografía y Cambio Global, Las Palma de Gran Canaria, Spain
Mahieu	Léo	PhD student	School of Environmental Sciences, University of Liverpool
Ratnarajah	Lavenia	Postdoctoral researcher	
Salaun	Pascal	Research scientist	
Tagliabue	Alessandro	Senior scientist	
Collot	Julien	Senior scientist	Service Géologique de Nouvelle-Calédonie, DIMENC, Nouméa, Nouvelle-Calédonie

9. ANNEXE 3: PUBLICATIONS (PUBLISHED OR ACCEPTED) AND COMMUNICATIONS (UPDATE NOV 2023)

In addition to the papers published (as in Nov 2023), there is a ongoing Research Topic (special issue) 'Hydrothermal and submarine volcanic activity: Impacts on ocean chemistry and plankton dynamics (Journal Frontiers in Microbiology and Frontiers in Aquatic Microbiology, <https://www.frontiersin.org/research-topics/49099/hydrothermal-and-submarine-volcanic-activity-impacts-on-ocean-chemistry-and-plankton-dynamics>. Already 4 published papers, 3 papers in review, several to be submitted in the following months (see update here: <https://docs.google.com/spreadsheets/d/1VuU-d-xc-em3-IURRAD6oNBr3CzSOAg5/edit#gid=893870304>)

Benavides, M., Bonnet, S., Le Moigne, F.A.C. et al. Sinking Trichodesmium fixes nitrogen in the dark ocean. ISME J 16, 2398–2405 (2022). <https://doi.org/10.1038/s41396-022-01289-6>

Benavides, M., Conradt, L., Bonnet, S., Berman-Frank, I., Barillon, S., Petrenko, A., Doglioli, A. Fine-scale sampling unveils diazotroph patchiness in the South Pacific Ocean. ISME Communications, 1(1), 3 (3p.). <https://doi.org/10.1038/s43705-021-00006-2>

Bonnet S. and Guieu C., Taillandier V., Boulart C., Bouruet-Aubertot P., Gazeau F., Scalabrin C., Bressac M., N. Knapp A.N., Cuypers Y., González-Santana D., J. Forrer H.J., Grisoni J-M, Grosso O., Habasque J., Jardin-Camps M., Leblond N., Le Moigne F., Lebourges-Dhaussy A., Lory C., Nunige S., Pulido-Villena E., L. Rizzo A.L., Sarthou G., Tilliette C. (2023). Natural iron fertilization by shallow hydrothermal sources fuels diazotroph blooms in the ocean. Science, 380(6647), 812-817. <https://doi.org/10.1126/science.abq4654>

Bonnet, S., Benavides, M., Le Moigne, F., Camps, M., Torremocha, A., Grosso, O., Spungin, D., Berman-Frank, I., Garczarek, L., Cornejo-Castillo, F., Diazotrophs are overlooked contributors to carbon and nitrogen export to the deep ocean. Isme Journal, 17(1), 47-58. <https://doi.org/10.1038/s41396-022-01319-3>

Dulaquais, G., Fourier, P., Guieu, C., Mahieu, L., Riso, R., Salaun, P., ... & Whitby, H. (2023). The role of humic-type ligands in the bioavailability and stabilization of dissolved iron in the Western Tropical South Pacific Ocean. Frontiers in Marine Science, Volume 10 - 2023 | <https://doi.org/10.3389/fmars.2023.1219594>

Filella, A., Riemann, L., Van Wambeke, F., Pulido-Villena, E., Vogts, A. Bonnet, S., Grosso, O., Diaz, J., Duhamel, S. and Benavides, M., Contrasting Roles of DOP as a Source of Phosphorus and Energy for Marine Diazotrophs. Frontiers In Marine Science, 9, 923765 (10p.). <https://doi.org/10.3389/fmars.2022.923765>

Forrer, H., Bonnet, S., Thomas, R., Grosso, O., Guieu, C., & Knapp, A. (2023). Quantifying N₂ fixation and its contribution to export production near the Tonga-Kermadec Arc using nitrogen isotope budgets. Frontiers in Marine Science, Volume 10 - 2023 | <https://doi.org/10.3389/fmars.2023.1249115>

Fourrier, P. Dulaquais, G., Guigue, C., Giamarchi, P., Sarthou, G., Whitby, H. and Riso, R., Characterization of the vertical size distribution, composition and chemical properties of dissolved organic matter in the (ultra)oligotrophic Pacific Ocean through a multi-detection approach. Marine Chemistry, 240, 104068 (15p.). <https://doi.org/10.1016/j.marchem.2021.104068>

Fuchs Robin, Baumas Chloé M. J., Garel Marc, Nerini David, Le Moigne Frédéric A. C., Tamburini Christian (2023). A RUpture-Based detection method for the Active mesopeLagic Zone (RUBALIZ): A crucial step toward rigorous carbon budget assessments. Limnology And Oceanography-methods, 21(1), 24-39. <https://doi.org/10.1002/lom3.10520>

Lory C., Van Wambeke F., Fourquez M., Barani A., Guieu C., Tilliette C., Marie D., Nunige S., Berman-Frank I., Bonnet Sophie (2022). Assessing the contribution of diazotrophs to microbial Fe uptake using a group specific approach in the Western Tropical South Pacific Ocean. ISME Communications, 2(1), 41 (11p.). <https://doi.org/10.1038/s43705-022-00122-7>

Méridguet, Z., Vilain, M., Baudena, A., Tilliette, C., Habasque, J., Lebourges-Dhaussy, A., ... & Lombard, F. (2023). Plankton community structure in response to hydrothermal iron inputs along the Tonga-Kermadec arc. Frontiers in Marine Science, Volume 10 - 2023 | <https://doi.org/10.3389/fmars.2023.1232923>

Thibon F., Weppe L., Churlaud C., Lacoue-Labarthe T., Gasparini S., Cherel Y., Bustamante and Vigier N. (2023), Lithium isotopes in marine food webs: Effect of ecological and environmental parameters. Front. Environ. Chem. 3, 1060651. <https://doi.org/10.3389/fenvc.2022.1060651>

Tilliette, C., Gazeau, F., Chavagnac, V., Leblond, N., Montanes, M., Leblanc, K., Schmidt S., Charrière B., Bhairy N. & Guieu, C. (2023). Significant impact of hydrothermalism on the biogeochemical signature of sinking and sedimented particles in the Lau Basin. Journal of Geophysical Research: Oceans, 128(12), <https://doi.org/10.1029/2023JC019828>

Tilliette C., Taillandier V., Bouruet-aubertot P., Grima Nicolas, Maes Christophe, Montanes M., Sarthou Geraldine, Vorrath M-e., Arnone V., Bressac M., González-santana D., Gazeau F., Guieu C. (2022). Dissolved iron patterns impacted by shallow hydrothermal sources along a transect through the Tonga-Kermadec arc. *Global Biogeochemical Cycles*, 36(7), e2022GB007363 (27p.). <https://doi.org/10.1029/2022GB007363>

Tilliette, C., Gazeau, F., Portlock, G., Benavides, M., Bonnet, S., Guigue, C., ... & Guieu, C. (2023). Influence of shallow hydrothermal fluid release on the functioning of phytoplankton communities. *Frontiers in Marine Science*, Volume 10 - 2023 | <https://doi.org/10.3389/fmars.2023.1082077>

10. ANNEXE 4: STUDENTS INVOLVED IN TONGA

The full list of students and post-doc involved in TONGA can be find here : <https://docs.google.com/spreadsheets/d/1OodmSnsHRpuHCJdyXITmRX0vEEJB6JYE/edit#gid=614005275>

TONGA "SHALLOW HYDROTHERMAL SOURCES OF TRACE ELEMENTS: POTENTIAL IMPACTS ON BIOLOGICAL PRODUCTIVITY AND THE BIOLOGICAL CARBON PUMP"



<https://twitter.com/tongaproject>



<http://tonga-project.org>